Supercooling of phase change materials: A review

I. Shamseddine, F. Pennec, Pascal Henry Biwole, F. Fardoun

▶ **To cite this version:**

I. Shamseddine, F. Pennec, Pascal Henry Biwole, F. Fardoun. Supercooling of phase change materials: A review. Renewable and Sustainable Energy Reviews, 2022, 158, pp.112172. 10.1016/j.rser.2022.112172 . hal-03548211

HAL Id: hal-03548211
https://uca.hal.science/hal-03548211v1

Submitted on 22 Jul 2024

HAL is a multi-disciplinary open access archive for the deposit and dissemination of scientific research documents, whether they are published or not. The documents may come from teaching and research institutions in France or abroad, or from public or private research centers.

L'archive ouverte pluridisciplinaire **HAL**, est destinée au dépôt et à la diffusion de documents scientifiques de niveau recherche, publiés ou non, émanant des établissements d'enseignement et de recherche français ou étrangers, des laboratoires publics ou privés.

Distributed under a Creative Commons Attribution - NonCommercial 4.0 International License

Version of Record: https://www.sciencedirect.com/science/article/pii/S1364032122000995
Manuscript_f540d7fd5a20c52ca423d5591533017c

Professor Pascal Henry BIWOLE, PhD

Université Clermont Auvergne (UCA)
Institut Pascal UMR 6602 UCA/CNRS/ INP
7 Avenue Aristide Briand,
03100 Montluçon, France
Tel: +33 4 70022000

MINES ParisTech, PERSEE –
Center for Processes, Renewable Energies and Energy Systems,
CS 10207, F-06 904 Sophia Antipolis, France

pascal.biwole@uca.fr

November 25, 2021

To Editor,
Renewable and Sustainable Energy Reviews, Elsevier

Dear Editor,

As an academic researcher in the area of construction materials for low energy buildings, I hereby submit a second revision of the review paper entitled "Supercooling of phase change materials: a review", for publication purpose in Renewable and Sustainable Energy Reviews. The revised manuscript takes into account all the comments previously made by the reviewers, as detailed in the "Response to reviewers" file attached to the submission. The amendments are highlighted in the manuscript and are visible in Microsoft Word software's Revision mode.

With the growing public awareness on the environmental vulnerability of our planet and the recent issue, in many countries, of stricter regulations in terms of carbon emissions and energy consumption, it has seemed to us important to publish a paper on the state of the art regarding the supercooling phenomenon in phase change materials (PCM). Depending on the application, supercooling can be either an advantage or disadvantage. PCM can be used in thermal storage systems to enhance the performance by decreasing the demand on energy supply and shift the peak hour demand. This is done by the alternating solidification and melting processes that serve in the release and absorption of latent heat. Supercooling negatively affects the performance of such system by delaying or preventing solidification. On the other hand, supercooling can be beneficial in the sectors of preservation and survival of plants. This paper first presents a comprehensive review of the daily applications where this phenomenon can appear. Then, a detailed analysis of the effect of different factors on degree of supercooling is done. It was found that there is still a lack of information regarding the correlation between different factors. Afterwards, a detailed explanation of the challenges encountering researchers when modeling supercooling is done, followed by a set of models showing the different methods followed to overcome the challenges. A final discussion on needed future work is provided.

This review paper involved the University of Clermont Auvergne and the Lebanese University. This paper is an original work and it is not currently being reviewed by any other journal.

Sincerely yours,
Pascal Henry BIWOLE, PhD

© 2022 published by Elsevier. This manuscript is made available under the CC BY NC user license
https://creativecommons.org/licenses/by-nc/4.0/

RSER Author Checklist Table

Item	Check	Important notes for Authors/Requirement
Article type	Review article (16703)	Papers will be indexed as Full-length articles, Review articles, Retractions, Corrigendum, Addendum or Editorials as explained above in this GFA.
Manuscript	This is the 'entire' article that the reviewers and authors will assess. It is used later to prepare the published article, so it is important that all details required by the GFA are included.	The manuscript should be a single MS Word file or pdf that includes the cover letter, the RSER Author Checklist table and the paper as per the layout in the GFA.
Cover letter	A maximum of two pages, dated and addressed to the Editors stating the name and affiliation of the authors, it should state the following clearly; • Title paper, key findings and why novel and meets the journal scope, • Article type and if relates to a conference special issue. • Any details relating to elements of the work already published as a Preprint/Archiv/Working paper/conference paper etc. or as a thesis or other with a precise explanation, • Any details of funding agencies etc., • Provide a declaration of interest, • List any recommended reviewers, • The corresponding author must sign the Cover letter as the person held responsible for all aspects of the paper	Note that the role of the corresponding author is very important as they are responsible for the article ultimately in terms of Ethics in Publishing, making sure that the GFA is adhered to, informing readers of any relationships with organisations or people that may influence the work inappropriately as discussed in the GFA, all the content of the article and that the Proof is correct. It is very difficult if not impossible to edit a paper once published. Most mistakes in articles occur when corresponding authors are changed after/during acceptance; examples include leaving out acknowledgements of funding agencies and the full and correct author affiliations.

	during and after the publication process.	
Layout of paper	• checked	Note read carefully the specific details of each element/heading in this GFA. The main headings i.e. 2.0 to 6.0 can vary from article to article, but all articles must include the title, author details, abstract, keywords, highlights, word count and list of abbreviations on page 1 of the paper.
English, grammar and syntax	checked	The authors must proof read and check their work. This is NOT the role of the editorial team, reviewers or the publishing team. Some guidance on English, grammar and syntax is provided in this GFA below, but it is ultimately the author's responsibility.
Title	checked	The title should not include acronyms or abbreviations of any kind. Excessive use of capitals letters should also be avoided.
Author names and affiliations	checked	The names of the authors in order of contribution or supervision or seniority depending on the funding agency/field requirements should be presented below the title of the article as follows: Last, First by initial e.g. Foley, A.M.[1], Leahy, P.[2] 1 = School of Mechanical & Aerospace Engineering, Queen's University Belfast, BT9 4AH, United Kingdom 2 = School of Engineering, University College Cork, Ireland
Corresponding author	checked	The corresponding author must be denoted in the article by an asterix superscript beside their name and a

		footnote, as follows: Foley, A.M.[1, *] * = corresponding author details, a.foley@qub.ac.uk Note that only one corresponding author can be identified.
Highlights	Yes	Details on highlights are in the GFA below.
Graphical abstract	no	Note submitting a graphical abstract is at the discretion of the authors. It this is not required by RSER.
Copyright	Figure 1: 5153100354364 Figure 5: 5020130495280 Figure 6: 5020130666861 Figure 7: 501636583 Figure 10, 16, 17: 501635876 Figures 11, 12, 30: 5015910203673 Figure 14: 5015911350097 Figure 17: 5015920201970 Figures 19, 20, 21,22: 5015920798442 Figure 23: 5015921019090 Figures 25, 40, 41: 5015930204800 Figure 27: 5015930455028 Figure 31, 32: 5015931045492 Figure 38, 39: 5015940071082	Authors are responsible for arranging copyright for any already published images, figures, graphs and tables borrowed from third parties. Citing a source is not enough, in fact this is an Ethics in Publishing issue. Guidance on arranging copyright is provided in the GFA below.
Referencing style	**yes**	The preferred journal style is Vancouver (i.e. [1], [2] etc., see details on using in this GFA. All references must be numbered chronologically starting at 1 in square brackets in the paper and the list of references. All references mentioned in the Reference List are cited in the text, and vice versa.
Single column	checked	Note an article submitted in two column format will be automatically rejected.
Logos/emblems etc.	checked	A paper must NOT be submitted with Elsevier logos/layout as if already accepted for publication.
Embed graphs, tables and figures/other images in the main	checked	Although you will be required to submit all images, images MUST appear embedded in the main body

body of the article		of the article where they are to appear in the final published article.
Figures/Graphs/other images	checked and adhered	Any captions for graphs should be below the graph in the Manuscript. Note that all figures must be individually uploaded as separate files in the correct format, check format requirement in this GFA. Ensure all figure citations in the text match the files provided.
Tables	Checked and adhered	Any captions for tables should be above the graph in the Manuscript. Note that all figures must be individually uploaded as separate files in the correct format, check format requirement in this GFA. Ensure all table citations in the text match the files provided.
Line numbering	checked and adhered	RSER journal uses automatic line numbering, so authors must submit their source files without line numbers.
Acknowledgements	checked	The questions authors need to ask themselves, when preparing their acknowledgement are as follows: • Was this work funded by a government agency, industry or other philanthropic organisation? If yes, the corresponding author must check and include any grant/award/funding details. • Were any data sources, models, images used or provided by others, who did not contribute to the article? If yes, then it is to good practice to name and thank them individually. • Did any colleagues, friends or family proof read your work? If yes then it is also polite to mention them.

Ethics in Publishing	**checked carefully by all the authors named on the paper.**	It is vital that all authors read our requirements for Ethics in Publishing. Once your name is on the article you all are responsible for any plagiarism issues. Note that a corresponding author must email the Editor in Chief to get approval for any changes in authorship before any Proof is finalised. A change in name of the corresponding author must also be done with the written consent of the author and the Editor in Chief nominated by the existing corresponding author.
Ethical Statement	**Upload an Ethical Statement or alternatively state in the Cover Letter.**	Read details in this GFA,

Supercooling of phase change materials: a review

Shamseddine, I.[1, 2], Pennec, F.[1], Biwole, P.[1, 3*], Fardoun, F.[2, 4]

[1=] Université Clermont Auvergne, CNRS, Clermont Auvergne INP, Institut Pascal, F-63000 Clermont–Ferrand, France

[2=] Université Libanaise, Centre de Modélisation, Ecole Doctorale des Sciences et Technologie, Hadath, Liban

[3=] MINES Paris Tech, PSL Research University, PERSEE - Center for Processes, Renewable Energies and Energy Systems, CS 10207, 06 904 Sophia Antipolis, France

[4=] Faculty of Technology, Department GIM, Lebanese University, Saida, Lebanon

*Corresponding author: pascal.biwole@uca.fr

Abstract:

Supercooling is a natural phenomenon that keeps a phase change material (PCM) in its liquid state at a temperature lower than its solidification temperature. In the field of thermal energy storage systems, entering in supercooled state is generally considered as a drawback, since it prevents the release of the latent heat. Conversely, when dealing with plants, animals or preservation processes, supercooling protects organs, tissues or blood from solidification that leads to damage or to death. This paper first reviews the most important applications and cases in which supercooling can take place and dramatically change the performance. Second, the paper discusses the factors affecting the occurrence and the degree of supercooling, such as cooling rate, PCM container characteristics, PCM thermal history, use of additives, etc. The paper includes a supercooling modeling section, which presents the main mathematical and numerical methods used to solve the challenges encountered by researchers. This review shows that to experimentally foster or reduce supercooling, most researchers tend to use similar methods such as controlling the cooling rate, changing container's characteristics or adding additives. The main challenge in supercooling modeling being its unstable and probabilistic nature, most authors tend to perform experimental measurements to obtain some key parameters, notably the supercooling degree, prior to the modeling. This strategy restricts the validity of the models to applications having the same conditions as the experiments. Nevertheless, this review offers the guidelines to select the appropriate experimental parameters and modeling strategies, depending on the specific and practical objectives of each application.

Highlights:

- The advantages and disadvantages of supercooling in nature and different daily applications are reviewed.
- The latest experimental studies are presented and factors affecting supercooling are discussed.
- The challenges in modeling supercooling of PCM are presented
- The most used techniques to model supercooling are discussed.

Keywords: Thermal energy storage – Phase change material – Supercooling – Solidification – Numerical modeling – Experimental validation

Word count: 16703

Nomenclature :

a_0, a_1, a_2: constants
Bi: Biot number, -
CR: cooling rate, $°C/min$
C_p: heat capacity, J/K
d: the molecular diameter, m

F_{cry}: crystallization probability function, -

Fo: Fourier number, -

f_c: crystallization factor, -

f: nucleation barrier reduction factor, -

f_{super}: phase supercooling indicator, -

H: latent heat, J/kg

h: Planck's constant, -

$\Delta h = \frac{latentheat \times molecularweight}{Avogadro'snumber}$

I: homogeneous nucleation rate

I_n: nucleation factor

k: Boltzmann constant, -

K_1: arbitrary constant, -

K_2: fitting parameter, K^{-2}

K_3: calibration parameter, -

L: length, m

L_{adj}: number of solid crystals in the adjacent segments, -

L_f: molar heat of fusion, J/mol

N: number of atoms of a system, -

n: total number of measurements, -

$P(T)$: nucleation probability function, -

Q:heat source, kW

R: molar gas constant, $J/(mol.K)$

Ra: surface roughness, μm

q: activation energy, kJ/mol

SF: solidified fraction, -

T: temperature, K

Δt: time step, s

T_a: average value of nucleation and solidification temperatures, K

ΔT_{am}: melting point depression, K

T_c: coolant temperature, K

T_{di}: density change temperature, K

T_E: equilibrium melting point temperature, K

t_{end}: duration of simulation, s

T_f: freezing temperature, K

ΔT_h: degree of overheating, K

$T_I w$: capsule's internal wall temperature, K

T_i: initial temperature, K

T_m: melting temperature, K

T_n: nucleation temperature, K

T_s: solidification temperature,K

ΔT_s: degree of supercooling, K

t_s: duration of supercooling, K

u: internal energy, J

$v(T)$: solidification rate, m/s

W: the normal surface velocity of the freezing front, m/s

Δx: size of the cell, m

X_i: the impurity fraction, -

β: state quantity, -

λ: thermal conductivity, $W/(m.K)$

ρ: density, $kg/m3$

α: $(water/PCM)$convection coefficient, -

$\emptyset$: solidification ratio, -

γ: surface tension, $N.m^{-1}$

ΔG_n: free energy variation, J

α: angle of notch, rad

σ: surface tension, N/m

1 Introduction

For a given phase change material, the melting temperature, T_m, is the theoretical temperature at which the material changes its phase from solid to liquid and vice versa. For a pure PCM, phase change is considered isothermal [1]. In reality, for most PCM used in engineering applications, phase change occurs in a range of temperature around the melting temperature, as shown in Figure 1.

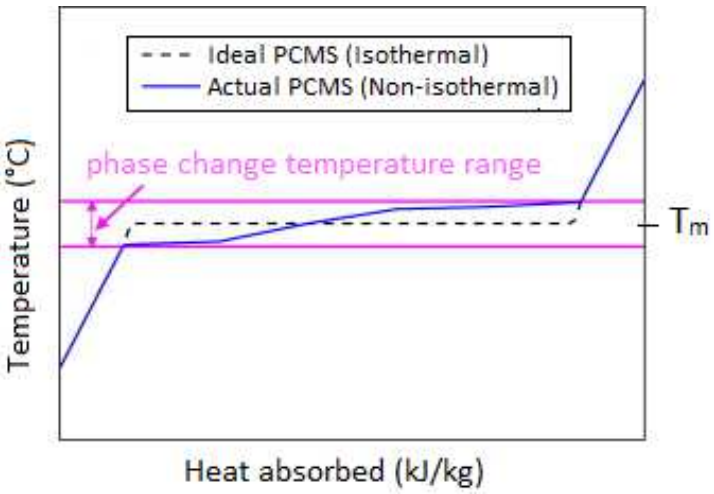

Figure 1 Temperature variation and phase change as a function of absorbed heat. The pink horizontal lines represent the actual phase change range. The blue line curve represents the actual temperature curve, whereas the black dotted curve represents the theoretical melting temperature [1]

A material remaining in liquid state at a temperature below its melting temperature is referred to a phenomenon known as supercooling, subcooling or undercooling. During supercooling, the material is in metastable state and plenty of factors can trigger solidification. The initiation of solidification results in the release of the latent heat, which causes a temperature rise within the material. If the energy contained in the liquid is sufficient, the temperature of the liquid will increase to its melting temperature as shown in Figure 2. The degree of supercooling is the difference between the theoretical melting temperature and the lowest temperature reached by the liquid phase, called the nucleation temperature hereafter denoted as T_n.

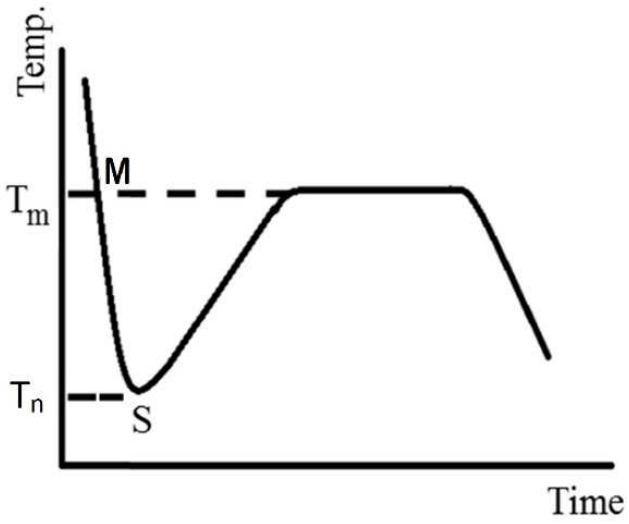

Figure 2 Plot of liquid undergoing supercooling upon cooling [2]

Depending on the given application, supercooling can be either useful or destructive. However, treating this phenomenon requires a good knowledge of its behavior under different conditions.

If supercooling is desired, a set of actions can be taken to increase the degree of supercooling and insure no solidification in the operating range below the melting temperature. For example, in applications of preservation, it is suitable avoid solidification while maintaining low temperatures. In this case, supercooling allows decreasing the quantity of energy needed to reach such temperatures, which is represented by the latent heat of solidification. However, if supercooling is not desired like in latent heat thermal energy storage systems, some parameters should be modified in a way to eliminate or decrease as much as possible the degree of supercooling. The importance of this phenomenon is reflected by the increasing number of articles, conferences and patents containing supercooling in their titles and abstracts, throughout the last decades. Based on Google scholar data, Figure 3 illustrates this trend.

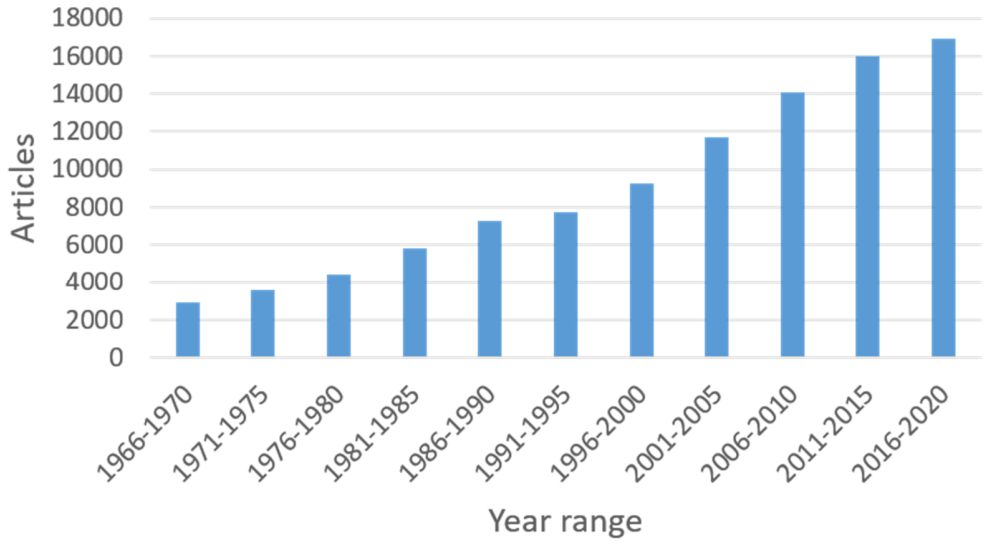

Figure 3 The increasing number of articles containing supercooling

Moreover, Figure 4 shows a statistical study done on a sample of 130 papers published in the year 2020 including the supercooling phenomenon. Those papers can be either a review paper, presenting a new numerical model, showing the current difficulty to address supercooling by numerical methods.

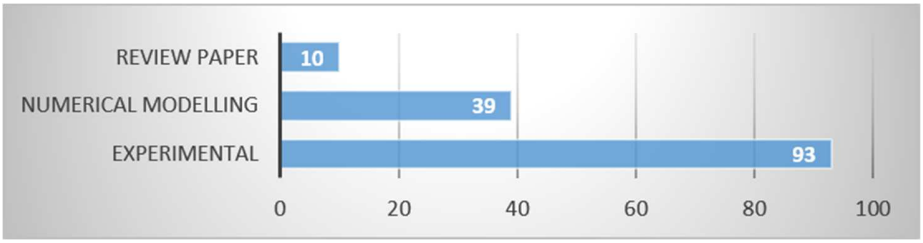

Figure 4 Investigation of type of publications of the year 2020 from a sample of 130 article

Existing reviews focus on one specific application such as food preservation [3]–[5], TES systems [6] or on very specific materials [7]–[9]. Such reviews only consider methods to reduce

supercooling [10]–[13] or to increase supercooling, depending on the application, without presenting both aspects. In the same way, most existing review focus either on experimental methods or on numerical modeling methods to deal with supercooling, with almost no paper discussing both. Only two recent reviews [14], [15] discussed both aspects but limited the study to man-engineered PCMs only, without considering supercooling in nature and preservation processes. Therefore, there is still a need for a foundational comprehensive review on all aspects of supercooling, cataloging and discussing its main occurrences in nature and human processes, the experimental methods to increases or decrease its occurrence depending on the application, and the existing numerical models. The present review paper aims at filling this gap.

First, an overall introduction to supercooling is conducted through its occurrence in nature or daily applications such as food preservation and thermal energy storage systems. The importance of considering this phenomenon in experimental and research works is explained by presenting its direct effects on the applications' performance and efficiency. In the second part, the paper details the most important factors having an effect on the degree of supercooling. According to the application, if these factors are well treated, the degree of supercooling can be increased, decreased or even eliminated at low cost using simple techniques. When trying to include supercooling in the numerical models, a set of challenges arises due to the metastable state of the material. The third section presents these challenges, along with the adapted solutions. The most recent models for supercooling, their methodology, the used mathematical equations and the taken assumptions are discussed. Then, the numerical results obtained by several researchers are compared and the gaps in the models are presented. At last, clear guidelines are provided for the optimal experimental design or numerical modeling of applications in presence of supercooling and the required future works are discussed.

2 Supercooling in nature and human applications

Supercooling is a natural phenomenon that depends on the surrounding circumstances, the liquid's properties and its response to different applied conditions. This variety of factors of supercooling presence causes this phenomenon to appear in various applications such as in plants, living creatures, food preservation and thermal storage systems using phase change materials.

2.1 Animals, plants and specimen organs

In nature and especially in freezing climate zones, the living creatures have three main options: they can either migrate to a warmer land, die freezing or survive by supercooling. Supercooling exists among plants and animals living in a very cold freezing climate in order to prevent these living creatures from dying due to the solidification of their body water content, body cells and blood. Some examples of animals are: Nematodes, insects that were found alive at a temperature of -80°C in Antarctica; Vallonia perspectiva, a small land snail [16]; Hippodamia convergens, a lady bird beetle; the larvae of goldenrod fly that were found alive at a temperature of -9°C and Chrysemys picta, a north american turtle that faces ice and freeze [17]. In addition, arctic fishes were found alive at a temperature of -1~-3°C [18].

Similarly, plants tissues can be damaged due to freezing of the water content inside the plant, especially the xylem tissues that are responsible of water and nutrients transport to several

parts of a plant such as leaves [19]. The experiment carried by Hacker *et al.* [20] on a cushion of Saxifraga caesia at bud stage and Saxifraga moschata during anthesis shows that the solidification of supercooled inflorescences occurs when reaching the minimum temperature and that 77% of caesia buds and 44% of moschata flowers solidified, causing lethal damage. However, the unfrozen inflorescences survived. Depending on the time spent in supercooling state and the temperature reached, Figure 5 shows in gray circles and black diamonds the number of solidification cases for caesia and moschata respectively.

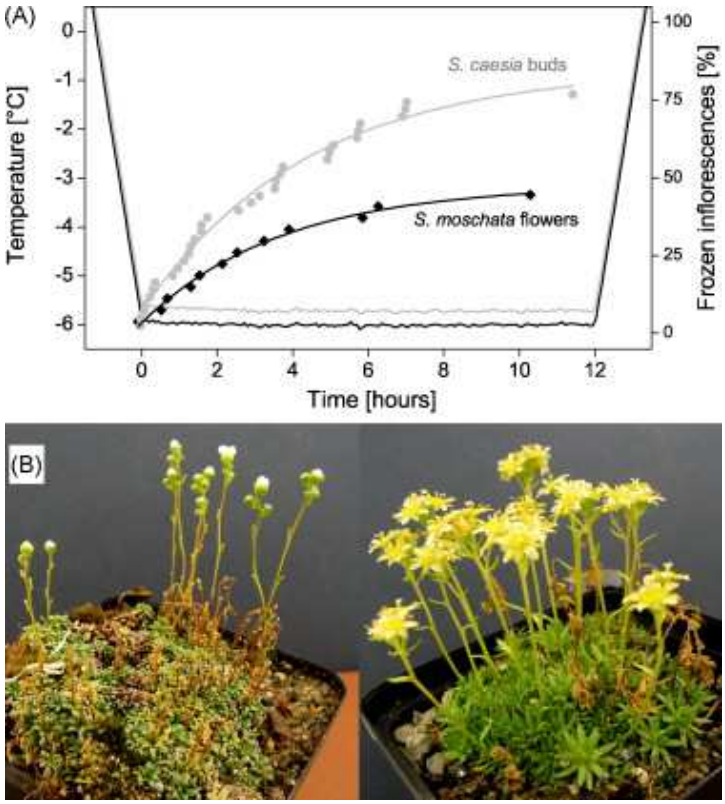

Figure 5 (A) Plot showing the percentage of frozen S. caesia and S. moschata with respect to temperature and time, (B) Captured photo of the experiment showing the impact of supercooling [20]

The preservation of mammalian body parts specimens is essential. It aims to have available cells, organs or tissues maintained at certain standards. In the presence of oxygen, the body is able to create energy by the degradation of aminoacids, carbohydrates, proteins and fats by aerobic metabolism process. According to Sicular *et al.* [21], for every 10°C of temperature decrease, the metabolism activity decreases by a factor of 1.5-2. Regarding the body temperature, preserving the organs at 4°C decreases the metabolism to 1/10, whereas the preservation at -4°C decreases it to 1/17. Monzen *et al.* [22] performed an experimental study on the preservation of rats' heart, liver and kidney in supercooled state, that is attained by an energized chamber using electric pressure. Preserving in supercooling state shows promising results, whereas cell and tissue damages are detected in the organs preserved at ordinary 4°C conditions. Moreover, the use of an electric field to attain supercooling state did not leave any trace or evidence of damage even when increased to 1000V. It is important to attain stable supercooling state to ensure that no solidification will take place which leads to organs damage. There are several

techniques used to reach the stable state, one of which is adding antifreeze agents. However, the agents used in the experiment of Rubinsky *et al.* [23] left traces in the organs that caused inevitable damages. This technique of preservation is essential because it extends the storage life of the specimens, especially from human donners.

2.2 Food preservation

Supercooling is considered very helpful in food preservation when knowing that a material undergoing supercooling does not release its latent heat because it remains in liquid state. Therefore, preserving food, at a given temperature, in supercooled state rather than solid state, will require less energy. In addition to economical savings, other benefits can be found. The growth of bacteria decreases with decreasing temperature, so preserving food in supercooled state keeps it fresh for a longer period with a high quality since the formation of ice ruins the food structure and properties. This technique leads to a decrease in food waste and an increase in the lifetime of fresh food at a lower cost [24]. The studies are still new, but they are promising in such fields as agricultural products [25], meat [26], [27] and fish [28], [29].

You *et al.* [30] conducted an experimental study on beefsteak, where the beef's internal temperature was held at a temperature of -4°C for 14 consecutive days using pulsed electric field and oscillating magnetic field. Figure 6 shows the obtained samples after 14 days for samples preserved by refrigeration (4°C), slow freezing (-10°C), fast freezing (-20°C) and fresh samples. By comparing these samples, no significant color change is observed between fresh (Figure 6a), rapid freeze (Figure 6e) and supercooled (Figure 6c) beef. Preserving by refrigeration (Figure 6b) shows an obvious change in color. The drawback of slow freezing (Figure 6d) is destroying the meat cells by the slow formation of ice. The slow formation of ice causes the ice to be formed as clusters that leads to drip loss, tenderization causing protein denaturation. Using rapid freezing can decrease the lipid oxidation and cell damage. Lipid oxidation causes a deterioration in the quality concerning the color, taste and nutritional value. However, low heat transfer rates in large sized food prevents using rapid freezing, which sets the technique of using supercooling in the scope of interest. Therefore, the quality of the beef represented by color, lipid oxidation, drip loss and texture can be attained similar to fresh meat by supercooling with less risk.

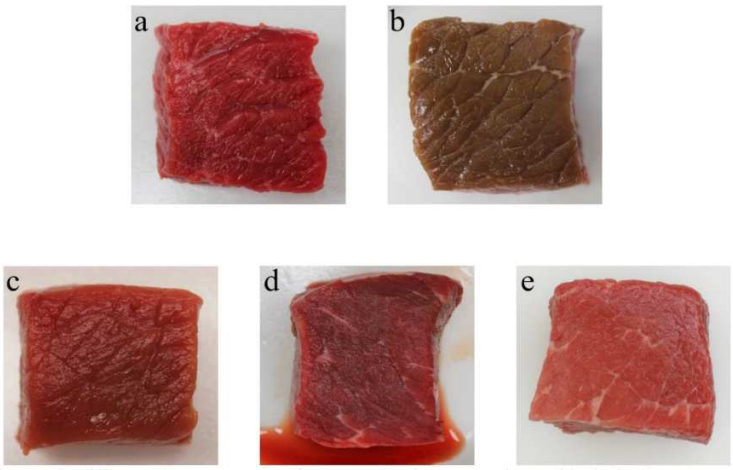

Figure 6 Images of a) fresh beefsteak compared to beefsteak samples preserved for 14 days by b) refrigeration, c) supercooling, d) slow freezing and e) rapid freezing [30]

Studies done on fish meat show that the meat preserved at a supercooling state has a firm structure [31], [32], fresher, since at a refrigeration temperature, meat can be preserved for a few days only and loses its firmness after that. Using standard refrigeration preserving conditions, the preservation of chicken is less than one month. However, a chicken preserved at supercooling state can endure preservation for months, which gives an extended margin for the merchant to distribute his products. Similarly, the supercooled garlic at -6°C shows a higher quality, as shown in Figure 7, where the color and structure of the cloves of garlic are better than those frozen at -30°C [33]. Similarly, Figure 8 shows the effect of temperature and preservation technique on the garlic and shallot, where a severe structure damage is clear in the freezing case [34].

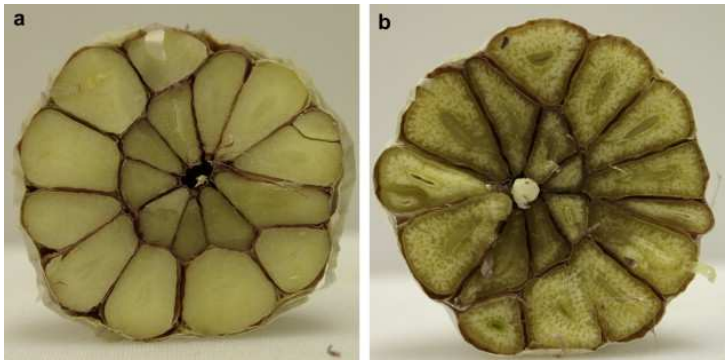

Figure 7 Garlic preserved unpeeled for one week a) supercooled at -6°C and b) frozen at -30°C [33]

Figure 8 Snapshots of a) garlic and b)shallot after being preserved unpeeled for a week at ambient temperature, chilled temperature 1.1°C, -6°C supercooled temperature and -30°C freezing temperature from left to right respectively [34]

James *et al.* [34], performed a series of experiments on vegetables and fruits. Table 1 summarizes the results, where the melting temperature is the temperature of phase change in case of no supercooling. From the below table, two things can be observed. The first is the dependence of the degree of supercooling on the type of sample, knowing that the supercooled material, water content, is the same. The degree of supercooling and standard deviation vary indeed from one to another. The second thing is the sensitivity of supercooling to any change. When performing an experiment on a given vegetable or fruit, efforts are done to take identical samples and apply similar external conditions. However, the degree of supercooling for some samples have a wide range and high standard deviation (sd).

Table 1 Supercooling experimental results performed on vegetables and fruits [34]

Sample	Average melting temperature (°C) and standard deviation	Number of samples $\left(\frac{supercooled}{Total}\right)$	Degree of supercooling		
			Min	Max	Avg (sd)
Broccoli	-2.1 (0.3)	9/10	0.4	7.7	2.5 (2.3)
Carrot	-1.6 (0.6)	9/10	0.4	2.6	1.1 (0.7)
Cauliflower	-1.5 (0.3)	7/10	0.6	6.9	3.8 (2.6)
Garlic	-2.7 (0.3)	15/15	4.9	12	10.3 (1.6)
Leek	-1.9 (0.3)	9/10	0.6	2.3	1.6 (0.6)
Parsnip	-2.2 (0.2)	4/10	0.4	0.9	0.7 (0.2)
Shallot	-1.6 (0.2)	10/10	1.1	4.7	3.3 (1.3)

As presented above, supercooling is beneficial for food preservation. A good knowledge of supercooling behavior helps applying the suitable techniques needed to obtain a narrow range of supercooling degree and low standard deviation with an optimal cost and better quality.

2.3 Thermal storage systems

Energy is the main demand for humans to fulfill their activities. The global energy demand is constantly increasing, with the increase in living standards and the growth of the economy and human population. The limited amount of traditional energy sources, such as coal and fuel,

prompts the search for other clean, inexpensive and unabated energy sources. The renewable energies are often intermittent and therefore need to be stored. Phase change materials (PCM) have drawn attention due to their importance in applications of thermal energy storage. PCM are promising materials that store energy in a relatively small volume of material. PCM store thermal energy by changing phase and taking advantage of their high latent heat. PCM in wallboards or HVAC systems serves in increasing the thermal comfort in the building by shifting the hour of peak load demand, decreasing this peak, reducing the sharp variation of daily energy demand and enhancing the building's thermal and energy behavior. In addition to that, using transparent PCM can serve in providing natural day light that also interferes in energy saving and adding comfort to the building. PCM can also act as a temperature regulator and heat sinks by delaying the rise in temperature of various electronic systems such as photovoltaic panels [35], [36]. Figure 9 shows the behavior of a PCM during heating and cooling, where making use of the big amount of latent heat serves to make PCM supplementary and even alternative to traditional cooling systems.

For that reason, PCM are precisely chosen according to their melting temperature to obtain the maximum efficiency of the thermal energy storage system in which they are integrated. One of the challenges facing the success of solid-liquid PCM systems is the supercooling phenomenon. The PCM remains liquid rather than solidifying, which prevents the system from benefiting of the latent heat. For such systems, researchers pay great attention to supercooling because of the direct negative impact on the efficiency, which may cause a damage and a fail in serving their purpose. Jin *et al*. [1] performed an experiment to study the supercooling degree of sodium acetate trihydrate (SAT). Three different cases were studied. The first starts the cooling process when the SAT is in solid state. In this case, no latent heat is released because there is no phase change and no supercooling. The second starts the cooling process when the SAT is in a partially melted state. In this case, the released latent heat and the degree of supercooling are relatively small. The third starts the cooling process when the SAT is in liquid state. Here, the liquid remains in supercooled state and latent heat is not released. The main challenging problem is that the degree of supercooling depends on several factors and differs from one fluid to another. There is no general methodology to obtain a specific degree of supercooling for each material. Therefore, experiments are conducted to study the effect of each factor separately. By the help of such experiments, a number of the used PCM have a well-known range of supercooling degree. In addition to the experiments, efforts are done to establish numerical models simulating the PCM behavior under supercooling. The following paragraphs discuss the details of supercooling in PCM.

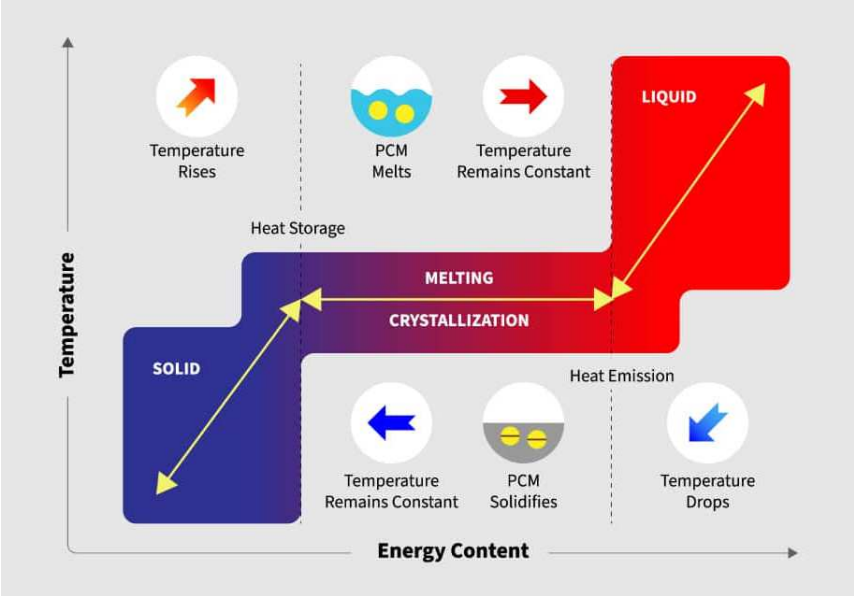

Figure 9 Schematic drawing representing a PCM during absorption and release of heat [37]

3 Effects of supercooling on PCM behavior

When choosing a PCM to include in a heating/cooling system, the main parameters taken into consideration are the melting temperature T_m and the latent heat H. The melting temperature has to be chosen close to the desired operating temperature or within the thermal comfort temperature range. Supercooling may be catastrophic to the PCM system efficiency. For example, in buildings, solidification mainly takes place naturally at night during a limited time. If the PCM undergoes supercooling instead of solidification, it will not be able to discharge the stored thermal energy. Therefore, the main goal of the presence of the PCM is not achieved during the day, leading to a system failure. Schranzhofer *et al.* [38] highlighted this problem by using a validated TRNSYS model, where they compared a brick wall layer with a PCM wall layer. The simulations highlight reduced temperature peaks with the use of PCM plaster since the latent heat plays an important role in shifting and decreasing the peak load. However, in the case of solidification prevention at night due to supercooling, the PCM remains liquid. In this case, the liquid PCM has a similar performance to that of the brick wall.

The following sections present a set of recent experimental and numerical results showing the effect of supercooling on the PCM behavior. The effect of supercooling degree on the temperature distribution, crystallization and quantity of released latent heat is outlined.

3.1 Different behaviors during cooling

Five typical cooling curves for water are presented in Figure 10, where T_i, T_{di}, T_f, T_n and T_c are the initial, density change, freezing, nucleation and coolant temperatures respectively. Five steps of PCM cooling process are displayed: (a): phase of release of sensible heat from liquid water and density changes until reaching freezing temperature; (b): metastable state of supercooled liquid; (c): process of dendritic ice formation and temperature increase; (d): release

of latent heat and solid formation; (e): cooling of solid water where temperature decreases by sensible heat release [39].

1. In Figure 10-1, water freezes without any presence of supercooling. Upon cooling, the temperature of water decreases by releasing its sensible heat until reaching T_f, after which the latent heat is released and phase change takes place. After releasing all latent heat, the solid water starts to cool down by releasing sensible heat. Since no supercooling takes place, dendritic ice is absent and crystalline ice is formed.
2. In Figure 10-2, the above five steps (a) → (e) take place, dendritic ice is formed during step (c) once T_n is reached. The temperature increases until it reaches T_f, and this is done by the release of the latent heat from the dendritic ice and its absorption by the supercooled liquid.
3. Figure 10-3 shows the case of water with low level of energy, which causes the freezing to take place immediately once T_f is reached.
4. Figure 10-4 shows a case similar to the case in Figure 10-3. However, the energy is low in a way that all the latent heat of the crystallized portion is released at a temperature lower than T_f and the latent heat is insufficient to raise the temperature to T_f.
5. In Figure 10-5, water stays in supercooled state and no phase change takes place. In this case, water stays in process (b) for an undetermined period. This can be due to a value of T_c higher than T_n and close to T_f ; or to a capsule material having low thermal conductivity, which fosters a higher degree of supercooling.

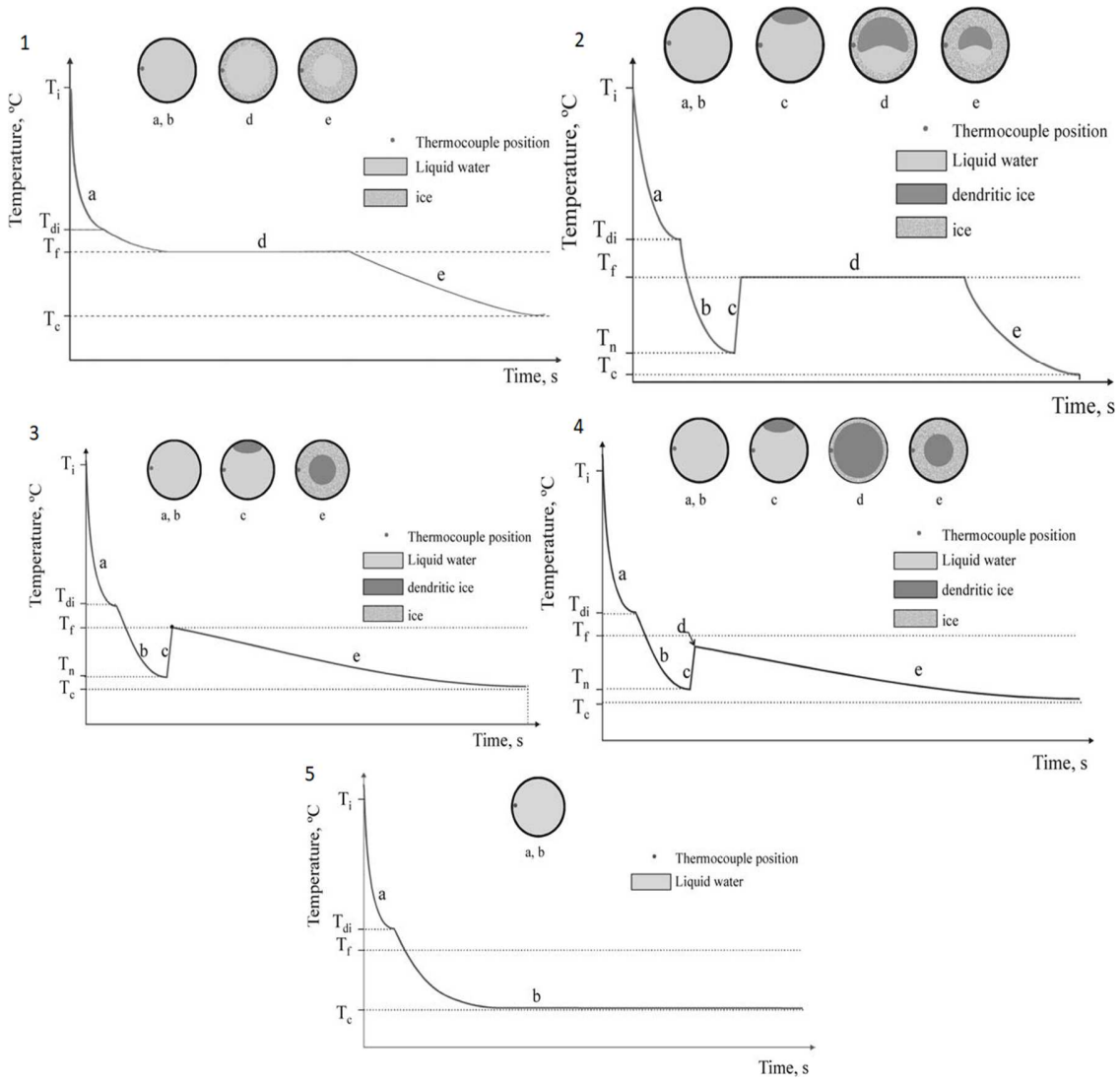

Figure 10 Process of 1) freezing with no supercooling, 2) instantaneous freezing with supercooling, 3) freezing with supercooling where all latent heat released to reach T_f , 4) freezing with hyper-cooling and 5) permanent supercooling with no process of freezing [39]

3.2 PCM performance

When choosing a PCM, its phase change temperature should be close to the comfort temperature or the desired functioning temperature of an apparatus, and the latent heat of fusion per unit volume should be high. The advantage of latent heat over sensible heat is the larger heat storage capacity with the same mass of material. However when solidification initiates in presence of supercooling, the liquid PCM absorbs part of this latent heat to increase its temperature from the nucleation temperature up to the melting temperature T_m as shown in Figure 10. The higher the degree of supercooling, the lower the amount of latent heat that is released at the actual phase change temperature. When comparing with a case not suffering supercooling, this consumed portion is equal to $c_{p,l}\Delta T_s$, where $c_{p,l}$ is the liquid phase heat capacity and ΔT_s is the degree of supercooling. If ΔT_s increases, more energy is needed to rise

the temperature to the melting temperature, which may cause a lack of useful energy needed during phase change. When solidification initiates, the temperature of the supercooled liquid increases sharply at a constant enthalpy. According to the experiments held by Sandnes *et al.* [40], this increase can be easily highlighted from enthalpy plots. They measured enthalpy-temperature curves for disodium hydrogen phosphate dodecahydrate, sodium acetate trihydrate and STL-47 that are well-known supercooling salt hydrates and found that the nucleation temperature decreases as the supercooling degree ΔT_s increases. This decrease of nucleation temperature causes a delay in the onset of crystallization, which is shown in the studies done by Hu *et al.* [41]. The one-dimensional mathematical heat transfer model of a PCM is initially set at the same temperature before decreasing the temperature of the left side. For different degrees of supercooling, Figure 11a shows the temperature distribution of the domain at a given instant, and Figure 12 shows the temperature variation at a given node. The temperature at the same location decreases with the increase of supercooling degree, because the initially liquid PCM, experiencing supercooling, releases sensible heat upon cooling, resulting in a temperature drop, while the other releases its latent heat and maintains a constant temperature. Moreover, as shown in Figure 11b, the heat flux variation depends on the PCM state and temperature. A PCM undergoing phase change has approximately equal temperature through all the sample. As a result, the maximum value reached increases before phase transition with the increase of supercooling degree; while during the whole process of solidification, it decreases [41].

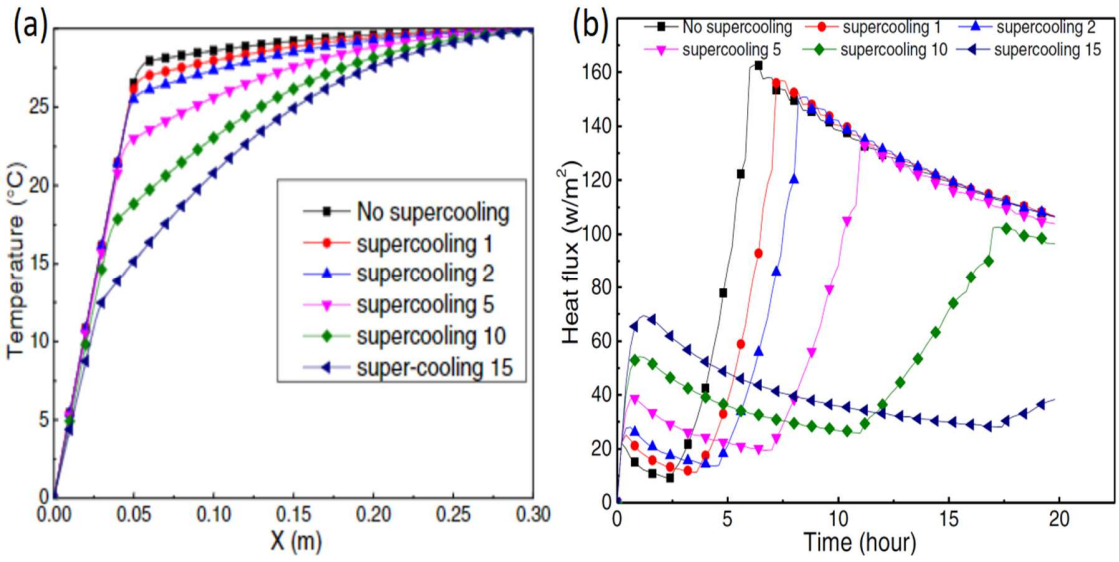

Figure 11 Plots showing the variation of the (a) temperature after 20 hours, (b) heat flux at a specific PCM node as a function of time under different degrees of supercooling [41]

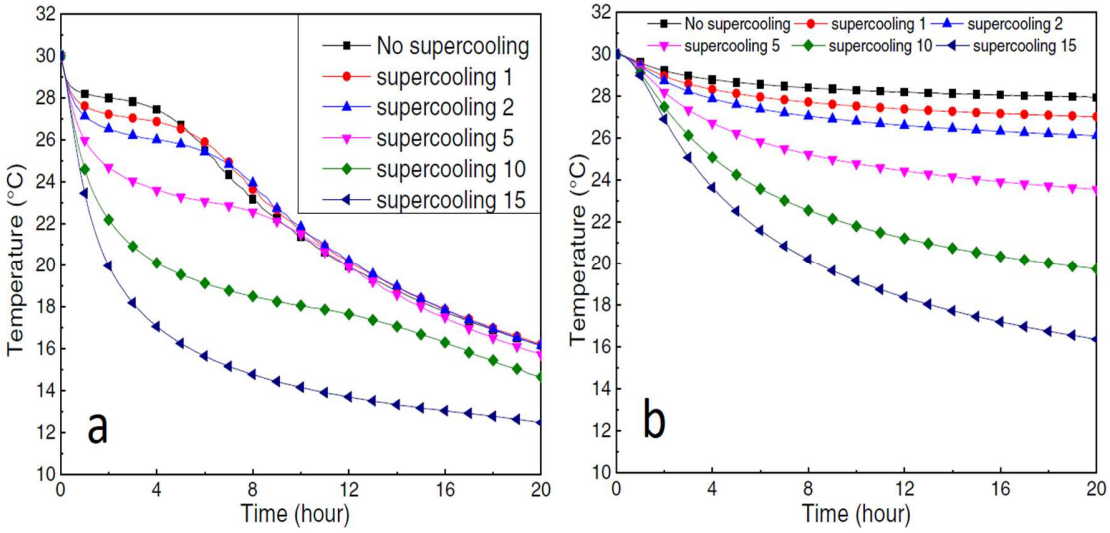

Figure 12 Temperature variation as a function of time for different degrees of supercooling at the same node having abscissa a) L/10, b) L/5, with t1=30°C, t2=0°C and a phase transition temperature range of 26–28°C [41]

Another effect of supercooling on the PCM is increasing the time required to discharge the stored heat. This phenomenon is due to the small temperature difference between the cold temperature applied at the heat exchange surface and the nucleation temperature T_n causing the PCM to approach the exchanger's temperature by sensible heat extraction. If $T_n$is lower than the exchanger temperature, the PCM fails to change phase, which means that the latent heat will not be extracted. The small temperature gradient just before reaching T_n causes a slow heat extraction. Using a numerical parametric study, Günther *et al.* [42] reproduce qualitatively the main effects of supercooling in the PCM. The PCM is connected on one side to a heat exchanger and on the other side to an insulating material. Another supercooling effect is represented by the phase change plateau's time span, which is the PCM buffering effect. By plotting the material average temperature versus time, the latent heat can be detected by a plateau of constant temperature. Increasing the degree of supercooling has several effects on the PCM behavior. First, the length of the plateau during which the release of latent heat takes place decreases meaning that less latent heat is released at T_m. In the case of severe degree of supercooling this plateau vanishes. Second, the temperature rise due to latent heat release becomes sharper, which causes problems in the performance of an application by releasing a sudden amount energy causing a sharp temperature variation. Moreover, this behavior causes numerical problems in simulation. Third, the instant of onset of solidification becomes late. Finally, the temperature of the PCM approaches the temperature of the node of heat exchanger, which decreases heat transfer rate between the PCM and the exchanger.

Even if the supercooling effect is inconspicuous, it does not mean its absence and it should be taken into account in numeral modeling since it may have a major impact on the heat transfer rate [43]. As shown above, the two main drawbacks of supercooling presence in heat storage systems are the shift in the phase change temperature, the reduction of the amount of useful latent heat energy and even its absence in some cases. Any loss in the latent heat is a loss of the useful heat and a decrease of the system's efficiency. The sudden and sharp increase of temperature due to latent heat release contradicts with the PCM goal to reduce sharp energy

demand variation. This phenomenon, if not taken into consideration, can cause severe effects on the PCM performance.

4 Factors affecting supercooling

Generally, the presence of chaotic and unexpected supercooling in an application is not recommended. Handling and controlling this phenomenon requires a good knowledge of the factors responsible for its presence. Precisely knowing the role of each factor and of the PCM behavior with their variations is essential to understand the basis of supercooling control. Controlling supercooling can be either increasing the degree of supercooling if its presence is desired, or decreasing it as much as possible if not. In this section, a number of important factors that have a direct responsibility in changing the degree of supercooling is presented.

4.1 Volume of the liquid PCM

The dimensions of the PCM container have a direct influence on the degree of supercooling, where a decrease in the sample's volume generally increases the degree of supercooling. Figure 13 shows the results obtained by Adachi *et al.* [44] of the experiments done on 99% pure Erythritol. The results reveal that decreasing the PCM container's volume from 16cm^3 to 0.025cm^3 increases the degree of supercooling of erythritol from 48K to 88K. As the volume of the container decreases, the solidification initiation shifts toward the surface of the container. In this way, the influence of suspended impurities in the PCM on the solidification initiation decreases compared to the influence of the container's wall. Similarly, the supercooling in metals is influenced by volume change, where a change from mm^3 to µm^3 scale may increase the degree by a factor of 3 [45]. Dumas *et al.* [46] found an increase of the supercooling degree in benzene from 19.5K to 71.5K when the volume decreased from 1cm^3 to few cubic micrometers. The same influence is observed for organic bodies [46]. Lafargue *et al.* [47] found crystallizations at a temperature of -40.5°C and -14°C for a water container of a few cubic micrometers and 10mm^3 respectively.

Conversely, when the supercooling effect is required, the use of a single volume of high dimensions should be avoided, especially in applications that seek longer-term storage. Indeed, such a volume has many germination sites, which facilitates crystallization and risks releasing all of the stored energy as soon as crystallization initiates. It then becomes necessary to compartmentalize the storage. Chen S.L. and Chen C.L. [48] studied the probability of crystallization per sample. They found that with a larger size sample, the probability of crystallization increases. The best solutions in this area remain the encapsulation or emulsion processes, where the material is divided into microscopic portions serving in increasing the heat exchange surface and improving heat exchange. Each capsule then has a reduced number of impurities, which limits solidification and accentuates the degree of supercooling.

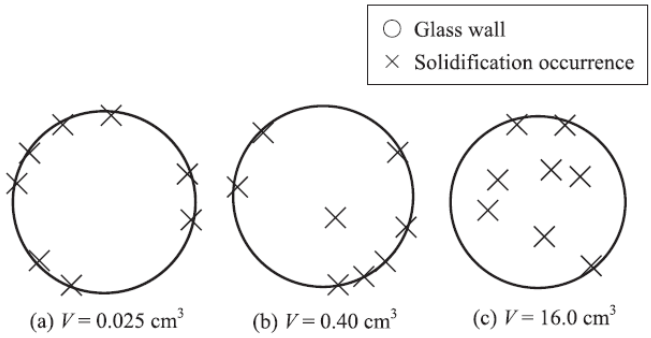

Figure 13 The position of solidification initiation for three different volumes having a measured degree of supercooling for the same PCM of a) 88°C, b) 58°C and c) 48°C [44]

When the mass of material is sufficiently low, a new phenomenon may appear, in particular during imposed thermal cycles. Due to the low number of impurities, crystallization is not possible until reaching a very low temperature corresponding to a very high degree of supercooling. However, the lower temperature of the sample also increases its viscosity, until it evolves into an amorphous solid. It is then necessary to wait until the material is heated again to allow the release of the stored energy. This phenomenon is called cold crystallization**.** Nakano *et al.* [49] finds that at a cooling rate of 1K/min of erythritol, the crystallization of 4.5g is possible at around 24°C while a mass of 3.5g remains supercooled till -50°C and doesn't crystallize until the temperature rises to -14°C approximately.

4.2 Rate of cooling

The rate of cooling directly affects the degree of supercooling on one hand, and the time spent in supercooling state on the other hand. Taylor *et al.* [50] conducted an experiment on commercial hydrated calcium chloride salts known as PC25 and PC29. As shown in Figure 14a, the degree of supercooling increases with the increase of the cooling rate. The cooling rate corresponds to the slope of the curves in Figure 14b before reaching the melting temperature and entering supercooling. So, as the bath temperature decreases, the cooling rate increases and the degree of supercooling increases too. Figure 14b confirms the observation of Figure 14a, where an increase in the degree of supercooling is observed for samples cooled with higher rates. It can be seen that the minimum temperature, reached before the initiation of solidification, decreases as the cooling rate increases. The figure also shows that the nucleation is delayed as the cooling rate decreases that is the PCM remains in supercooled state for a longer period. For example, the crystallization of samples cooled by 0°C and 20°C baths, corresponding to cooling rates of 166.3°C/min and 31°C/min respectively, is delayed for about 100s and 1400s respectively. In other words, this figure shows that decreasing the cooling rate decreases the degree of supercooling and delays nucleation initiation. This result is also observed in the experimental study done by Chen *et al.* [51] on water inside horizontal cylinders. Moreover, holding the PCM at a lower temperature increases the probability of solidification as shown in Figure 14b. This observation is also highlighted in the experiments of Dannemand *et al.* [52] on 10 samples sodium acetate trihydrate, where 73% of the containers remained supercooled at a degree of supercooling $\Delta T = 23K$, while only 42% remained in this metastable state at $\Delta T = 45K$.

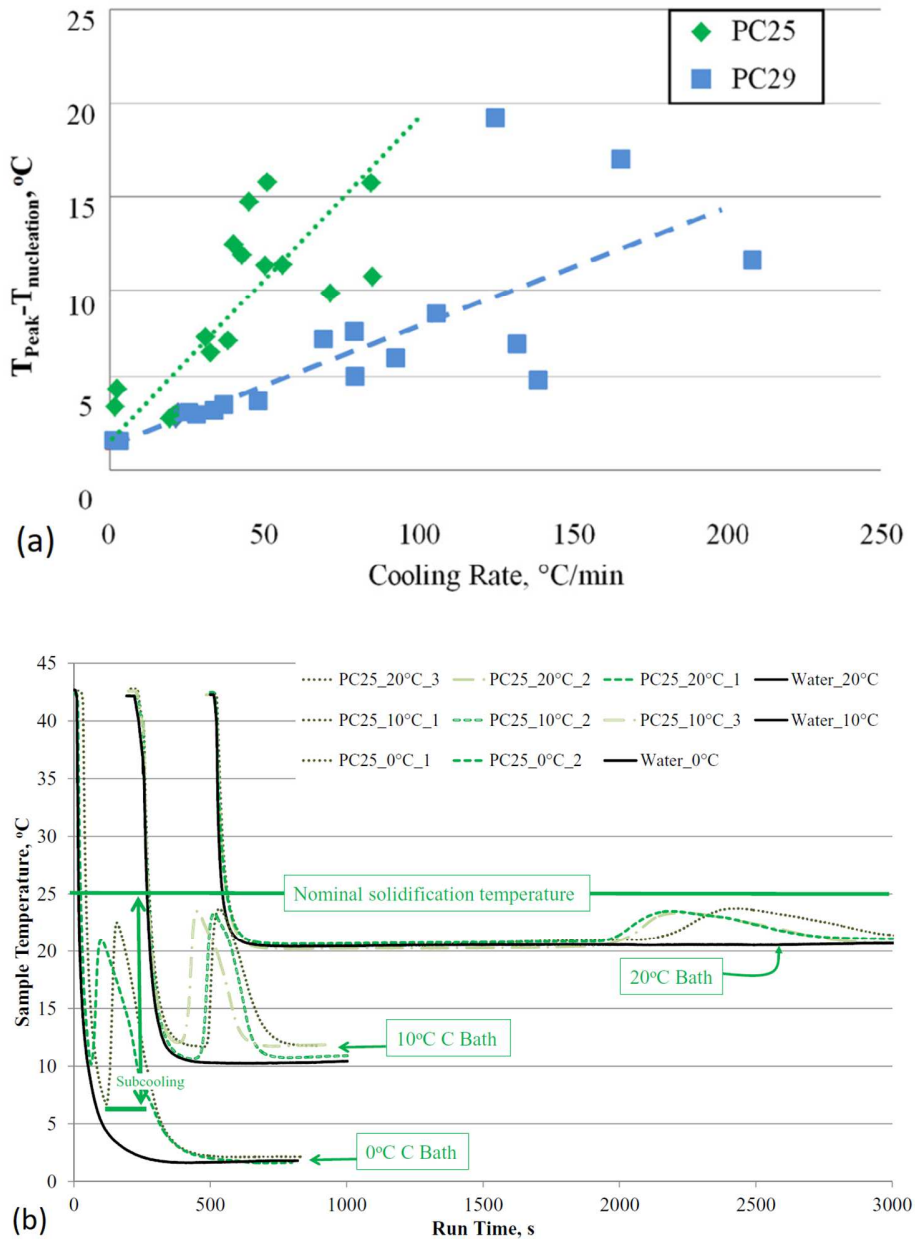

Figure 14 Plots showing (a) the variation of degree of supercooling as a function of cooling rate, (b) instantaneous temperature for PCM cooled in different bath temperatures [50]

The effect of coolant temperature and capsule's material on the probability of nucleation of encapsulated water is shown in Figure 15 [39]. The capsule material is represented by its thermal conductivity and roughness. By comparing the cases having similar surface roughness, the plot shows that the probability of nucleation decreases with decreasing cooling rate and with lower thermal conductivity materials. In other words, to reduce supercooling in an application having low cooling rate recommends using materials having high thermal conductivity. The cooling rate is also dependent on the surface of heat transfer. There are several passive and active techniques used to enhance the heat transfer rate [53]. An example

of passive technique is adding fins to increase the heat transfer area. On the other hand, adding a certain percentage of additives can also increase the thermal conductivity of a PCM as reported by Kant *et al.* [54]. Asgari *et al.* [55] studied the effect of fin structure and thickness on the heat transfer rate in addition to using nanoparticles. They showed that thin branch-shaped fins and nanoparticles with 0.04 volume fraction help in increasing contact surface area and thus the heat transfer rate.

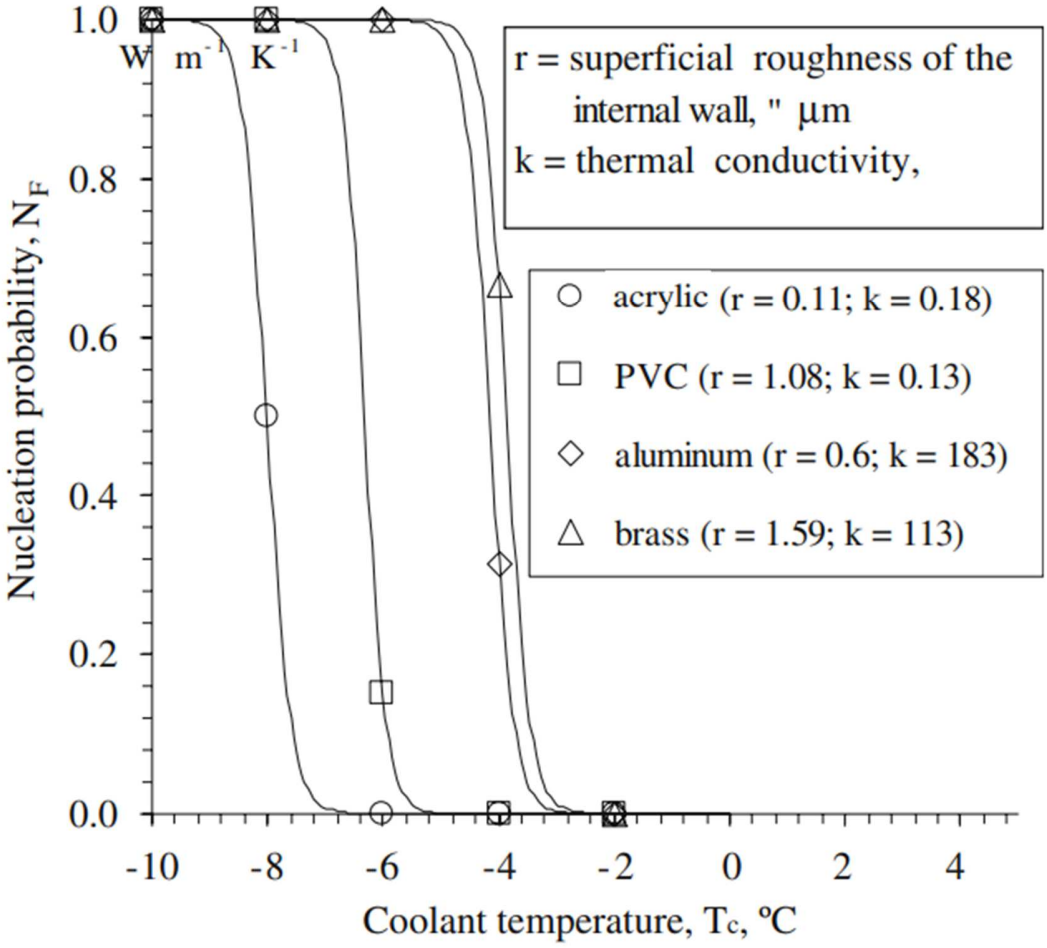

Figure 15 Variation of nucleation probability as a function of cooling temperature for materials with different thermal conductivities and various roughness of the internal wall [39]

From Figure 10, the cooling rate, CR, can be obtained by evaluating the temperature variation of capsule's internal wall T_{Iw}, from the beginning until the end of supercooling or by dividing the degree of supercooling, ΔT_S, by the duration of supercooling, t_s, [39]:

$$CR = \frac{\sum_{i=1}^{n} CR_i}{n} = \frac{\sum_{i=1}^{n} \frac{((T_{Iw})_i - (T_{Iw})_{i-1})}{t_s}}{n} \quad (1)$$

$$CR = \frac{\Delta T_S}{t_s}$$

where i is the index of the measurement and n is the total number of measurements.

Figure 16 shows the time spent in supercooled state for four different containers. Regardless the thermal conductivity and wall roughness of the container, Guzman *et al.* [39] obtained the same results as Taylor *et al.* [50] concerning the supercooling period: the time spent in supercooled state increases as the cooling rate decreases. As the rate of cooling increases, it becomes dominant over other factors, where the graph becomes confined.

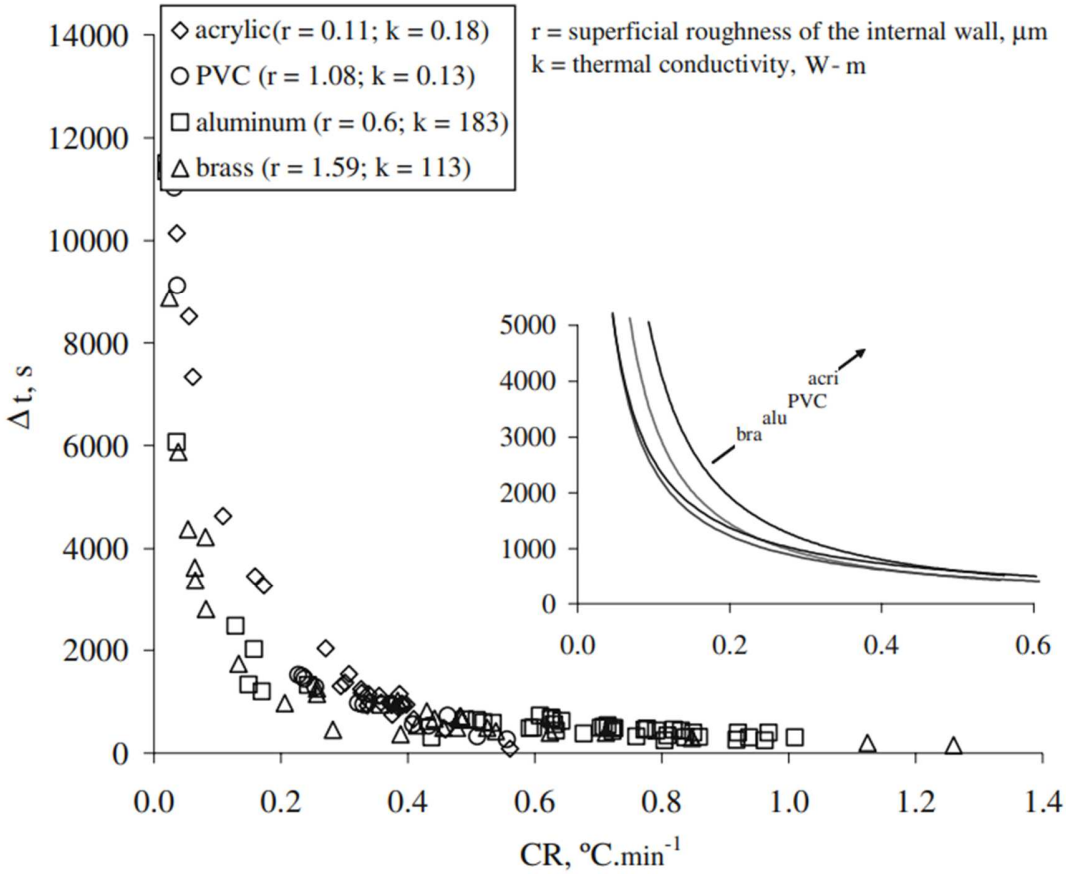

Figure 16 Time spent in supercooling state for different materials as a function of cooling rate. r is the container surface roughness and k is the thermal conductivity [39]

4.3 Thermal history of the PCM

The degree of supercooling is directly affected by the PCM history which has an impact on crystal growth, nucleation and their properties [56]. This dependence can be illustrated as a relationship between the degree of supercooling and the degree of over-heating (ΔT_h). The degree of superheating is given by $\Delta T_h = T_{PCM} - T_m$. This relationship has been studied for different (semi)metals (Sn, Bi, Ga) [47] and alloys [57]. Figure 17a shows this relation, where the degree of supercooling changes sharply beyond a certain value of degree of superheating. In a

molten metal, the imbedded impurities may stay in solid clusters. Heating the melt above a critical temperature, will lead to the melting of these impurities and change their structure later. In addition to that, metals tend to change their physical properties depending on their thermal history and temperature variation. For example, Rudolph *et al.* [58] show that the degree of supercooling changes according to the time spent by the PCM at molten phase as shown in Figure 17b . In addition to the before mentioned effect, Mei and Li [59] results show a significantly reduced melting temperature of Al encapsulated in Al_2O_3 after several cooling-heating cycles.

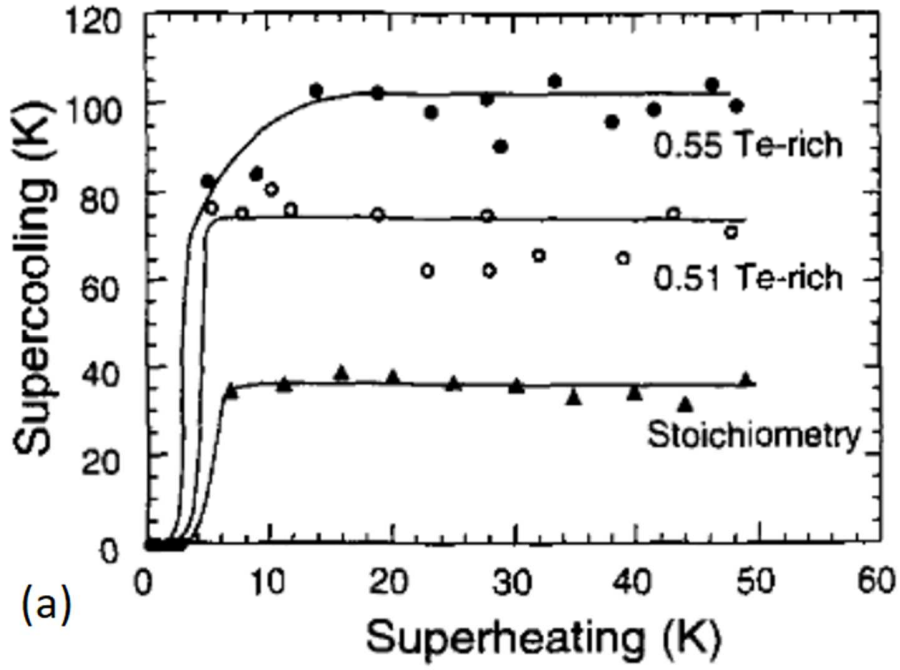

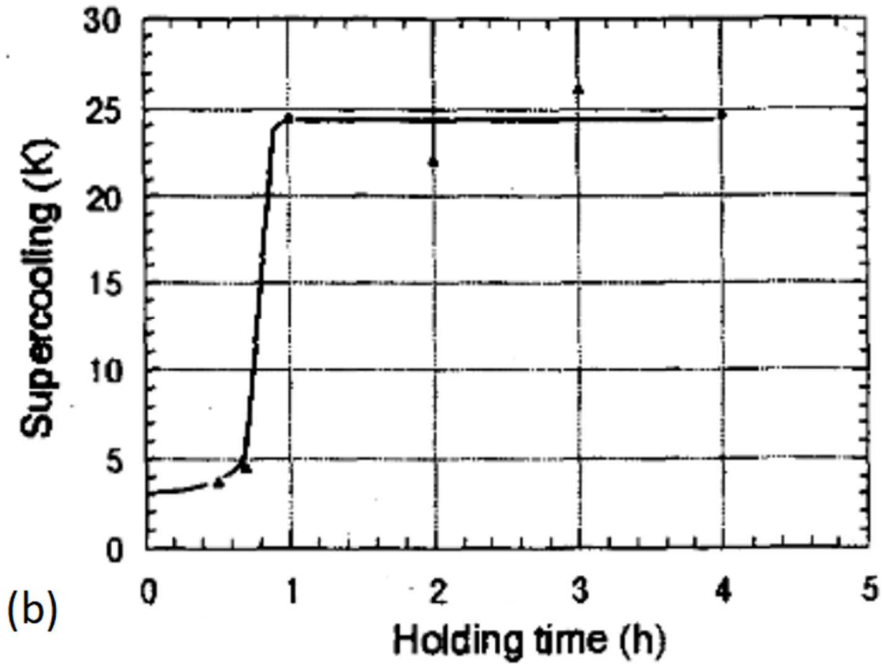

Figure 17 Variation of the degree of supercooling as a function of (a) degree of superheating of CdTe for stoichiometric, 1% and 5% excess mole fraction of Te, (b) holding time at 10°C superheated state of stoichiometric CdTe [58]

Fatty acids are known for their low degree of supercooling and large applications in different heat storage systems. Fatty acids have a threshold temperature above which if heated and held for a given time, the alkyl chain becomes more mobile and the molecular clusters break apart [60]. Upon cooling, the clusters do not reform quickly causing a barrier to nucleation that leads to supercooling. The obtained results by Noël *et al.* [60] are in agreement with those of Rudolph *et al.* [58] and show the significant difference in the degree of supercooling between samples heated above the threshold temperature and others that are not. Figure 18 shows the influence of holding dodecanoic acid at a temperature above its melting temperature. The figure shows that, as the difference between the holding temperature and the melting temperature increases, the degree of supercooling increases too. For a 125°C holding temperature, a dramatic change in the degree of supercooling is observed, which approximately corresponds to the above mentioned threshold temperature. Similarly, the probability of crystallization of emulsions varies with the number of cooling-heating cycles [61], [62].

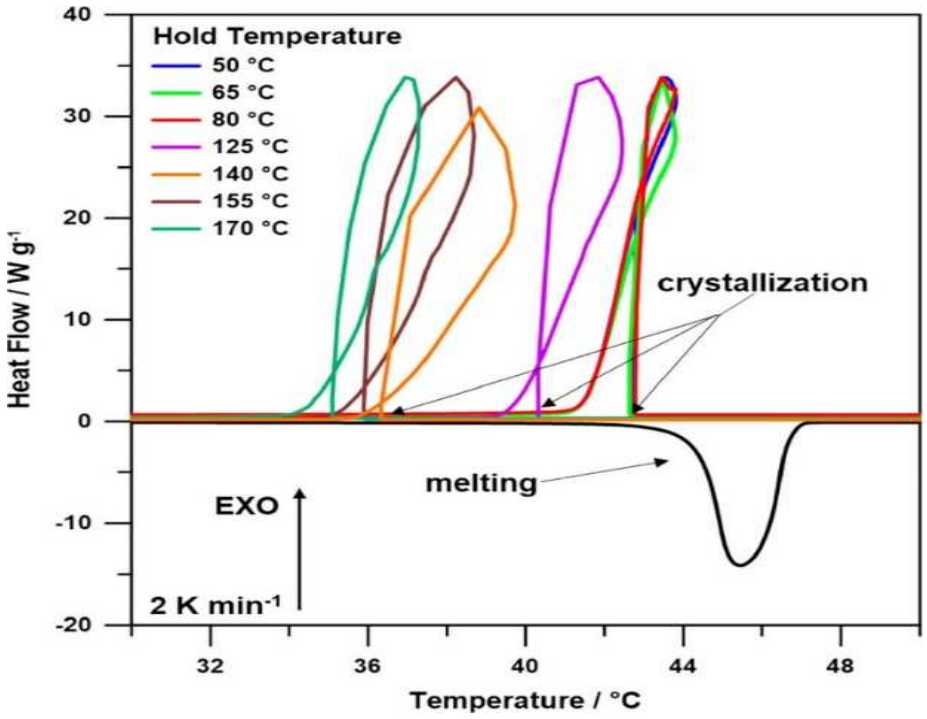

Figure 18 Thermal cycling of dodecanoic acid [60]

For the case of salt hydrates, Wada *et al.* [63]–[65] performed studies on sodium acetate trihydrate (SAT), by investigating its thermal stability after several cooling-heating cycles. SAT has a melting temperature of 58°C and is used in solar heating systems. SAT can undergo stable supercooling if extra heat is needed. The problem comes from the phase separation during supercooling and the probability of solidification of the supercooled SAT. Indeed, melting phase separation can affect the solubility, volume and density, which in turn may cause a change in the thermal conductivity, heat transfer rate and the amount of latent heat available for the next cycle. Some solutions consist of adding excessive water, thickening agents or mixing. However, although adding water or thickening agents is helpful, attention should be given to the functioning range of the system and the change in the properties of the SAT solution, such as melting temperature, density and thermal conductivity. After each thermal cycle, part of SAT solidifies and precipitates, which also eventually leads to a change in the properties. In [63]–[65], the probability of solidification decreased to zero upon heating above 80°C, due to the melting of the entire precipitated solid. Similar results are obtained by Fashandi and Leung [66], where heating the encapsulated SAT in nanocapsules above 70°C causes a significant increase of the supercooling degree as shown in Figure 19. In addition, the use of sodium dodecyl (SDS) as a thickening agent decreases the degree of supercooling to almost zero as shown in Figure 20. Furthermore, the particle size of the SAT powder used to prepare the solution also has an effect on the degree of supercooling as shown in Figure 21. The increase of the particle size interferes in increasing the degree of supercooling. This may be explained by a change in the solution homogeneity and by a phenomenon called sifting due to the phase segregation of the solution. Thus, heating history can play a role in changing the initial properties of the used PCM by changing size and structure of additives, thickening agents or impurities.

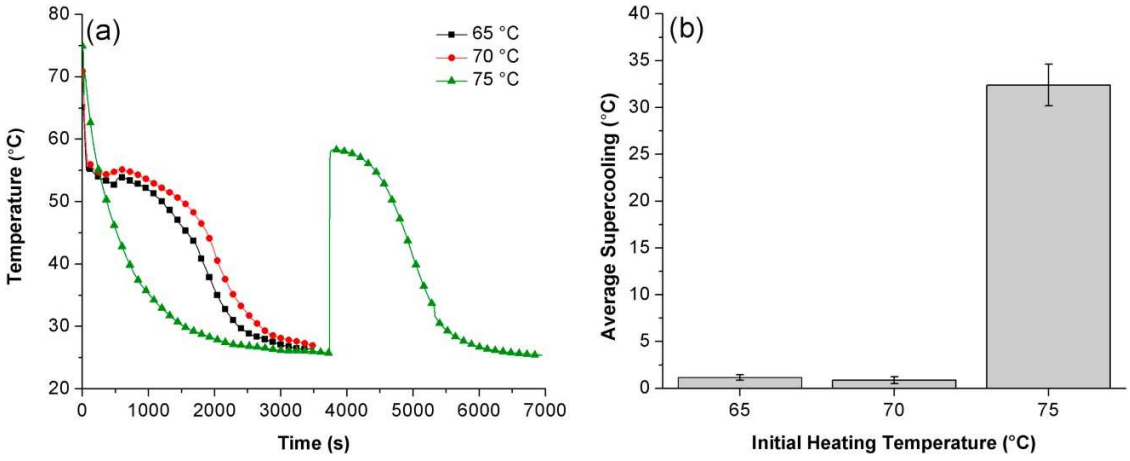

Figure 19 Effect of preheating a) on the temperature variation as function of time during cooling and b) on the degree of supercooling [66]

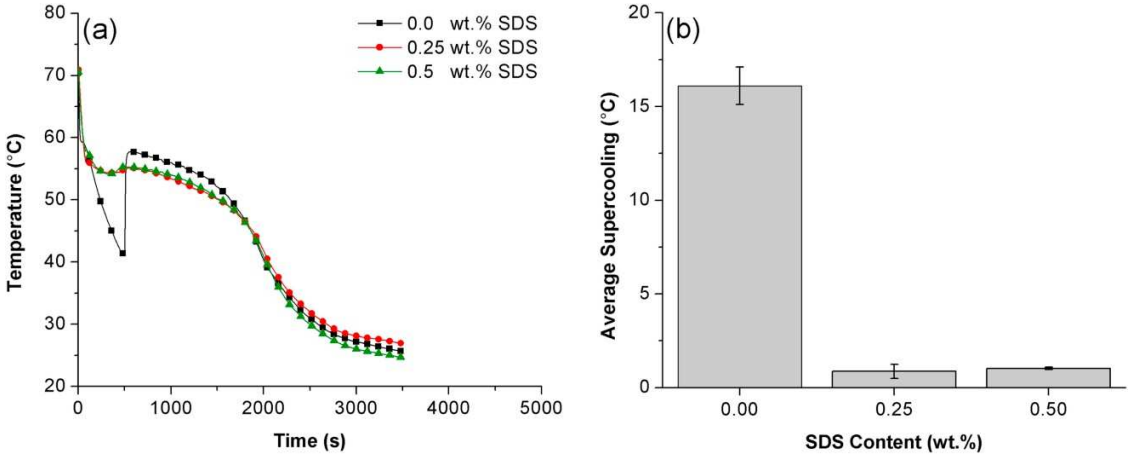

Figure 20 Effect of percentage of thickening agent a) on the temperature variation as function of time during cooling and b) on the degree of supercooling [66]

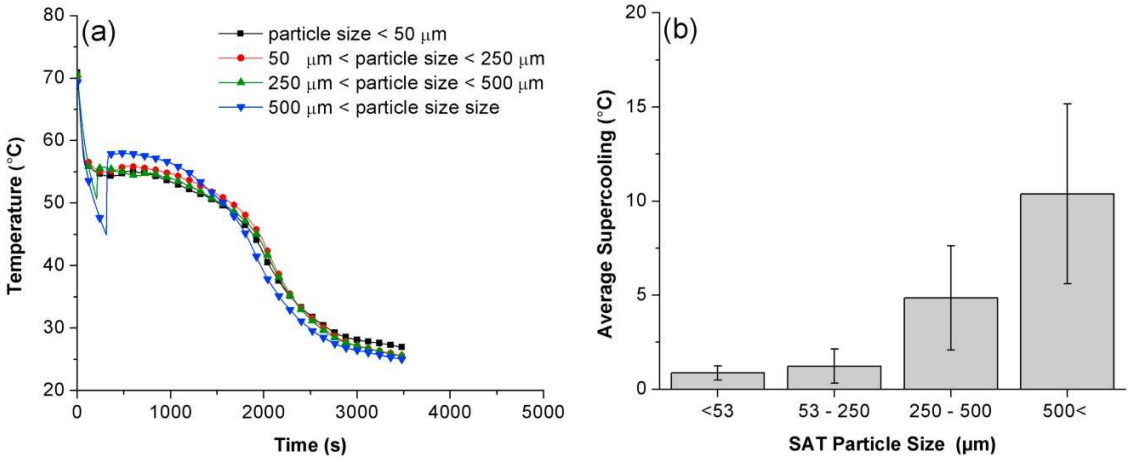

Figure 21 Effect of particle size a) on the temperature variation as function of time during cooling and b) on the degree of supercooling [66]

The threshold temperature may also vary with respect to the history of the PCM. Johansen [67] also supposes that this is due to a decrease in the number of potential germination sites or to phase separation due density difference. In Wada's study mentioned above [63]–[65], a zero probability of nucleation is achieved by heating up to 80°C a sample kept 30 minutes at 20°C, while a sample left for 96 hours at 20°C requires heating up to 93°C. However, beyond this time, this threshold temperature remains constant. On the other hand, cooling the solid to -20°C for 96 hours requires a reheat to 83°C.

4.4 Roughness of contact surfaces

The degree of supercooling is directly affected by the surface roughness of the container that embraces the PCM. Rough surfaces are a factor in lowering and even eliminating supercooling [68] because the surfaces trigger the initiation of solidification. This direct impact can be observed using several techniques. The first technique is introducing the PCM in a very smooth container and scratching one of its sides. The second technique is performing the same experiment on a number of identical samples contained in containers of different roughness. The degree of supercooling is lower in the case of more rough surfaces. Below are couple of experiments performed on different PCM.

According to Faucheux *et al.* [69], the degree of supercooling of aqueous solution of ethanol decreases when changing the surface roughness of aluminum tubes from 0.63µm to 13.3µm. The used container has rough walls while the bottom has a smooth glassy poly (methyl methacrylate), PMMA. In all the experiments, the crystallization initiated from the container's rough surface rather than the smooth bottom. In this study, a correlation between the degree of supercooling and the surface roughness is demonstrated by the aid of the free energy variation equation and the conditions to permit nucleation and then phase change. This correlation is given by equation (2) [69]:

$$\Delta T_S = \sqrt{\frac{8\pi\gamma^3 T_m^2}{3H^2\Delta G_n}\left(1 - cos\frac{\alpha}{2}\right)} = aRa^b \qquad (2)$$

where γ is the surface tension, ΔG_n is the free energy variation and α is the angle of notch where crystallization takes place. H is the latent heat and Ra is the surface roughness. a and b are constant coefficients, obtained from experimental results by least square optimization [69]:

$$\Delta T_S = 7.15 Ra^{-0.196} \quad (3)$$

Similar results are reached by Sakurai *et al.* [70] for silver electrode embedded with SAT crystals and immersed in a supercooled SAT. In this experiment, low values of roughness of Ag anode leads to stability of the supercooled solution of SAT, while a higher surface roughness leads to a larger number of repeated cycles of electrical nucleation allowing the controlled release of latent heat.

Akio *et al.* [71] studied supercooling in water. In the first experiment, one side of the smooth container is scratched and as a result, crystallization is first formed on this rough scratched surface. In the second study, water contained in rough surfaces containers experience a lower degree of supercooling.

4.5 Additives

Nucleation is a spontaneous process that requires energy to solidify the liquid phase on its surface. The free energy volume, that is proportional to the heat released by crystallization, and surface energy are two components in competition forming a barrier between the liquid and crystallization. There are two types of nucleation: homogeneous and heterogeneous. In the homogeneous nucleation, the impurities have no impact on the nucleation process, which happens suddenly by generating crystal nuclei. On the other hand, the presence of any impurity or contact surface with the liquid play a role in triggering the nucleation process. This latter phenomenon is called heterogeneous nucleation.

The surface of nucleation is not limited to the surface of the container. Impurities embedded in the solution are also surfaces for nucleation. In this case, the role of nucleating agent additives becomes more obvious in increasing the nucleation probability, where additives increase the area of nucleating surfaces with the PCM. Chen *et al.* [51] confirmed the before mentioned researches by experiments done on water. Their results show that additives with higher surface roughness had a greater effect in decreasing degree of supercooling.

As mentioned in subsection 4.4, the contact surfaces with the PCM motivate crystallization. Any impurity present in the PCM reduces the required free energy surface and can be a surface for crystallization onset. From this concept, additives are chosen with a melting point higher than that of the PCM to ensure that they are solid during the phase change interval. Fashandi and Leung [66] studied the supercooling of SAT. In their study, a bio-derived nucleating agent called Chitin nanowhisker is added to the SAT contained in nanocapsules. The addition of nucleating agent affects significantly the degree of supercooling as shown in Figure 22a. The sample with no nucleating agent suffers from a severe degree of supercooling and does not solidify. However, the addition of the additive triggers solidification. First, the degree of supercooling decreases as percentage of additive increases to a given value after which it starts to increase again. The estimated value, at which the supercooling degree reaches the minimum value, is 1%

as shown in Figure 22b. This is most probably due to the gathering of the additive particles, which leads to a decrease in the density of nucleation sites.

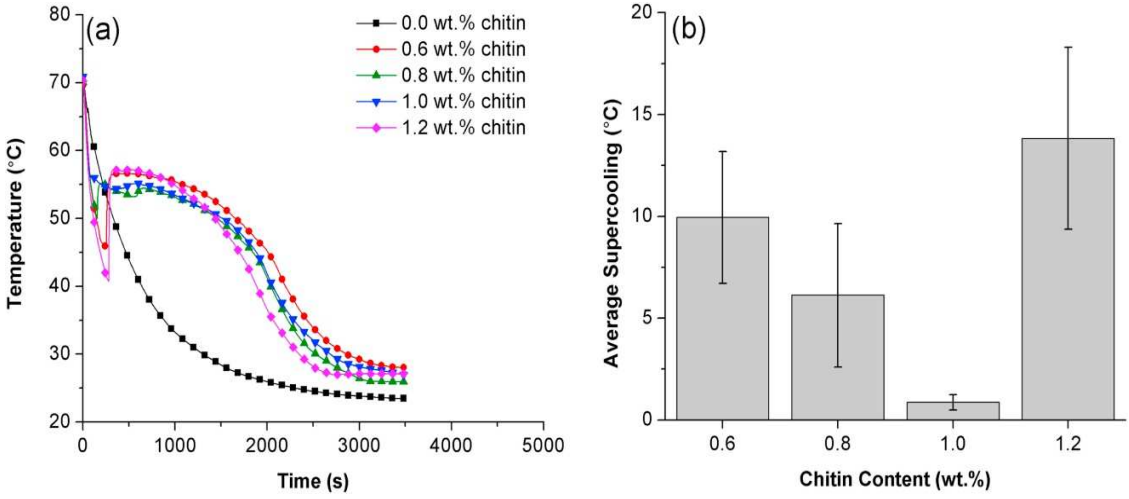

Figure 22 Effect of the percentage of nucleating agent a) on the temperature variation as function of time during cooling and b) on the degree of supercooling [66]

Shamberger *et al.* [72] added $Cu_3(OH)_5(NO_3)\cdot 2(H_2O)$ as an additive to decrease the degree of supercooling of $LiNO_3\cdot 3H_2O$. The addition of additive decreased the degree of supercooling by up to 66%. On the other hand, it increased the stability of $LiNO_3\cdot 3H_2O$ for more than 900 phase change cycles and increased the aging at elevated temperature for extended periods of time (t > 250 days). Chen *et al.* [48] studied, for different cooling rates, the effect of nucleation agents by using several types of additives such as lead iodide, mud powder, silver iodide and river sand. A significantly lower degree of supercooling is noted for water with additives in comparison with pure water. Silver iodide shows an attractive performance while sand is the most recommended for its cheap price. Crystal mesh size variation of the additives must be 15% less than that of PCM to be crystallized [69,70]. This result has been the scope of work of many studies. Lane *et al.* [75], for example, studied the nucleating agents of several materials that distinguish them into isostructural materials or not. These studies report the difficulty to define the type and amount of the nucleating agent to be added to a specific PCM. Crystallization is not dependent only on these agents, and studying under all circumstances is time consuming. The most used variable is the nucleating agent-PCM mass fraction. Beaupere *et al.* [11] presented the results of several PCM nucleating agents' effectiveness in Figure 23. Similar to other conclusions, the best percentage to use is about 1%. This result is the average obtained by several researchers as shown in Table 2.

Table 2 Set of experiments showing the effect of different additives on the degree of supercooling (ΔT_s) and on the latent heat of fusion (H) for different PCM

Author (year)	PCM	Additives	Results
Hu *et al.* [76] (2011)	Sodium acetate trihydrate	Nothing added	$T_m = 58\ °C$ $\Delta T_s = 17\ °C$ $H = 238.54\ kJ/kg$

		AlN nanoparticles	3 wt%	$\Delta T_s = 2.4\ °C$
		CMC*	4 wt%	
		AlN nanoparticles	4 wt%	$\Delta T_s = 1\ °C$
		CMC	4 wt%	
		AlN nanoparticles	5 wt%	$T_m = 52.5\ °C$ $\Delta T_s = 0\ °C$ $H = 227.54\ kJ/kg$
		CMC	4 wt%	
Li *et al.* [77] (2016)	$CH_3COONa{\cdot}3H_2O$	Nothing added		$T_m = 58\ °C$ $\Delta T_s = 28.3\ °C$
	$CH_3COONa{\cdot}3H_2O$–2%KCl			$T_m = 54\ °C$ $\Delta T_s = 9.2\ °C$
	$CH_3COONa{\cdot}3H_2O$–4%KCl			$T_m = 53\ °C$ $\Delta T_s = 3.5\ °C$
	$CH_3COONa{\cdot}3H_2O$–6%KCl			$T_m = 52\ °C$ $\Delta T_s = 3.1\ °C$
	$CH_3COONa{\cdot}3H_2O$–8%KCl			$T_m = 50\ °C$ $\Delta T_s = 7.1\ °C$
	$CH_3COONa{\cdot}3H_2O$–10%KCl			$T_m = 50\ °C$ $\Delta T_s = 9\ °C$
	$CH_3COONa{\cdot}3H_2O$–8%KCl	Nucleating agent: Al_2O_3 nanoparticles and 4 wt% CMC	0.5%	$\Delta T_s = 3..5\ °C$
			1%	$\Delta T_s = 0.1\ °C$
			2%	$\Delta T_s = 2.3\ °C$
			2.5%	$\Delta T_s = 4.6\ °C$
			3%	$\Delta T_s = 5.3\ °C$
Pilar *et al.* [78] (2012)	MgCl2·6H2O	Nothing added		$\Delta T_s = 36.8\ °C$ $H = 168.9\ kJ/kg$
		$SrCO_3$	0.5 wt%	$\Delta T_s = 14.2\ °C$ $H = 159.7\ kJ/kg$
			1 wt%	$\Delta T_s = 6.4\ °C$ $H = 157.7\ kJ/kg$
			2 wt%	$\Delta T_s = 1.8\ °C$ $H = 112.3\ kJ/kg$
			3 wt%	$\Delta T_s = 1.2\ °C$ $H = 100\ kJ/kg$
		$Sr(OH)_2$	0.5 wt%	$\Delta T_s = 4.3\ °C$ $H = 149.4\ kJ/kg$
			1 wt%	$\Delta T_s = 5.2\ °C$ $H = 150.9\ kJ/kg$
			2 wt%	$\Delta T_s = 0.1\ °C$ $H = 111.4\ kJ/kg$
			3 wt%	$\Delta T_s = 0\ °C$ $H = 94.4\ kJ/kg$
		$Mg(OH)_2$	0.5 wt%	$\Delta T_s = 18.9\ °C$ $H = 160.1\ kJ/kg$

			1 wt%	$\Delta T_s = 18.9\ °C$ $H = 143.6\ kJ/kg$
			2 wt%	$\Delta T_s = 14.8\ °C$ $H = 102.4\ kJ/kg$
			3 wt%	$\Delta T_s = 16\ °C$ $H = 108.2\ kJ/kg$
Ushak *et al.* [79] (2016)	bischofite	Nothing added		$\Delta T_s = 36\ ℃$ $H = 115.5\ kJ/kg$
		CaO	0.5 wt%	$\Delta T_s = 16.3\ °C$ $H = 95.3\ kJ/kg$
			1 wt%	$\Delta T_s = 19.9\ °C$ $H = 57\ kJ/kg$
			1.5 wt%	$\Delta T_s = 21.4\ °C$ $H = 50.8\ kJ/kg$
			2 wt%	$\Delta T_s = 20.4\ °C$ $H = 46.6\ kJ/kg$
			3 wt%	$\Delta T_s = 11\ °C$ $H = 28.5\ kJ/kg$
		$Sr(OH)_2$	0.5 wt%	$\Delta T_s = 18.2\ °C$ $H = 104.4\ kJ/kg$
			1 wt%	$\Delta T_s = 2.9\ °C$ $H = 36.6\ kJ/kg$
			1.5 wt%	$\Delta T_s = 20.4\ °C$ $H = 73.1\ kJ/kg$
			2 wt%	$\Delta T_s = 18.7\ °C$ $H = 78.6\ kJ/kg$
			3 wt%	$\Delta T_s = 0\ °C$ $H = 71.1 kJ/kg$
		$SrCO_3$	0.5 wt%	$\Delta T_s = 23.7\ °C$ $H = 118.8\ kJ/kg$
			1 wt%	$\Delta T_s = 22.4\ °C$ $H = 106.8\ kJ/kg$
			1.5 wt%	$\Delta T_s = 15.7\ °C$ $H = 92.3\ kJ/kg$
			2 wt%	$\Delta T_s = 5.51\ °C$ $H = 94.5\ kJ/kg$
			3 wt%	$\Delta T_s = 1.7\ °C$ $H = 89.3\ kJ/kg$
		$LiOH.H_2O$	0.5 wt%	$\Delta T_s = 24.2\ °C$ $H = 99.7\ kJ/kg$
			1 wt%	$\Delta T_s = 18\ °C$ $H = 84.9\ kJ/kg$
			1.5 wt%	$\Delta T_s = 21.9\ °C$ $H = 82.7\ kJ/kg$
			2 wt%	$\Delta T_s = 23.6\ °C$ $H = 85.6\ kJ/kg$
			3 wt%	$\Delta T_s = 18.3\ °C$ $H = 63.5\ kJ/kg$

		Li_2CO_3	0.5 wt%	$\Delta T_s = 27.8\ °C$ $H = 85.9\ kJ/kg$
			1 wt%	$\Delta T_s = 18.8\ °C$ $H = 76.3\ kJ/kg$
			1.5 wt%	$\Delta T_s = 22\ °C$ $H = 76.3\ kJ/kg$
			2 wt%	$\Delta T_s = 19.1\ °C$ $H = 64.1\ kJ/kg$
			3 wt%	$\Delta T_s = 25.6\ °C$ $H = 59.9\ kJ/kg$
Sutjahja *et al.* [80] (2016)	$CaCl_2.6H_2O$	Nothing added		$\Delta T_s = 1.8\ °C$ $Induction\ time^* = 178\ min$
		$SrCl_2.6H_2O$ (1 wt%)		$\Delta T_s = 0.3\ °C$ $Induction\ time = 19\ min$
		$BaCO_3$ (0.5 wt%)		$\Delta T_s = 0.95\ °C$ $Induction\ time = 50\ min$
		K_2CO_3 (0.5 wt%)		$\Delta T_s = 0.92\ °C$ $Induction\ time = 107\ min$

* CMC: Thickener: Carboxyl methyl cellulose

* Induction time is the time required for temperature to rise from nucleation temperature to melting temperature due to latent heat release and initiation of solidification

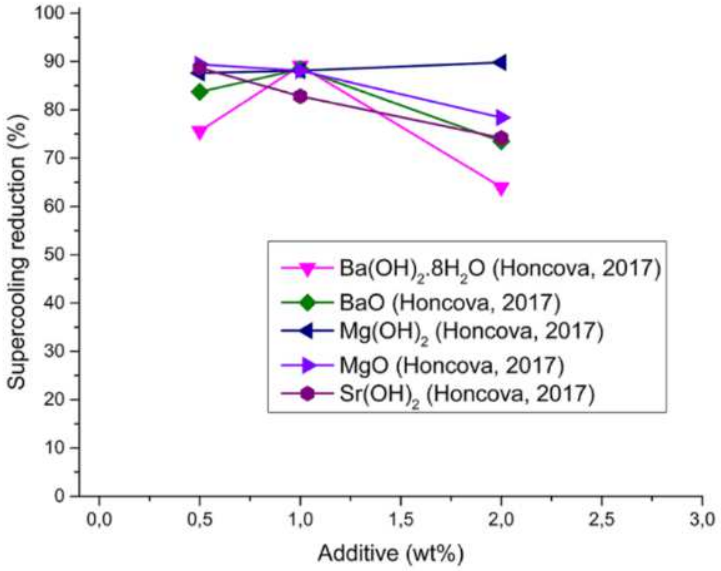

Figure 23 Percentage of supercooling reduction as function of several additives percentage [11]

In a PCM application, using the appropriate concentrations of nucleating agents is an effective method used to reduce or even eliminate supercooling along with triggering crystallization in a shorter period. In the study of Liu *et al.* [81] on a nanofluid, the degree is reduced by 69.1% and nucleation time is shortened by 90.7%.

The above subsections present the main factors that contribute to change the behavior of a supercooling prone PCM. These factors are considered of great importance because they appear in almost all applications, experiments and even create problems in modeling the PCM behavior with supercooling. Table 3 summarizes these factors by presenting the results of a number of experiments performed on different types of PCM. It is worth noting that there are plenty other factors that interfere in influencing supercooling such as stirring, magnetic field, electric field, mechanical vibrations or shocks. These factors are not mentioned in this paper, but more details can be found in [12].

Table 3 Summary of major experimental results on supercooling over the past 50 years

Author (Year)	Body/material	Method/measuring technique	Results
Packard *et al.* [17] (2001)	Turtles	Statistical analysis: Factorial analysis of variance (ANOVA)	Lower ambient temperatures improve the capacity for supercooling of acclimated turtles, the ingestion of particle of soil (as nucleating agents) may reduce the degree of supercooling.
Scholander *et al.* [18] (1971)	Fish	Thermometer	- Supercooling serves in the survival of the fish. - Ice formation can be triggered by contact with a freezing surface.
Hacker *et al.* [20]	Plants	Infrared thermography	- Ice formation is triggered by reaching minimum temperature and is affected by the duration of supercooling state. - Only the plants in supercooled state survived, where plants use hydrophobic barrier to prevent nucleation in its sensitive parts.
Wisniewski *et al.* [25] (2008)			
Fakuma *et al.* [29] (2012)	Fish meat	- Statistical analysis: one-way ANOVA - Measuring and analysis tools	- Fish meat achieves supercooling state by slow cooling due to insufficient kinetic energy necessary for the formation of ice nuclei.
Ando *et al.* [31] (2007)			
You *et al.* [30] (2020)	Beefsteak		- Beef steak achieves supercooling by pulsed electric field (PEF) and oscillating magnetic field (OMF).
Jeremiah *et al.* [27] (2001)	Muscle steak	- Low-temperature incubators - Temperature data loggers - pH meter	- Stability of supercooling varies according to the material to be conserved. - Instability of supercooled state: any shock can trigger solidification. - Storing at refrigeration and freezing temperatures shows very rapid muscle deterioration, which causes softening.

Duun *et al.* [32] (2008)	Fillet salmon	- Reflectance spectrophotometry	- Storing in supercooled state shows similar color, odor, drip loss and shear as fresh food. - Storing in supercooled state provides better quality (hardness) and increases storage life by limiting bacterial growth. - Drip loss is recorded during supercooling but it is not considered as a disadvantage. - Recommendations to use supercooling in preservation
James *et al.* [33] (2009) [17] (2011)	Garlic vegetables Sea food		
Yehya [37] (2015)	Paraffin based, organic 99% pure octadecane	Thermocouples, probes and meters	- Supercooling causes a vertical discontinuity in the temperature curve. - Increasing the cooling rates causes a higher degree of supercooling, however PCM stays in supercooled state for a shorter time. - Increasing the thermal conductivity increases the probability of nucleation. - Quantity of energy, needed to increase liquid's temperature to melting temperature, increases with the increase of supercooling degree.
Guzman et. al [39] (2005)	water		
Sandnes *et al.* [40] (2006)	Salt hydrates - Disodium hydrogen phosphate - Dodecahydrate sodium acetate trihydrate -STL-47		
Adachi *et al.* [44] (2014)	Organic 99% pure Erythritol	Differential scanning calorimetry (DSC) used to calculate latent heat and melting temperature	Time spent in supercooled state decreases as: - cooling rate increases - volume of container increases As the volume of the container decreases, solidification initiates from surface of container rather than impurities embedded in liquid. Probability of nucleation increases as: - cooling rate increases - the volume container increases - the roughness of contact of surfaces increases Degree of supercooling decreases with: - decreasing the cooling rate - increasing the surface roughness
Chen *et al.* a)[51] (1998) b)[82] (1998)	Pure degasified water a) horizontal cylinders b) cylindrical capsules	Flow meters and thermocouples	
Taylor *et al.* [50] (2016)	Calcium chloride hexahydrate-based salts PC25 and PC29	-T history method -Distilled water as a reference sample -Temperature measured by NTC thermistors	

Akio *et al.* [71] (1990)	Pure water	Thermocouples	- decreasing the particle size - adding thickening agents - adding additives, maximum reduction is obtained by adding 1% of additives Degree of supercooling increases dramatically by heating above a critical value - Stable supercooling is achieved when coolant temperature is higher than nucleation temperature - Crystallization starts from rough rather than smooth surface
Fashandi and Leung [66]	Inorganic salt hydrate Sodium acetate trihydrate		
Faucheux *et al.* [69] (2006)	Organic Ethanol/water mixture	K-type thermocouples	- Concentration of the mixture has no significant effect on the degree of supercooling compared to roughness factor. - Power relation between the degree of supercooling and roughness is obtained.
Nakano *et al.* [49] (2015)	Organic- sugar alcohol 97% pure meso-Erythritol	Differential scanning calorimetry (DSC)	PCM in and around 2D mesoporous silica shows that as the pore diameter decreased: - amount of latent heat decreased - nucleation temperature increased Influence of thermal history on the behavior of PCM upon cooling and heating Heterogeneity of the solution induces surfaces for crystallization initiation.
Rudolph *et al.* [58] (1996)	Metals CdTe and PbTe	Direct temperature measure	The thermal history represented by the degree and time held at superheating affects: - the quality of the crystals - the crystal growth - degree of supercooling

Yin *et al.* [57] (2004)	Cast nickel-based super alloy M963	-X-ray diffraction measurement -ISM-6301F scanning electron microscope (SEM)	
Yang *et al.* [83] (2014)	Metal Pure Sn	DSC Dielectric measurements	Supercooling degree increases as the cooling rate increases until reaching a critical value of cooling rate after which the supercooling degree starts to decrease strongly depending on the volume of capsule and purity of PCM.
Mei and Li [59] (2016)	Metal Pure Al		Low cooling rate does not affect the supercooling degree.
Noël *et al.* [60] (2018)	Fatty acids - Octanoic acid - Dodecanoic acid - Tridecanoic acid - Hexadecanoic acid		Dependence of degree of supercooling on the degree of superheating, presence of a threshold temperature above which if heated, PCM undergoes significant degree of supercooling.
Zhou *et al.* [84] (2000)	Alloy metal Pure $Bi_{95}Sb_5$	Temperature measurement by thermocouple	Four factors affecting supercooling degree are investigated and listed from more to less important: - cooling rate - degree of superheating - number of cycles - soaking time
Johansen *et al.* [67] (2014)	Inorganic salt hydrate Sodium acetate trihydrate-water mixture	Heat conductivity measurement by Isomet heat transfer analyzer	- Graphite enhances the thermal conductivity of the mixture but does not affect the degree of supercooling. - Use of gelation agent to overcome the problem of phase separation over long periods of cycles. - The used gelation agent (carboxyl methylcellulose CMC) is affected by high temperatures causing its degradation and change in color.
Sakurai *et al.* [70] (2018)	Inorganic salt hydrate Sodium acetate	X-ray photoelectron spectroscopy- XPS	- Increasing the voltage applied to the Ag anodes immersed in the solution, decreases the time spent in supercooling state.

	trihydrate-water mixture	Scanning electron microscopy- SEM	- After 30000 cycles estimated by 10 years, the response to applied voltage becomes faster. - Roughness of the Ag surfaces affects the behavior of solution upon cooling. For a given interval of roughness, the behavior upon cooling is stable for repeated cycles.
Liu *et al.* [81] (2015)	Organic Water-based graphene oxide	Thermostatic water bath and thermocouple	Supercooling degree decreases when adding graphene oxide nano sheets. Structure of the sheet affects the onset of crystallization.

As presented above, it is clear that each factor has a direct impact on the degree of supercooling and this dependency is detailed as a function of each factor separately. However, some correlations exist between them and some factors have a higher impact. As an example, Figure 15 and Figure 16 show that as the thermal conductivity of a material increases, the impact of surface roughness on the probability of nucleation and time spent in supercooled state decreases. Moreover, some factors can affect PCM properties. For example, adding additives can change the thermal conductivity of the solution along with the ratio of the PCM volume compared to total volume, which in turn decreases the latent heat of the solution. When using a PCM, a set of procedures can be taken to control supercooling. These procedures should not prevent the PCM from performing its role. For example, in a thermal energy storage system, the procedures should not change the thermal conductivity, quantity of latent heat or melting temperature to a value outside the acceptable range, whereas in a preservation process, they should not cause a damage for preserved materials. It is essential to follow a combination of several techniques, where tradeoffs are done to obtain the optimal performance in terms of energy saving on one side and economical cost on the other side.

5 Challenges in modeling

Modeling is essential in almost all applications, where a well-modelled system gives fast and more accurate results than experiments. The advantage of modeling is the ability to track, at any time and any position of the model, the change of desired parameters and to apply desired conditions without facing the problem of devices' accuracy and effect of their presence on the system. This particularly suits an application with supercooling occurrence. However, modeling requires an accurate presentation of the system by means of mathematical equations. As previously mentioned, there are plenty of factors affecting supercooling. The correlation of these factors adds complexity and challenges to model this phenomenon, where any change of any factor can dramatically change the performance of the system. A set of theoretical equations exists and has been validated for pure elements, which is not the case for all PCMs used in thermal storage systems. For example, any impurity or surface roughness can play the role of surface for crystallization onset. Moreover, considering all the factors requires time and high computational cost. The following subsections present a set of common challenges that encounter when modeling supercooling and the methods developed by different authors to overcome these challenges.

5.1 Degree of supercooling and nucleation

The determination of crystallization initiation is still an open challenge. As shown above, the behavior of PCM changes for different supercooling degrees, where the crystallization onset depends on several factors and is sensitive to different circumstances. Different techniques are adapted to include the nucleation temperature in the models and simulations. The most used method is to preset the temperature of crystallization. The PCM stays liquid upon cooling until reaching the preset temperature. However, choosing that temperature is also challenging, so the used value is obtained from an experimental result or from the literature. Besides, using accurate values is challenging, because they are affected by several parameters, especially for impure PCMs. Some researches use a mathematical relation between the supercooling degree and the impurity fraction in the solution. To overcome this problem, Yehya [37] performed experimental studies on octadecane as PCM to obtain the real enthalpy curve and supercooling degree. In buildings, octadecane contained in a Plexiglas enclosure is considered as an innovative technique, where the translucency of the PCM provides natural day light. The presence of soluble impurities lowers the melting temperature, widens the melting range and changes the heat flux curve as shown in Figure 24. This phenomenon is referred to as the "melting point depression" and this depression can be calculated according to the following relation [85]:

$$\Delta T_{am} = T_a - T_m = \frac{R T_a^2 X_i}{L_f} \tag{4}$$

where T_a and T_m are the melting temperatures for pure and impure PCM respectively and X_i is the impurity fraction. R is the molar gas constant and L_f is the molar heat of fusion.

The obtained values of melting temperature due to depression and degree of supercooling are implemented into a numerical model. When using the preset temperature method, experiments and simulations are done repeatedly to obtain accurate average solutions.

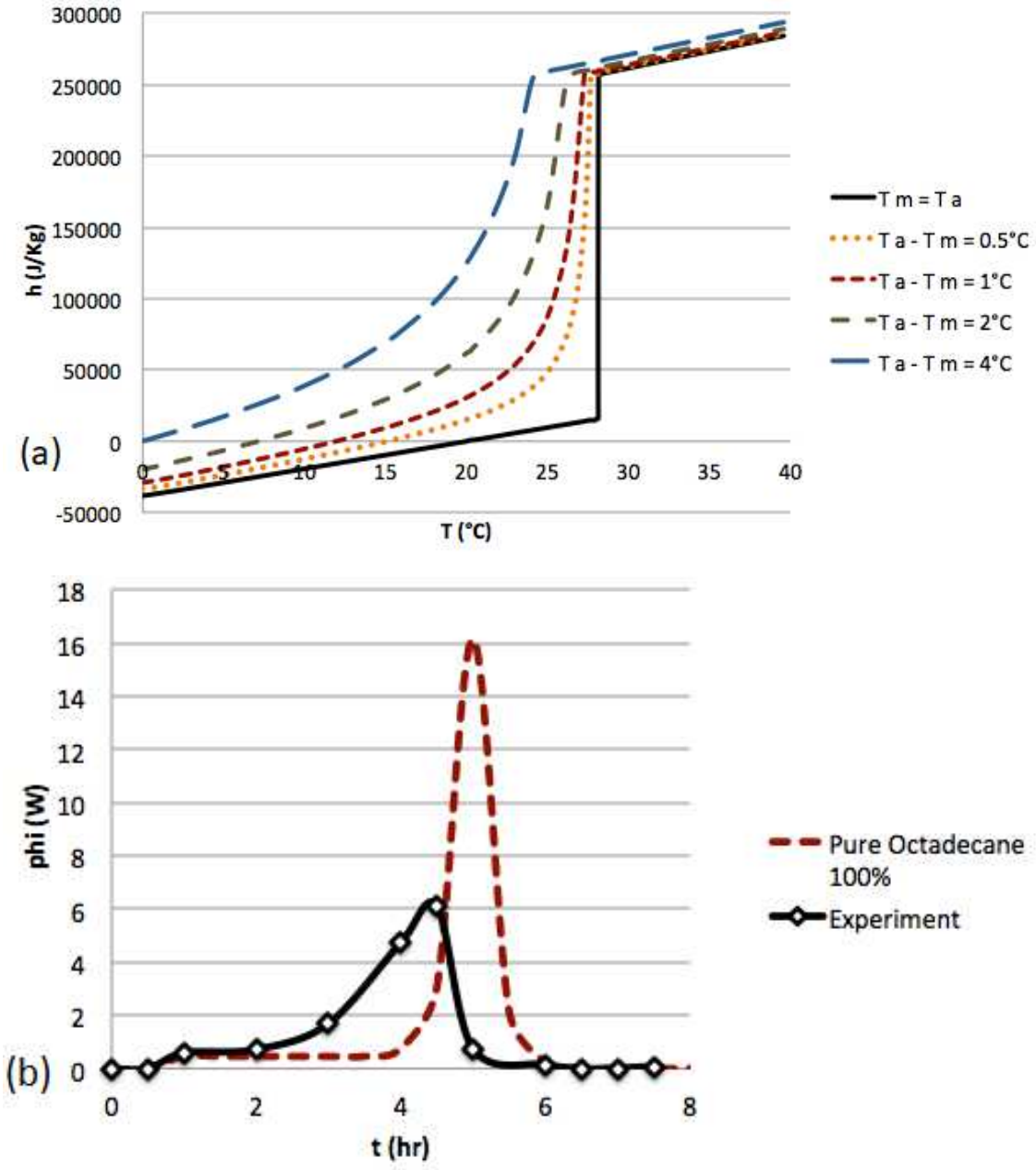

Figure 24 Effect of soluble impurities in octadecane on (a) the enthalpy-temperature curve variation for different depression values and (b) the heat flux variation as a function of time [37]

Another suitable method consists of representing the nucleation temperature by means of a probability function. Because of the stochastic nature of nucleation, Waser *et al.* [43] proposed a crystallization probability function F_{cry} dependent on time, location and temperature given by:

$$F_{cry}(t_s, I_n) = 1 - e^{-t_s \cdot I_n} \qquad where \begin{cases} I_{nuc}(\Delta T_s, f) = K_1 . e^{-f \cdot \frac{K_2}{\Delta T_s^2}} \\ f(L_{adj}) = 1 - \frac{L_{adj}}{K_3} \end{cases} \tag{5}$$

The supercooling time t_s and the nucleation factor I_n are the variables of this probability function. I_n depends on the degree of supercooling ΔT_s and the reduction factor of nucleation barrier f. K_1 is an arbitrary constant and K_2 is a fitting parameter that affects the critical degree of supercooling for which probability of crystallization increases. Solidification may take place due to contact between a supercooled liquid with a solidified PCM; f represents this phenomenon where L_{adj} corresponds to the number of solid crystals in the adjacent segments and calibrated by K_3. The values of these constants are obtained from the experimental study. Figure 25a shows that the probability function is mainly affected by the degree of supercooling where the probability of solidification increases as the degree of supercooling increases. This is because as the liquid become colder, its ability to trigger solidification increases. This result is in total agreement with the classic nucleation theory [86]. As L_{adj} decreases the number of solid particles in the adjacent node decreases too, meaning that the ability to solidify due to contact of liquid with solid also decreases. This is shown in Figure 25b, where the decrease of L_{adj} is represented by the increase of f causing the degree of supercooling increases too.

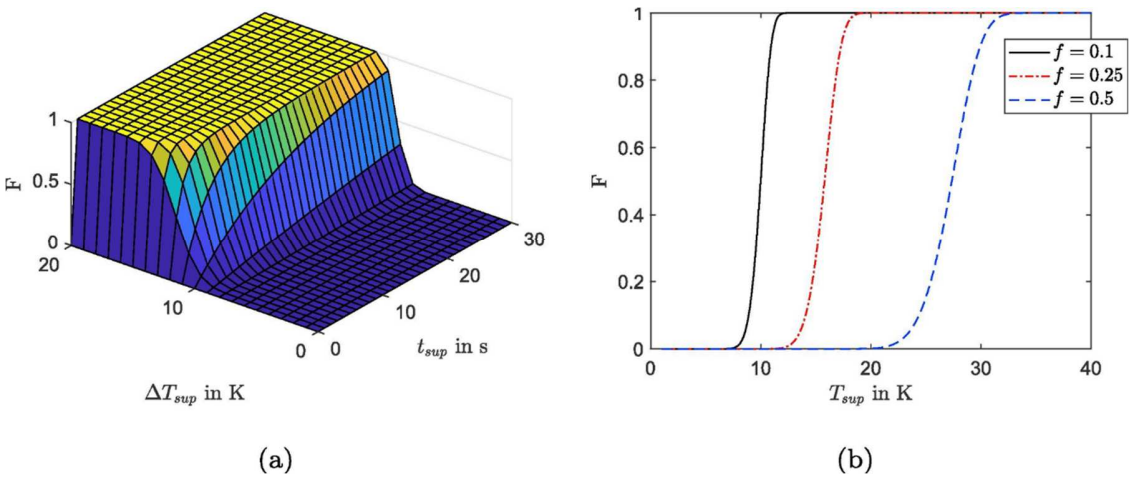

Figure 25 Variation of the probability function against a) supercooling time (tsup) and degree (ΔTsup) for f=0.1; b) degree of supercooling for different values of f at tsup = 0.1s [43]

Yehya *et al.* [37] proposed another probability function to predict nucleation at a given temperature T:

$$P(T) = 1 - \left[\frac{1}{1 + e^{-\Delta T_S \cdot (T - T_a)}}\right] \tag{6}$$

where $T_a = (T_s + T_n)/2$, T_s et T_n are the temperatures of solidification and nucleation respectively. Figure 26 shows the difference between nucleation and solidification temperature

where solidification takes place in the region between them. This probability function can change from one PCM to another according to the different parameters and conditions, so experiments and analytical studies are done to modify and calibrate it.

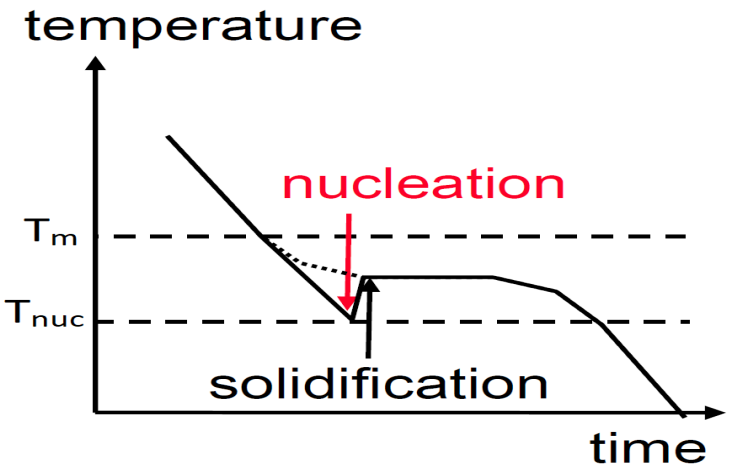

Figure 26 Solidification process [37]

5.2 Rate of solidification

Usually crystallization has a very high rate that may cause system instability in solidification modeling. The model requires fine grid with small time steps, which increases the simulation effort, time and complexity. To model the solidification phase efficiently, an equation relating the rate of solidification to the degree of supercooling is required. A logical assumption is that the rate of solidification increases with the increase of degree of supercooling, because the sample is colder. However, as shown by the solid line in Figure 27, accounting for a typical form of the relation between the solidification speed and the degree of supercooling, this assumption is true until a limit. Indeed, beyond this limit, the molecules of PCM lack thermal energy and become more sluggish causing a decrease in the rate of solidification.

According to the classical nucleation theory [87], the homogeneous nucleation rate I can be written as:

$$I = \frac{NkT}{h} exp\left[\left(\frac{-16\pi}{3}\right)\left(\frac{\sigma_{LC}^3}{H^2}\right)\left(\frac{T_m^3}{\Delta T_s^2}\right)\left(\frac{1}{kT}\right)\right] \quad (7)$$

where N is the number of atoms of a system, k and h are Boltzmann and Planck's constant respectively, σ is the surface tension of the interface between the nucleus and its surrounding, H is the latent heat and T_m is the equilibrium melting temperature.

Font *et al.* [88] used the approximated results of solidification rate obtained by Ashby *et al.* [89]:

$$v(T) = \frac{d\Delta h}{6hT_m}(\Delta T_s) exp\left(\frac{-q}{kT}\right) \quad (8)$$

where d is the molecular diameter, $\Delta h = (latentheat \times molecularweight)/(Avogadro's\ number)$, and q is the activation energy.

The dashed line in Figure 27 is obtained from the linearization of equation (8).

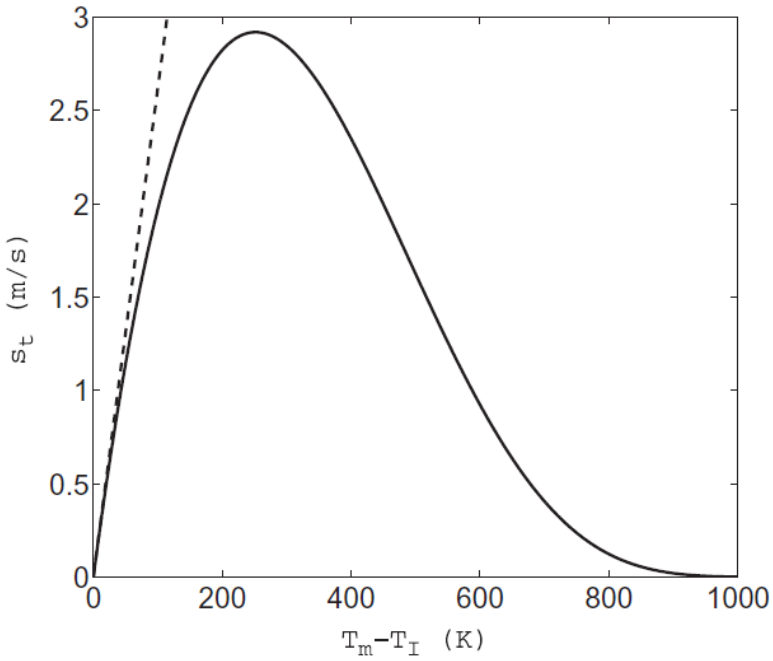

Figure 27 Variation of solidification speed of copper as a function of supercooling degree (T_l is the phase change temperature) [88]

In the numerical models, the rate of solidification is taken into account by different methods. Font [88] and Alexiades [90] use a one dimensional Stefan problem where the model consists initially of supercooled PCM. Both relate the rate of spread to the temperature gradient. The first supposes the solid/liquid interface temperature is equal to the nominal phase change temperature while the latter chooses the interface temperature as an unknown to be solved and uses an exponential function or an approximation to this function. Le Bot *et al.* [91] performed an experiment to obtain the required data of indium solidification and rate of spread. The obtained data from the experiment and an analytical model are used in their numerical model that starts solidification by the implementation of a small solid fraction. According to Günther *et al.* [42], solidification can start for two reasons: the PCM reaches the preset temperature or by direct contact of solid PCM node with its neighbor supercooled node. In their model, the rate of spread is thus controlled by isolating each node during its solidification, meaning that a node cannot trigger solidification in the neighboring node until it is totally solid. According to them, the rate of spread $v(T)$ is also temperature dependent and is given as [42]:

$$v(T) = v_0.(a_0 + a_1 T + a_2 T^2) \tag{9}$$

where $a_0, a_1\ and\ a_2$ are constants, determined by using a quadratic fit to measured data.

Uzan *et al.* [92] introduces a solidification ratio ∅ that is initially zero for total liquid node and is given as:

$$\emptyset^{n+1} = \emptyset^{n} + v.\,\Delta t/\Delta x \tag{10}$$

where n is the number of time steps and v is the speed of solidification.

The speed of solidification is given as [92]:

$$v = \frac{d}{6\mathrm{h}} exp\left(\frac{-q}{\mathrm{k}T}\right)\frac{L(T_m - T)}{T_m} \tag{11}$$

where d is the molecular diameter and q is the activation energy.

Moreover, Uzan *et al.* [92] improved Günther's isolation method, by defining a solid-liquid ratio ∅ . Once a certain node reaches $\emptyset_{max}$, it can trigger solidification in the adjacent node before completing its solidification.

Davin *et al.* [93] use a relative factor β which is the inverse of crystallization factor f_c given by:

$$f_c = a_0 + a_1\Delta T_s + a_2\Delta T_s^2 \tag{12}$$

Note that ΔT_s can have different values according to the mode of solidification (i.e. reaching preset temperature or by solid-liquid contact). As previously mentioned, the proportionality relation between crystallization rate and f_c factor is sensitive to several parameters. During parameterization, if the enthalpy-temperature curve is available, f_c is estimated by curve fitting. However, if the rate of crystallization v_c is known, the same law for f_c is used such that calibration for the factor is needed by actual rate computing and checking. A very high value of f_c means a rapid solidification that requires a very fine grid since the time step of the solidification (time needed for a node to complete its solidification process) should be greater than that of the simulation to overcome divergence and simulation errors. The beginning of solidification may also be chaotic as shown in Figure 28. On the other hand, a very low value of f_c can cause energy balance errors and in some cases solidification appear in two different locations. It is therefore recommended to assign a lower limiting value for f_c, to avoid a reach of crystallization temperature by a node different from the current one.

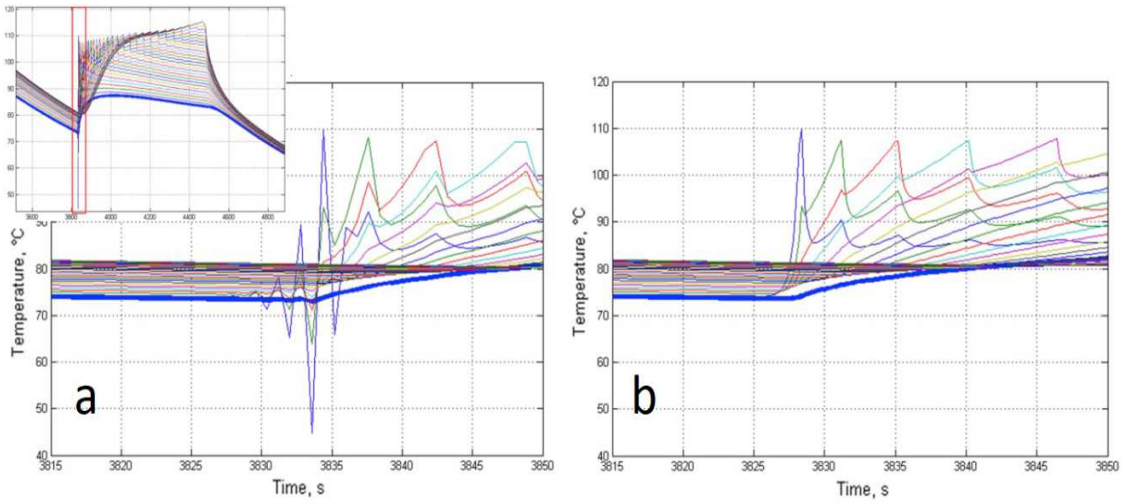

Figure 28 a) Chaotic behavior of temperature curve at the beginning of solidification of supercooled PCM and b) the enhancement due to fc limitation [93]

5.3 Thermal behavior

Another challenge in the modeling of the cooling process of a supercooled PCM is the simulation of the suitable thermal behavior of PCM. As shown in section 4.2, the behavior of PCM upon cooling is not the same in all cases. Once solidification initiates, the PCM enters the kinetic solidification phase, which is the phase where the latent heat is released to increase the PCM temperature. In this phase, several factors interfere in the kinetics of temperature increase. Figure 29 shows the different possible types of temperature increase [94]. The cases characterized in Figure 29a and Figure 29b are the same, where poor nucleation leads the PCM to attain supercooling. However, for higher values of thermal diffusivity, the temperature rises sharply (Figure 29b) to reach the melting temperature. In Figure 29c, the PCM attains supercooled state due the low crystal growth rate. This case shows the "kinetic controlled process", where the critical factor is the poor crystallization kinetics rather than the heat transfer rate. On the onset of PCM nucleation, the temperature stabilizes at a temperature lower than melting temperature rather than increasing to the melting point. This phenomenon is due to the balance between latent heat and heat removal. In Figure 29d, nucleation starts normally at the melting temperature, but the liquid undergoes supercooling during its solidification. The possible explanation for this case is the high rate of heat removal. The liquid in Figure 29e undergoes supercooling but is not seen in the temperature-time plot. This is due to the slow decrease of the temperature and the late reach to the melting temperature point and to a liquid with poor thermal diffusivity. Another explanation may be a difference between the position of the sensor and the solidification zone.

Davin *et al.* [93] developed a model based on the apparent specific heat capacity model by using a new formulation to represent the crystallization kinetics. The results show that by setting different coefficients for the crystallization factor law, it is possible to recover several typical thermal behavior of Figure 29. The results are discussed later in section 6 (Figure 37).

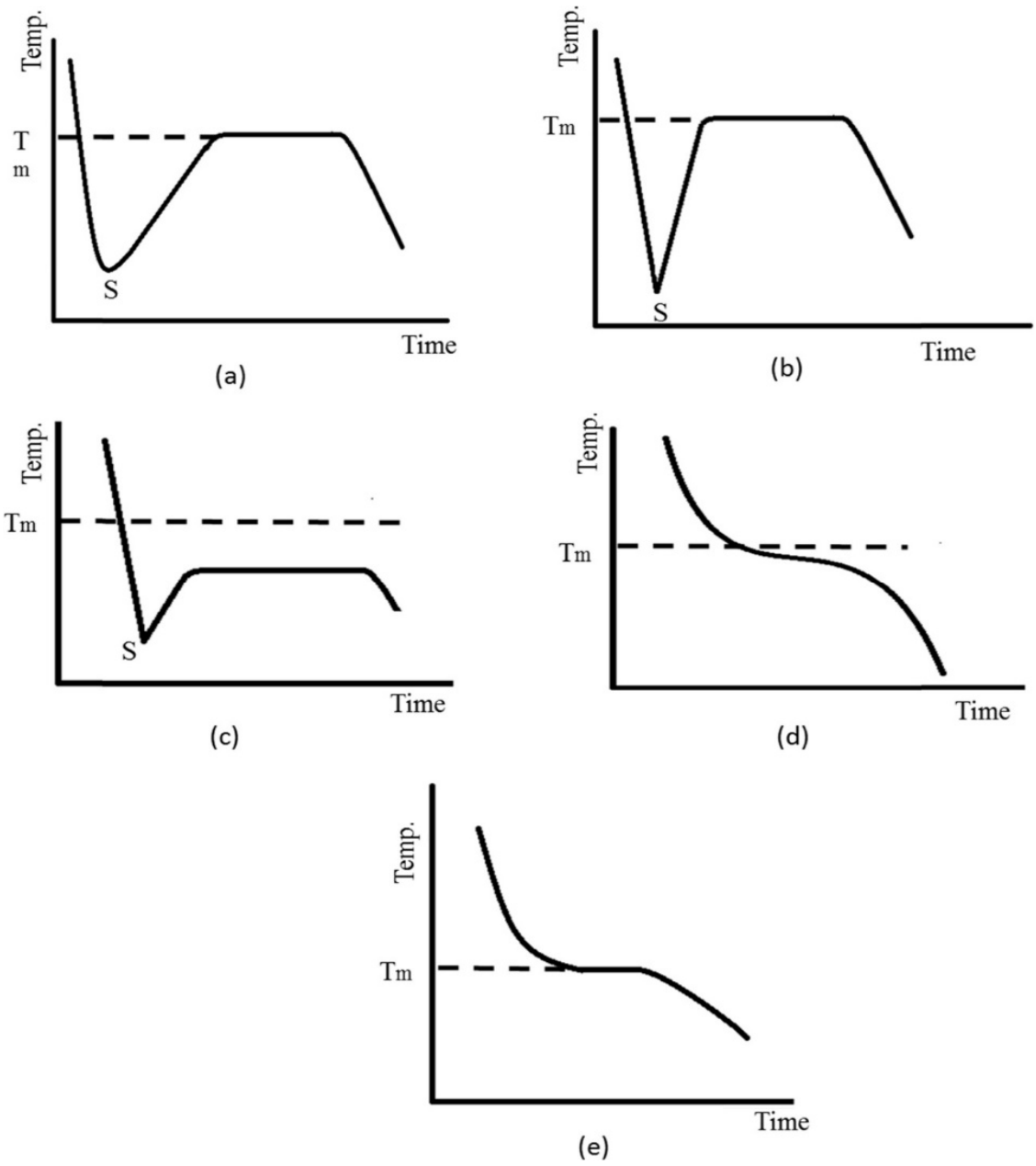

Figure 29 Plots showing different thermal behavior of PCM suffering supercooling [2]

As shown in the above subsections, the important parameters that represent supercooling are the degree of supercooling and rate of crystallization spread. It is challenging to represent these two parameters in a general equation to use in any application. These two parameters are also dependent on other factors previously mentioned which increases this challenge. Efforts are done to define some correlations; however, these equations still need calibration and validation by experimental results to become valid for a specific PCM under certain well-defined conditions.

6 Existing models

As shown in the previous sections, different methods are adopted to model the parameters of the solidification process that are the degree of supercooling and the rate of spread. Some assumptions are often taken into consideration to simplify the model; such as neglecting the volume change due to thermal expansion, the natural convection and radiation heat exchange, etc. In order to model supercooling, researchers modify the different methods used in modeling phase change problem. Each method has its own advantages and disadvantages when modeling a phase change process as shown in Table 4. The below sections present different models, the method used, the taken assumptions and the technique followed in each model to deal with the additional difficulty of supercooling modeling.

Table 4 Advantages and disadvantages of different methods used in modeling phase change problems

Method	Criteria	Advantages	Disadvantages	Authors using this method
Enthalpy method	The enthalpy function includes both sensible and latent heat	1- Fast 2- Can handle sharp and gradual phase changes	Temperature oscillation at typical points of a grid	[95][96]–[105]
Heat capacity method	The heat capacity function includes both sensible and latent heat	1- Variable are only dependent on temperature 2- Easily programmable	1- Accurate results require fine grids and small time steps. 2- Requires a gradual phase change (phase change range) rather than sharp change 3- Latent heat is underestimated.	[96], [97], [106]–[120]
Temperature transformation method	The values of heat capacity and a source term are equivalent to both sensible and latent heat	1- can handle sharp and gradual phase changes 2- Can be used for large time steps and coarse grids	This method is not commonly used	[121]–[125]
Heat source method	The value of a source term is equivalent to latent heat	1- Latent and sensible heats are represented by different variables	1- An optimal value for relaxation factor is required to apply an under-	[126]–[130]

		2- Can handle sharp and gradual phase changes	relaxation. 2- Low computational efficiency 3- Difficulty in modeling supercooling	

6.1 One-dimensional Models

Modeling is a method used to obtain the needed results to follow accurately the behavior of the tested material in a reliable period. Using a one-dimensional model reduces the complexity, where the heat equation is a function of time and one-direction. Moreover, the model is divided into several phases defined by state variables and functions. These variables and functions are introduced in the heat equation to represent the different phases and the values of different parameters. After dividing the model to a number of phases, some parameters do not affect the results a lot, so if neglected, this reduces the complexity and simulation time.

Frémond *et al.* [131] in 2001 developed a macroscopic predictive theory of supercooling to model the evolution of a supercooled body from its liquid state to its solid state. The domain is separated into two portions, solid and liquid, by the help of a state quantity β representing the volumetric fraction of liquid material. In this model, for simplicity, the latent heat is equal to 1 and solid-liquid portions are separated by a surface of discontinuity having a temperature related speed [132]. This leads to a problem having free boundary. Introducing the viscosity term in β leads to an irreversible model that is represented by differential equations obtained after deriving the energy equations as an affine function of local temperature u. The differential equations obtained in the continuous differentiable domain are [131]:

$$\frac{\partial \beta}{\partial t} + W(u)|\nabla \beta| = 0 \tag{13}$$

$$\frac{\partial u}{\partial t} + \frac{\partial \beta}{\partial t} - \Delta u = 0 \tag{14}$$

where W is the normal surface velocity of the freezing front. In these equations, when assigning the values for β, the free boundary appears explicitly. In the irreversible model, the end of the supercooling of liquid involves microscopic movements. During phase change, macroscopic effects occur due to these microscopic movements, which causes a slight change in density and volume. Since β is the state of the PCM, its change with time $(\partial\beta/\partial t)$ represents the microscopic velocities. Similarly, six differential equations are formed [132] and proved that there exists at least one solution.

Günther *et al.* [42] proposed in 2007 a linear and one-dimensional model based on the enthalpy method. Their model is connected to a heat exchanger on the left side and to an insulating material on the other side. The total volume of the container is equally divided into volume elements.

This model considers conduction as the only heat transfer mechanism and neglects the variations of volume resulting from phase change. The explicit finite volume method is used. The

duration of the simulation is preset, and the used time step has a fixed value and is obtained from the CFL criterion [133]. In an enthalpy method, the enthalpy function is injective. To include supercooling in the enthalpy-temperature relation, two enthalpy curves for stable and metastable states are used and when the crystallization temperature is reached, switch is done between both curves. The drawback of this method is the discontinuity of the enthalpy due to phase change that may cause simulation errors and misrepresents the real case of phase change. In the ideal case, the PCM has a fixed melting and nucleation temperatures whereas the more realistic case is having a temperature interval to accomplish the two processes. For an ideal case, the heat capacity is considered constant; however, this is not accurate, so experimental values of $h(t)$ are implemented in the model.

Another challenge is to control the rate of crystallization. As mentioned before, the used PCM has a known degree of supercooling that is obtained by performing similar scenario experiments. Solidification can start when the PCM reaches the preset nucleation temperature or due to solid-liquid interaction. The used rate of spread is given as a function of temperature according to equation (9). In some cases, to decrease the computational effort and to use a finer mesh, the rate of solidification is decreased using the isolation method. This method restricts the ability of solidification by solid-liquid interaction, where a node cannot trigger solidification in the neighboring node until it completely finishes its solidification process [42].

$$v(T) = v_0.(a_0 + a_1T + a_2T^2) \tag{9}$$

Hu *et al.* [41] developed in 2017 a model that is solved by using the finite differences method. Using the equivalent specific heat capacity method, the heat capacity is considered constant during phase change along with isothermal system as shown in Figure 30. The model uses implicit scheme to discretize the control equations and boundary conditions.

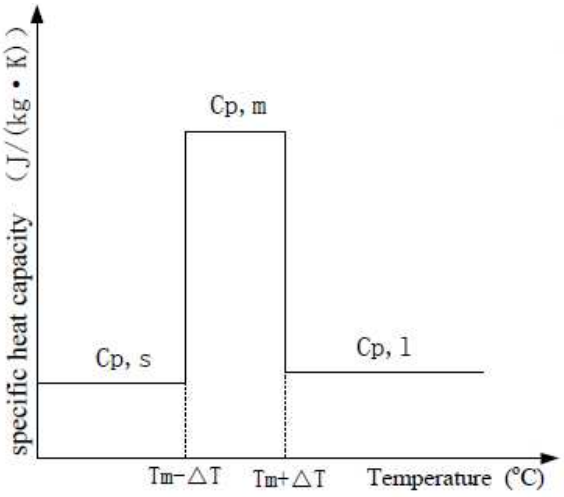

Figure 30 Equivalent rectangular specific heat capacity [41]

Bony [134] started from the existing type 60 in TRNSYS, dedicated to stratified fluid tanks based on sensible energy storage, and made an extension. The physical model consists of a water heat exchanger tank filled with PCM modules of different shapes (cylinders, plates, spheres), which

allows a bidimensional calculation model. The tank is vertical and constituted of multiple segments or nodes. An assumption of constant node temperature is taken. He uses the enthalpy method to calculate the heat transfer. The numerical equations are solved using the explicit method and to avoid calculation divergence, some conditions are applied on the nodes and the time step as follows [134]

For a surface node $$Fo(2 + Bi) \leq 1/2 \quad (15)$$

For a node inside material $$Fo \leq 1/4 \quad (16)$$

with: $Fo = \lambda.\Delta t/(\rho.C_p.\Delta x^2)$ and $Bi = \alpha.\Delta x/\lambda$

where Fo and Bi are Fourier and Biot numbers respectively, α is the convection coefficient between the water tank storage and the PCM container, λ is the thermal conductivity.

The maximum time step that can be used is [134]:

For a surface node $$\Delta t \leq \frac{\rho.C_p.x^2}{2\lambda\left[2 + \left(\frac{\alpha x}{\lambda}\right)\right]} \quad (17)$$

For a node inside material $$\Delta t \leq (\rho.C_p.x^2)/4\lambda \quad (18)$$

Hysteresis and supercooling phenomena are taken into account in the model as shown in Figure 31 by introducing a specific indicator for each of them. Due to the vertical shape of the container, the lower part of the cylinder is colder than the top. As a result, the lower part undergoes higher degree of supercooling and is the first to reach the preset crystallization temperature. Once solidification starts, it propagates to the above nodes with an instantaneous rate of spread (Figure 32). The thermal conductivity of PCM takes two different values for liquid and solid phases and is calculated by linear interpolation during the phase change. Concerning the convection coefficient between water and PCM, it is calculated according to the PCM container shape and the type of fluid flow.

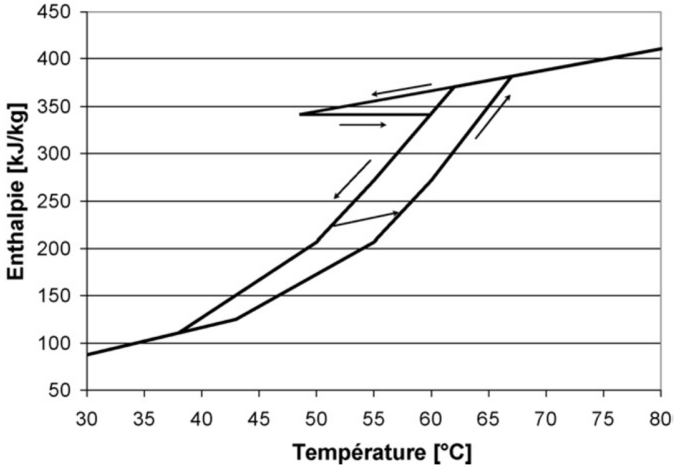

Figure 31 : New enthalpy functions to represent hysteresis and supercooling [134]

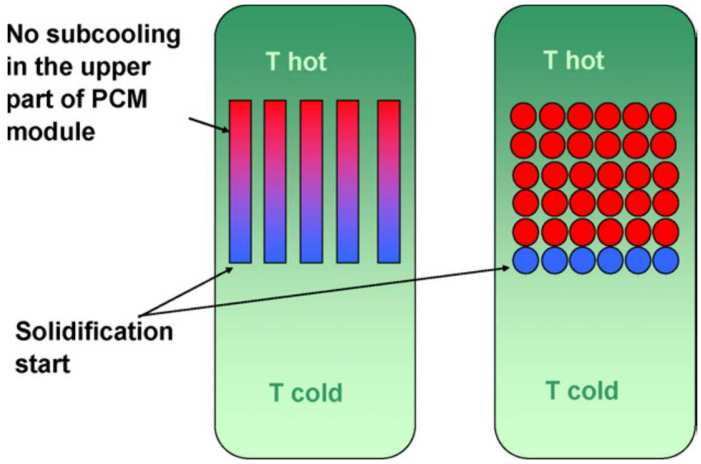

Figure 32 Solidification propagation according to the PCM module shape [134]

In 2020, Davin *et al.* [93] used, like Hu *et al.* [24], the apparent specific heat capacity method. The particularity of their method is related to the introduction of a negative Cp to accurately take into account supercooling. Their model is based on the lumped system or nodal method to discretize the heat equation as shown in Figure 33, with the main governing equation described in equation (19) [93]:

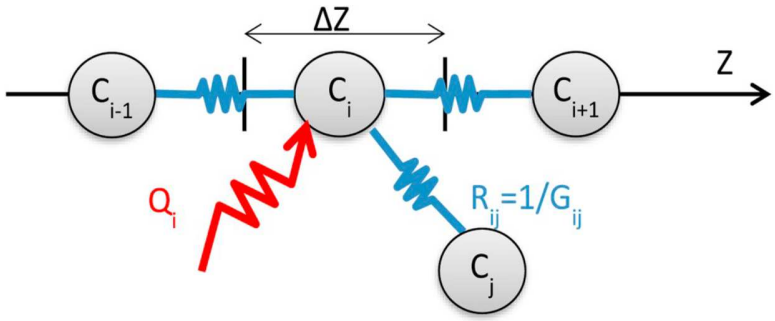

Figure 33 Lumped system network used for heat equation discretization [93]

$$\sum_j \lambda_{ij}(T_i - T_j) + Q_i = C_i \frac{dT_i}{dt} \qquad \forall i \in [1, N] \tag{19}$$

where λ is the thermal conductance, Q represents the heat sources and the boundary conditions, C is the heat capacitance that can insure phase change and i, j are the node indices.

Using an explicit scheme, the temperature is calculated for each time step. Similar to the before mentioned models using enthalpy method, the crystallization initiates either by reaching the present nucleation temperature T_n or by the liquid-solid interface. To reduce numerical errors and better represent the heat transfer, the Gaussian approximation is used to account for the specific capacity $C_p(T)$. Figure 34c shows two formulations for heat capacity change during the cooling phase at the crystallization temperature T_C. The first, blue arrow, considers the easy simple formulation while the second, green arrow, is more complex but represents the

crystallization process. f_{super} is a phase supercooling indicator that allows to differentiate the specific capacity regarding the phase history. During fusion (Figure 34a), the Gaussian law is used and $f_{super} = 0$. During cooling (Figure 34b), the PCM stays liquid until crystallization starts and f_{super} is set to 1. When crystallization starts (Figure 34c), f_{super} is incremented to 2. Finally, f_{super} returns to 0 as soon as crystallization ends and the solid begins to cool down (Figure 34d).

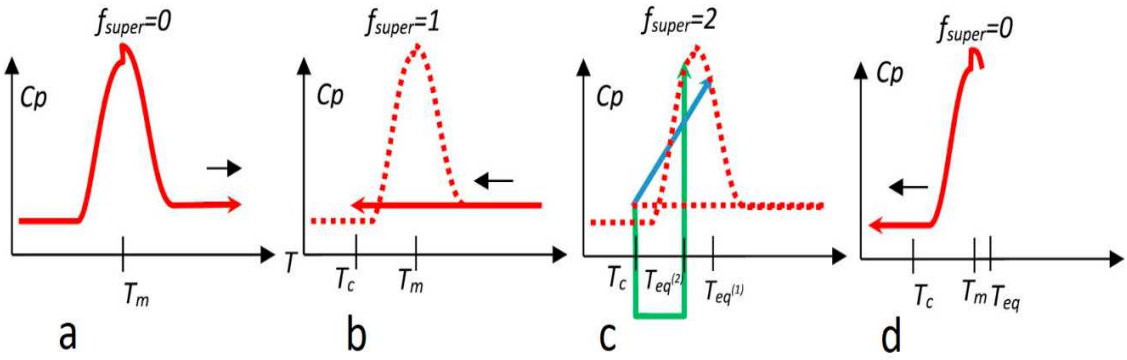

Figure 34 The different steps followed to represent supercooling: a) heating b) cooling until crystallization starts c) two formulations of crystallization and temperature rise represented by blue and green lines d) cooling of the solid PCM [93]

In formulation 1, the temperature directly increases from T_C to $T_{eq}^{(1)}$ by considering a very high rate of crystallization. The heat capacity for formulation 1 can then be written as [93]:

$$C_p(T) = \begin{cases} C_p^{gauss}(T) & if\ f_{super} = 0 \\ C_p^l & if\ f_{super} = 1 \\ C_p^{gauss}(T) & if\ f_{super} = 2 \end{cases} \quad (20)$$

where C_p^{gauss} is the Gaussian approximation, C_p^l et $C_p^s$are the heat capacity in liquid and solid phases respectively. Moreover, in case $f_{super} = 2$, $T = T_{eq}^1$ and $f_{super}(t + \Delta t) = 0$.

According to [42], [92], [135], C_p^{gauss}can be written as:

$$C_p^{gauss} = C_p^0 + \frac{H}{\Delta T\sqrt{\pi}} exp\left[\frac{-(T - T_m)^2}{\Delta T^2}\right] \quad (21)$$

where ΔT is the Gaussian standard deviation of Cp and H is the latent heat.

In Figure 35, A_0 corresponds to the enthalpy stored during heating process as shown in Figure 34a; A_1 corresponds to the enthalpy released during the cooling process in liquid or metastable state as shown in Figure 34b, and A_2 corresponds to enthalpy released during the cooling process from the equivalent phase change temperature T_{eq}^1 as shown in Figure 34d. The model has the same initial and final temperature. Thus, the enthalpy of heating is equal to that of cooling and the following equality relation is obtained [93]:

$$A_0 = A_1 + A_2 A_0' = A_1' \tag{22}$$

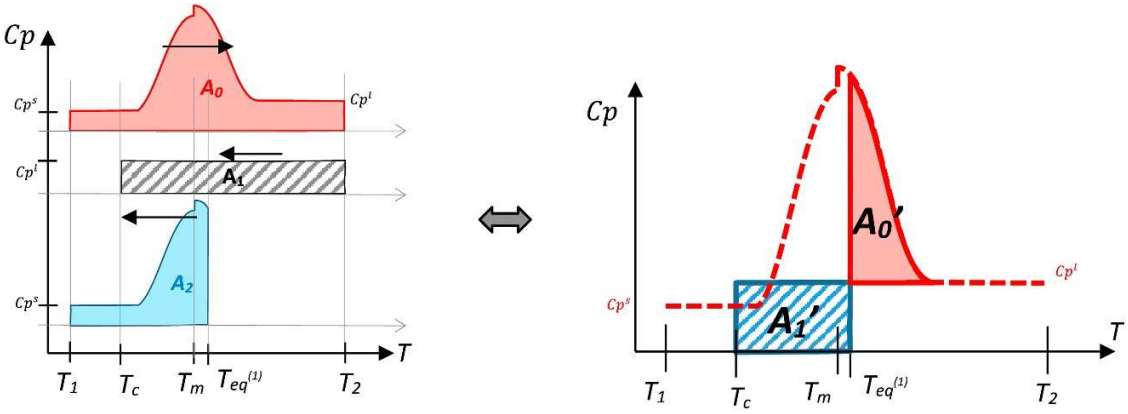

Figure 35 Blocks representing the equivalent enthalpy of the processes (heating/cooling) of formulation 1 [93]

By solving the equality of enthalpy blocks, performing change of variable, introducing error function and supposing ΔT is very small, $T_{eq}^{(1)}$ can be finally deduced as [93]:

$$T_{eq}^{(1)} = T_m + \Delta T.\, erf^{-1}\left[1 - \frac{2C_p^l(T_m - T_c)}{H}\right] \tag{23}$$

Formulation 2, shown in green in Figure 34c, is more complicated to model but more realistic. It is intuitive with a negative heat capacity chosen during phase change (i.e.: $f_{super} = 2$); the expression of the heat capacity for $f_{super} = 2$ in equation (20) becomes [93]:

$$C_p(T) = -\beta C_p^l(T); \quad if\ T \geq T_{eq}^2,\ f_{super}(t + \Delta t) = 0 \tag{24}$$

Figure 36 represents the enthalpy blocks of all stages mentioned before and equality of heating and cooling enthalpies is applied to determine T_{eq}^2.

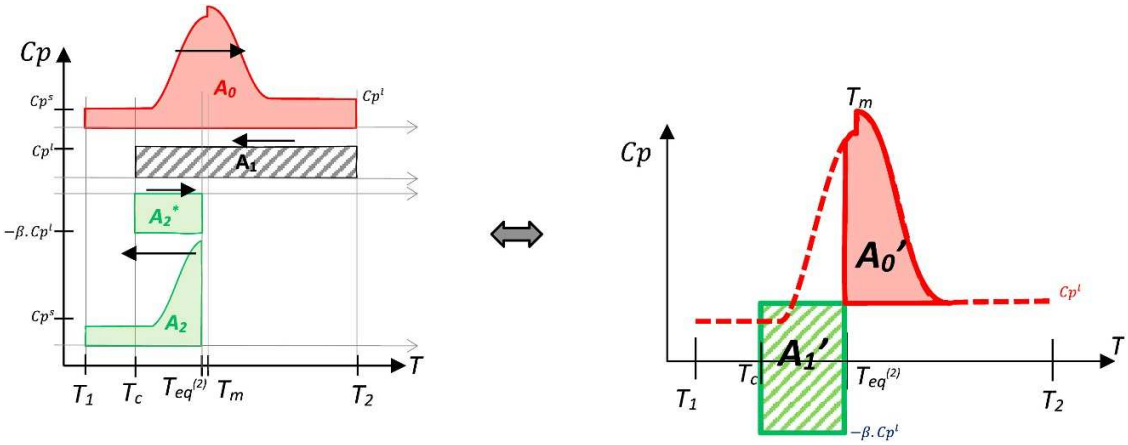

Figure 36 Blocks representing the equivalent enthalpy of the heating and cooling processes for formulation 2 [93]

Similar assumptions of formulation 1 are taken to obtain the expression of T_{eq}^2 [93]:

$$T_{eq}^2 = T_m + \Delta T.erf^{-1}\left[1 - \frac{2C_p^l(1+\beta)(T_m - T_c)}{H}\right] \quad (25)$$

Note that erf^{-1} accepts input value that belongs to the interval [-1,1]. In other words, if T_{eq}^2 is outside the melting range, then $C_p^l(1+\beta)(T_m - T_c) > H$ and an error occurs. In this case, the expression of T_{eq}^2 is replaced by equation (26) [93]:

$$T_{eq}^2 = \frac{H + T_m.\left(C_p^s - C_p^l\right) + T_c.C_p^l.(1+\beta)}{C_p^l.\beta + C_p^s} \quad (26)$$

The factor β is found to be the inverse of the crystallization factor f_c and is defined in equation (12), where the rate of crystallization is discussed in details. The value of β indicates the speed that a supercooled liquid reaches the phase change. If β is set to zero, then equations (23) and (25) become identical meaning that phase change takes place immediately.

The model has Neumann boundary conditions for elements in contact with the air including the natural convection coefficient. Heat transfer takes place in one direction so that the solid liquid/interphase is always planar. The heating source, insulation, capsules and other parts used in the experiment were included in the model.

To test this model, the simulated results are compared to experimental results. The study was done on erythritol, which presents a high degree of supercooling ($Tm = 118°C, Tn = 78°C$) and a relatively low crystallization rate. Erythritol is heated from 50°C to 150°C by a plate and cooling is done by ambient air through the same plate. During the cooling phase, several polynomial laws for the crystallization factor fc have been tested as shown in Figure 37. The actual crystallization rate is the calculated ratio of the distance between two nodes divided by the time between the two nodes crystallizations. These results show that it is possible to model different thermal behavior of supercooling for the PCM material.

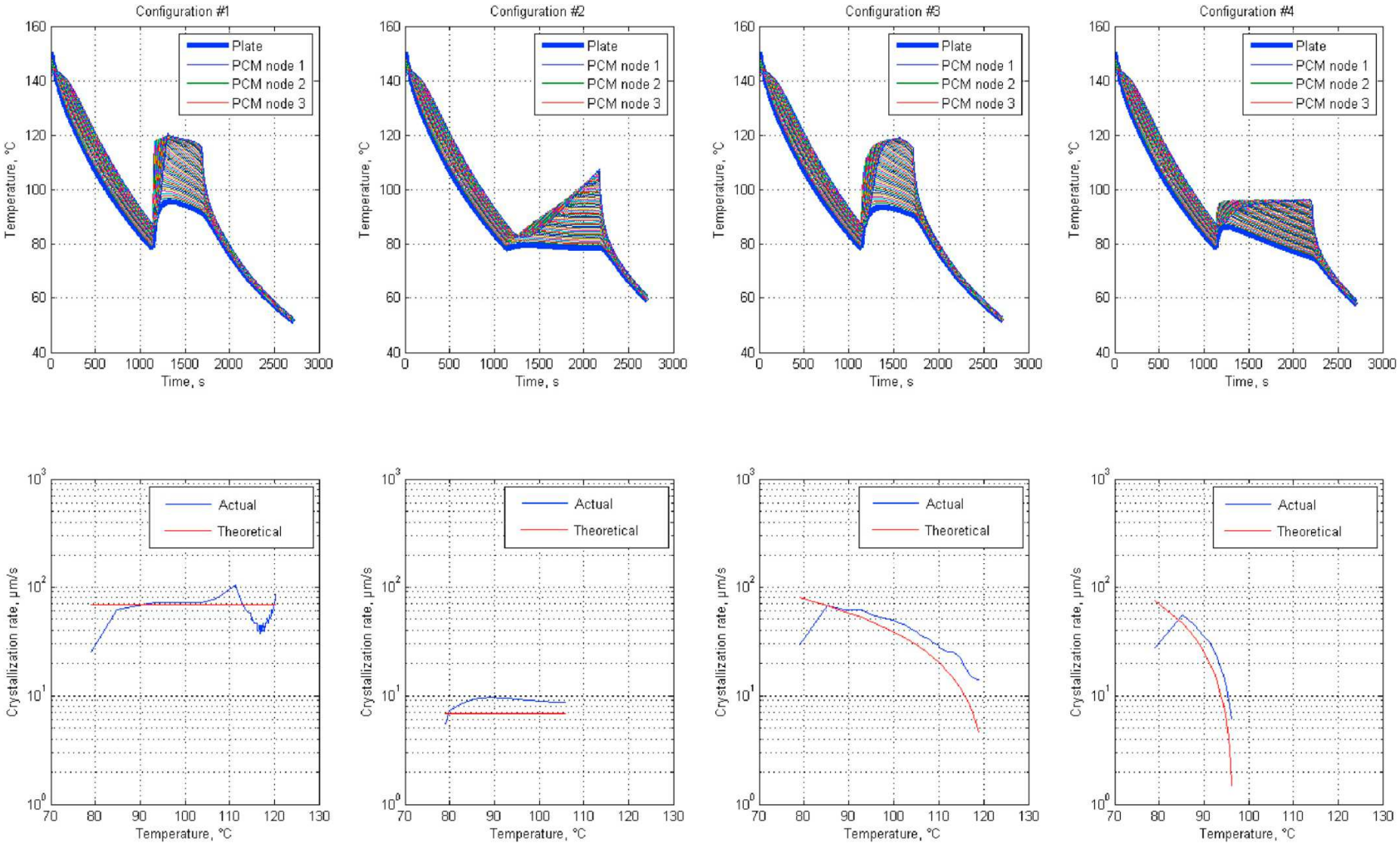

Figure 37 Simulation results showing the influence of the crystallization rate factor $fc(T)$ on the temperature and the crystallization rate [93]

6.2 Multi-dimensional Models

In a multi-dimensional model, an extra dimension is added to the one-dimensional model. In this case, reproducing a more realistic image of the simulated case is better, where the effect of convection in the PCM can be detected by the deviation of the solid/liquid interface. This accuracy and these results cost more computational time and add complexity to the model

The model developed by Uzan *et al.* [92] in 2017 is based on the enthalpy formulation and resolved by using finite volumes. The two-dimensional model is able to simulate the solidification of a supercooled liquid using explicit numerical scheme. Upon cooling the cylindrical model from the bottom, the liquid's temperature decreases and the PCM is in supercooled stage until solidification starts either by reaching the preset temperature or by the solid-liquid interaction. After solidification, the temperature of the solid continues in decreasing. Similar to Günther [42], Figure 38 shows the phase change process that takes place during an interval of temperature to overcome the sharp variation of enthalpy that may cause simulation errors. The difficulty of using the enthalpy method is the undefined enthalpy values for supercooled liquid. Experimental results of gallium and analytical solutions are compared with the results of the model.

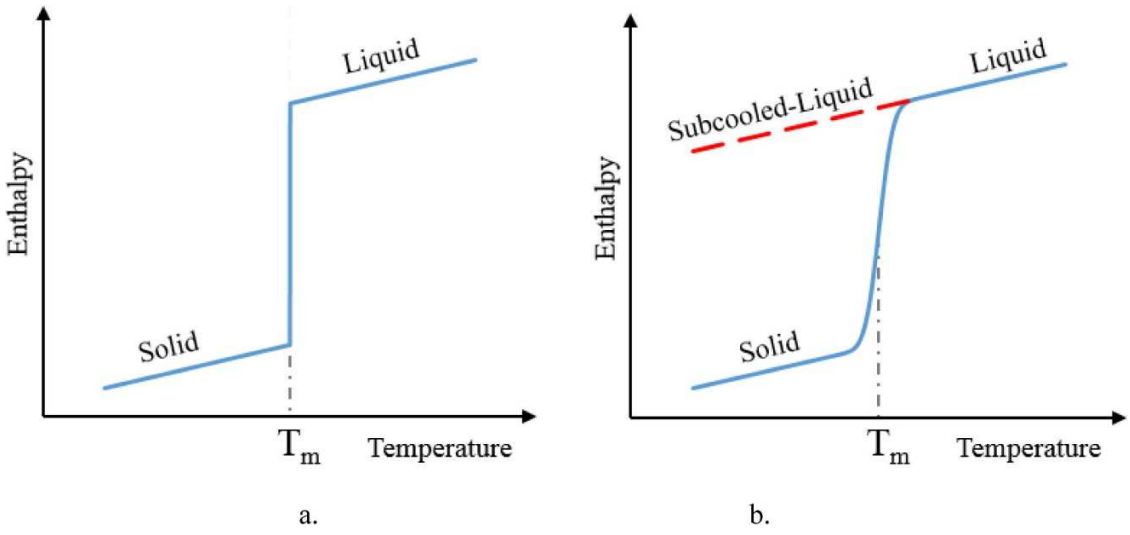

Figure 38 Enthalpy energy relation: a) used by enthalpy method; b) used by Günther and Uzan [92]

The heat capacity is in the form of a Gaussian function and a parameter "p" is used, as in the model of Günther *et al.* [42], to determine the state of the PCM. This indicator p is assigned for each node. A ratio for solid/liquid fraction $\emptyset$ and the speed of solidification v are calculated according to equation (10) and equation (11) respectively [92].

$$\emptyset^{n+1} = \emptyset^{n} + \frac{\Delta t}{\Delta x} v \tag{10}$$

$$v = \frac{d}{6h_P} exp\left(\frac{-q}{k_B T}\right) \frac{L(T_m - T)}{T_m} \tag{11}$$

The temperature is calculated at each time step according to the following equation (27) [92]:

$$T = \frac{\emptyset}{\emptyset_{max}} T(Solid) + \left(1 - \frac{\emptyset}{\emptyset_{max}}\right) T(Liquid) \quad (27)$$

where $\emptyset$ is the solid-liquid fraction, and $\emptyset_{max}$ must be previously defined using the energy conservation equation. $T(Solid)$ and $T(Liquid)$ are obtained by using the enthalpy relations in stable solid and liquid phases as described in equations (28) and (29) respectively. If $\emptyset < \emptyset_{max}$ part (a) of equation (29) is used, else part (b) [92].

$$h(T) = C_p(T - T_m) + \frac{L}{2} erf\left(\frac{T - T_m}{\delta T}\right) \quad (28)$$

$$h(T) = \begin{cases} C_p(T - T_m) - 0.5L \ \ (a) \ \ solid \\ C_p(T - T_m) + 0.5L \ \ (b) \ \ liquid \end{cases} \quad (29)$$

Moreover, a solidified fraction SF defines the ratio of solid mass over total mass. Reaching its maximum means the end of the kinetic solidification, which is the increase of the liquid temperature to its melting point. As shown in equation (30), SF_{max} is a function of the degree of supercooling and material properties [92]:

$$SF_{max} = \frac{1}{1 + \frac{L - C_{ps}(T_m - T_n)}{C_{pl}(T_m - T_n)}} \quad (30)$$

where C_{ps} and C_{pl} are the solid and liquid heat capacities respectively.

Günther's model isolates each node until it finishes solidification. However, in this model, once the node reaches the $\emptyset_{max}$, it triggers solidification in the adjacent node.

For simplicity, the model neglects volume and density changes. First, the model considers heat transfer in radial direction only (1D problem) and after 1D validation, heat transfer along z direction is included to obtain a 2D model (Figure 39). Similar procedure for differential equation discretization is followed. For both 1D and 2D models, the cylinder's wall has constant temperature and zero heat flux at the centerline. For 2D model, the base of cylinder has constant temperature while the top is insulated.

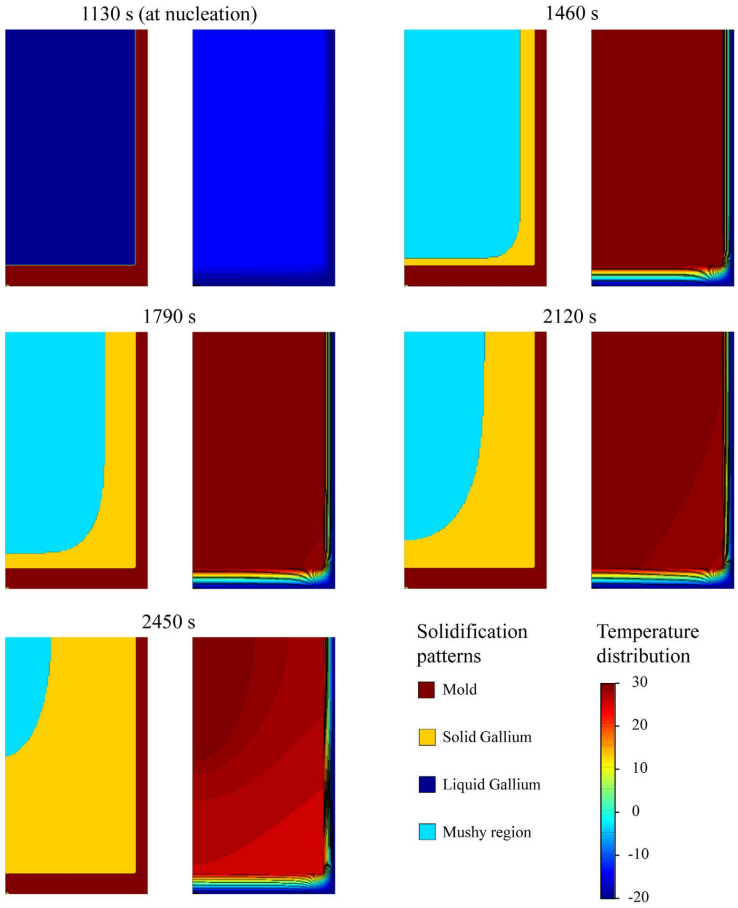

Figure 39 2D model simulated results from the start of cooling: solidification maps on the left and temperature fields on the right [92]

Waser *et al.* [43] proposed a 3D model consisting of a fin tube heat exchanger shown in Figure 40. To reduce the computational cost, the following assumptions are taken into account: convection heat transfer in PCM is neglected, as well as thermal losses to the ambient from the PCM. The material properties are constant, and the only considered heat transfer is from the PCM to the heat transfer fluid (HTF). The 3D model is reduced to 1/8 with symmetrical boundary conditions and a convective boundary condition is applied at the inner tube surface. Concerning the HTF, its model is one-dimensional with n segments and discretized using an upwind scheme to calculate the temperature in each segment. The energy equation of the PCM is discretized using finite volume method; the time discretization scheme used is implicit of first order and the spatial discretization scheme is second order. Using the enthalpy method, the latent heat is included in the enthalpy term of the energy equation. A temperature dependent state indicator

β is used to indicate whether the PCM is in solid, liquid state or in the mushy zone. The mushy zone is a zone where phase transition takes place, and its role is to prevent the sudden phase change that causes simulation instabilities. The indicator β is written as [43]:

$$\beta = \begin{cases} 0 & if\ T < T_s \\ \frac{T-T_s}{T_l-T_s} & if\ T_s < T < T_l \\ 1 & if\ T > T_l \end{cases} \quad (31)$$

where T_s is the maximum temperature of the PCM when it is totally solid, T_l is the minimum temperature reached by the liquid PCM and T is the instantaneous temperature of the PCM. The indicator β can also be used to determine the enthalpy and the amount of the latent heat released.

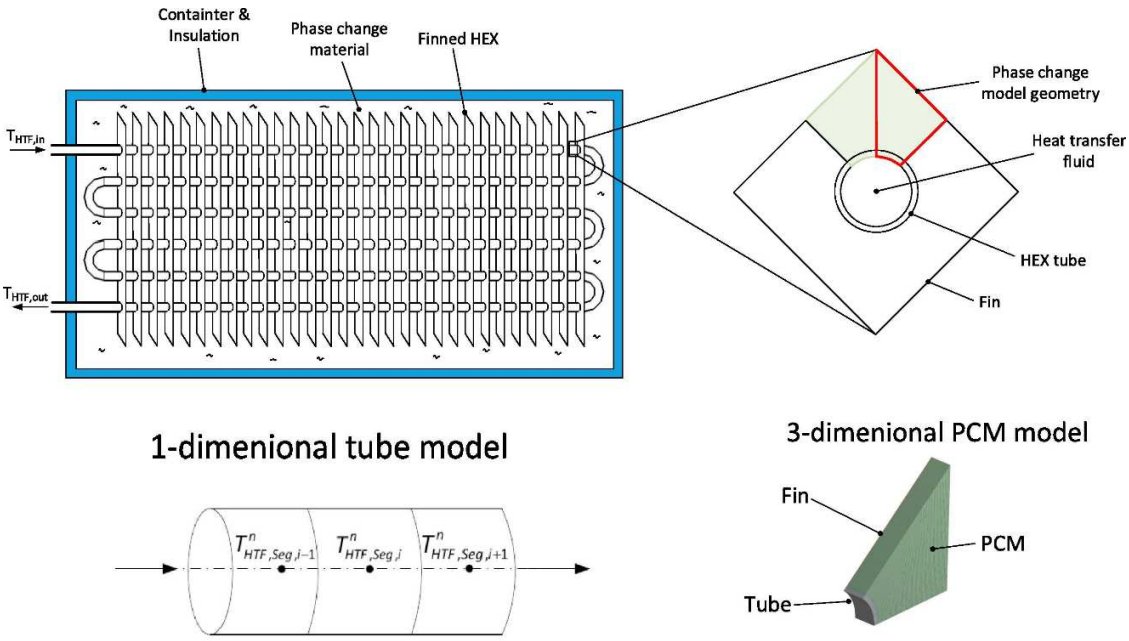

Figure 40 Illustration of the 3D model done by Waser et al. [43]

The temperature of the inflow is constant and PCM temperature is initially 68°C (10°C higher than melting temperature) and decreases to 15°C. As mentioned before, equation (5) shows the used crystallization probability function, which is calibrated by an experimental study [43].

$$F_{cry}(t_s, I_n) = 1 - e^{-t_s . I_n} where \begin{cases} I_{nuc}(T_s, f) = K_1 . e^{-f.\frac{K_2}{\Delta T_s^2}} \\ f(L_{adj}) = 1 - \frac{L_{adj}}{K_3} \end{cases} \quad (5)$$

Figure 41 gives $K_2 = 7250K^{-2}$ and $K_3 = 0.7$ for the minimal deviation of 140W. Both models are linked to each other by the heat flow rates from PCM to HTF. The heat flow rates are generated by the 3D model and collected in two datasets. The former contains data as the

phase change occurs and the latter contains data when PCM remains liquid. The heat flow rates are then used as source term in the 1D tube model.

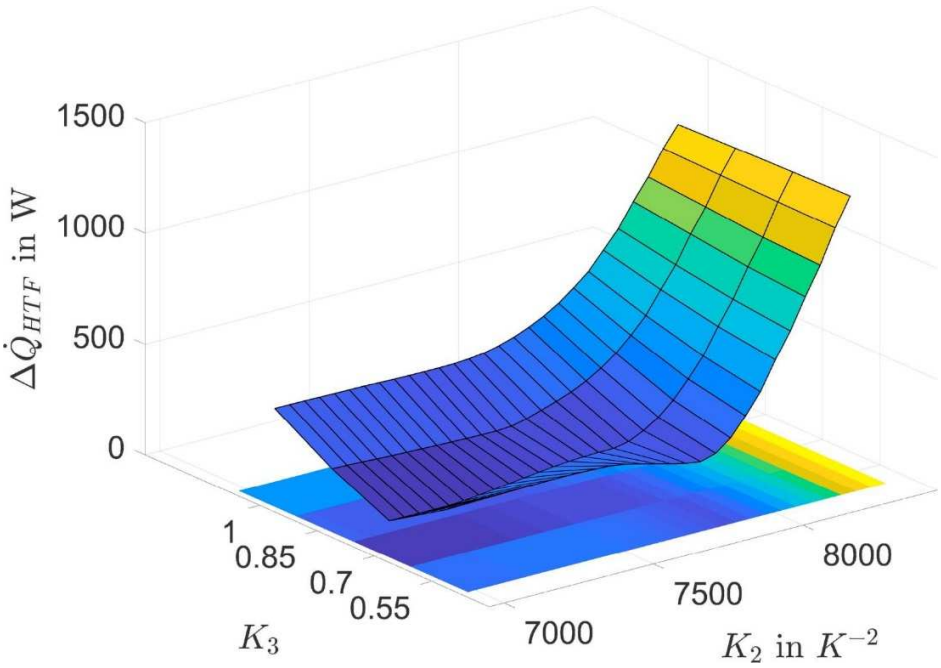

Figure 41 Averaged deviation between experimental and numerical results obtained for different values of K2 and K3 [43]

As shown above, the researchers tend to use different methods to include supercooling in numerical simulations. Simplifying the model is an important issue used to decrease the time and complexity of the simulation. Table 5 summarizes the above-discussed models showing the dimension, methods and assumptions taken.

Table 5 Summary of the most recent methods used for the numerical modeling of supercooling

Author (year)	Dimension	Method used	Assumptions	Results
Hu *et al.* [41] (2017)	1D	- Finite difference method - Heat capacity method - Implicit scheme to discretize the control equations and boundary conditions	Isothermal phase transition process	- Supercooling delays the onset of solidification. - As the degree of supercooling increases, the maximum value of heat flux reached before phase change increases. - The overall value of heat flux decreases as the degree of supercooling increases.
Frémond *et al.* [131] (2001)	1D	- Assigning a state quantity β representing the liquid volume fraction - Reversible and irreversible models, where the latter is obtained by adding the viscosity term in the partial differential equation of the moving front - Free velocity of freezing surface function of temperature	- The model consisted of two zones, liquid and solid, separated by a surface of discontinuity. - During phase change, the medium is at rest. - Latent heat value set to 1 kJ/kg.	Presence of a unique solution for the obtained differential equations for both cases
Bony *et al.* [134] (2007)	1D	- Enthalpy method to calculate heat transfer - Explicit method to solve numerical equations - Applying conditions on the nodes and the time step using Fourier and Biot numbers	Constant rate of crystallization	- Assuming constant rate of crystallization leads to inaccurate results - Temperature oscillations are observed

				during phase change that need to be reduced without dramatically increasing the calculation time.
Günther *et al.* [42] (2007)	1D	- Finite volume method - The values of enthalpy are implemented as a function of time to overcome the reality that enthalpy function is no longer injective. - Solidification is triggered either by reaching a preset temperature or by the solid front. - Rate of spread is a function of time. - A node could trigger solidification in the neighboring node when it finishes completely its phase change to solid.	- Conduction is the only heat transfer mechanisms - Constant volume during phase change - Melting and crystallization take place in a range and not at an exact value.	Using two curves of enthalpy to include supercooling causes a discontinuity of the enthalpy due to phase change. It causes simulation errors and misrepresents the real case of phase change
Davin *et al.* [93] (2020)	1D	- Lumped system or nodal method to discretize the heat equation - Time-explicit scheme to calculate the temperature at each time step - Enthalpy method based on heat capacity as a function of temperature - Modification of the heat capacity in the phase change range to include the latent heat to the equations (using negative heat capacity) - Solidification is triggered by either reaching a preset temperature or by the solid front. - Gaussian approximations for the heat capacity	- Rate of solidification is a function of a crystallization factor which is a function of temperature. - One direction heat transfer - The crystallization factor is bounded in an interval for computational reasons concerning divergence and errors.	- Using different values for heat capacity, especially the negative values, may cause robustness problems - The crystallization rate factor and the time step are the major parameters that influence stability of the system - The onset of heat release is a critical point - Decreasing the crystallization rate and using smaller time step improve the stability of

				algorithm - Using low values for crystallization rate factor can cause energy balance errors.
Uzan *et al.* [92] (2017)	2D	- Finite volumes method to resolve the enthalpy formulation - Solidification is triggered by either reaching a preset temperature or by the solid front. - Explicit numerical scheme to solve the solidification process - A node can trigger solidification in the neighboring node after reaching a preset value of percentage of solidification.	- Phase change takes place in a range and not at an exact value to overcome sharp variation of enthalpy. - No volume and density changes	- The model shows acceptable results compared to experimental data - Ability of the model to predict temperature behavior at different positions and to demonstrate the effect of boundaries - Ability to be a basis of complex multidimensional modeling
Waser *et al.* [43] (2008)	3D	- The model consists of PCM and - Upwind scheme to discretized the inner heat transfer tube - Finite volume method to discretize the energy equation of the PCM - Implicit first order to discretize the time scheme - Second order spatial discretization scheme - Enthalpy method - Used a phase indicator as a function of temperature - Used an experimentally calibrated crystallization probability function	- No convection heat transfer - No thermal loss with the surrounding ambient air - Constant material properties - No heat transfers between the segments of the model - The model was reduced by symmetry by a factor of 8	The proposed crystallization probability function must be calibrated using suitable experimental data.

			- The inner heat transfer tube is 1D	

7 Discussion

Obtaining an optimal performance with minimal supercooling degree is the main goal when using PCM in thermal storage systems. Each factor affecting supercooling was separately discussed and it was shown that the effect of some factors do not necessarily follow a monotonic tend such as the percentage of additives on the degree of supercooling. The effect of additives decreases after a mean value. The main challenge is to determine the combination between several factors like surface roughness, cooling rate, thermal conductivity, percentage of additives and thermal history that can lead to a PCM with optimal performance. For example, in Figure 15, the use of an aluminum capsule having surface roughness $r = 0.6$ and thermal conductivity $k = 183W/m.K$ gives approximately similar nucleation probability curve as a brass having higher $r = 1.59$ and lower $k = 113W/m.K$. Similarly, the decrease of container's volume, for example by the use of micro-encapsulation, leads to an increase in supercooling degree, but also to an increase of the heat transfer area in a thermal storage system.

The dependency of the supercooling phenomenon on many factors complicates its modeling. As shown above, most authors tend to perform experimental measurements to obtain the required parameters like supercooling degree and rate of spread. Nucleation theories are often used in the numerical models, but the implemented equations still need calibration using experimental data to fit the given case. It is better to increase the number of identical samples used to take the mean value and standard deviation, in order to overcome experimental inaccuracies, including changes in applied conditions and in materials properties. Implementing all known parameters/datasets in the simulations coupled to a statistical tool is still difficult, because of the models complexity and the simulation time that are restricted by the available computational power. Therefore, researchers take approximations, assumptions and neglect parameters to decrease this complexity.

So, it is recommended to use micro-capsulations to increase the heat transfer area and avoid sudden release of huge amount of latent heat. The whole knowledge of PCMs behavior should help in choosing a better PCM that can be a combination of several PCMs to obtain the desired melting temperature. For example, paraffins have high latent heat with a melting temperature near the indoor comfort temperature, which is needed in thermal energy storage in building walls; however, their thermal conductivity is low. Experimental results are important to validate the obtained results, but until now, they are being used to obtain several values to implement in equations and conditions in the model. This strategy restricts the field of work of the model to the applications having same conditions as the experiments. As a future work, it is important to be able to predict the degree of supercooling, which requires building the system of dependency between all parameters. Furthermore, the optimal performance of a PCM in terms of energy may not be the desired one in terms of investment. The chosen parameters should also include cost, energy saving and payback period studies. The ability of modeling a PCM regardless the changing parameters will provide an ability to choose the optimal conditions to be applied in a system from the energy, exergy, economic and environmental viewpoints.

Based on the above, the following guidelines should be followed for the optimal experimental design of an application:

1. Classification of the application: in this step, one should determine whether supercooling is desired (preservation process, animals and plants survival) or not desired (thermal storage systems). Supercooling chaotic behavior can dramatically change the system efficiency.
2. Determination of the parameters that can be modified and have a direct effect on the supercooling degree. For example, modifying the structure, roughness and size of the container of PCM is more easily achieved in thermal energy storage systems than in the processes of preservation. However, in preservation processes, controlling the cooling rate is easier than in thermal energy storage systems integrated in the walls of a building or a greenhouse, which depends on the exterior atmosphere.
3. Study of the correlation between the parameters to be changed. Some parameters have higher impact than others do; for example, the thermal conductivity and surface roughness of the container (see Figure 15).
4. Tradeoff between system performance and cost. The chosen techniques to increase or decrease supercooling should serve in increasing the system's efficiency with the lowest possible cost. Figure 42 summarized the most important decisions to take according to the application and whether supercooling is favored or not.

Regarding the numerical modeling of supercooling, the following guidelines might be followed:

1. Build a physical model with a simple geometry and dimension structure, to reduce computational time and cost.
2. Choose the appropriate modeling method: each method has its advantages and disadvantages. Table 5 summarizes the major characteristics of each model.
3. Make simplifying assumptions to reduce computational time and avoid divergence. Some parameters have negligible effect on heat transfer and PCM behavior while their implementation requires a high computational effort. For example, during solidification, conduction heat transfer is dominant over natural convection. Several assumptions have also been taken by different authors to initiate crystallization (preset temperature, probability equation, state functions)
4. Build the equations representing the temperature rise during latent heat release. Most authors tend to obtain it from experimental results. The manner of crystals spread differs for different temperatures and degrees of supercooling. This modeling challenge adds up to the modeling requirements for crystallization initiation (onset and position). A set of relations have been developed, but they are still limited to specific PCM, container properties and initial values.

8 Conclusions

The present paper is a comprehensive review of the supercooling phenomenon. The review of its principal occurrences in nature and human applications shows that it is usually beneficial for animal and plants survival and for the preservation of food and organs, while it is detrimental to the performance of most thermal energy storage systems. The investigation of the factors affecting the onset and degree of supercooling leads to the following conclusions:

- The occurrence and degree of supercooling increase with a decrease in the percentage of PCM impurities. Decreasing the cooling rate decreases the degree of supercooling but

increases the time spent in supercooled state. Overheating the PCM over repeated cycles and the absence of mechanical shocks on the system also foster supercooling.

- Conversely, the onset and degree of supercooling are reduced by increasing the mixture's thermal conductivity, the container's surface roughness and volume, or by reducing the PCM mixture melting temperature. Adding suitable nucleating agents to the PCM is one of the most used methods to reduce the supercooling degree.

By reviewing the existing numerical models for the simulation of supercooling, it was found that:

- The main challenges are the instable, non-deterministic nature of supercooling and the lack of knowledge on the exact correlations between the various factors affecting its onset.
- Therefore, most models rely on experimental data to provide important parameters such as the degree of supercooling or the rate of crystallization spread. Preset nucleation temperatures, probability equations and state functions are the most used methods to initiate crystallization. However, this strategy limits the validity of the numerical models to very specific experimental cases.

Future experimental and numerical work should include:

- The research of general correlations relating the most important factors affecting supercooling, towards the better prediction of the degree of supercooling and of the onset of crystallization. The correlations should also take into consideration the degradation of the material that takes place due to repeated thermal cycles.
- The investigation of changes in material thermophysical properties as a function of the supercooling degree. This is especially important for high supercooling degrees where the traditional assumptions (density, thermal conductivity, rate of spread, etc.) are no longer applicable.
- The investigation of the PCM temperature increase due to latent heat release. This point is still not well established due to several factors such as degree of supercooling, the change in material's properties and the high rate of spread. Once the behavior is known, the numerical simulation of the system behavior may become more accurate.
- In a holistic approach, the evaluation of the energy and economic impact of supercooling on each application.

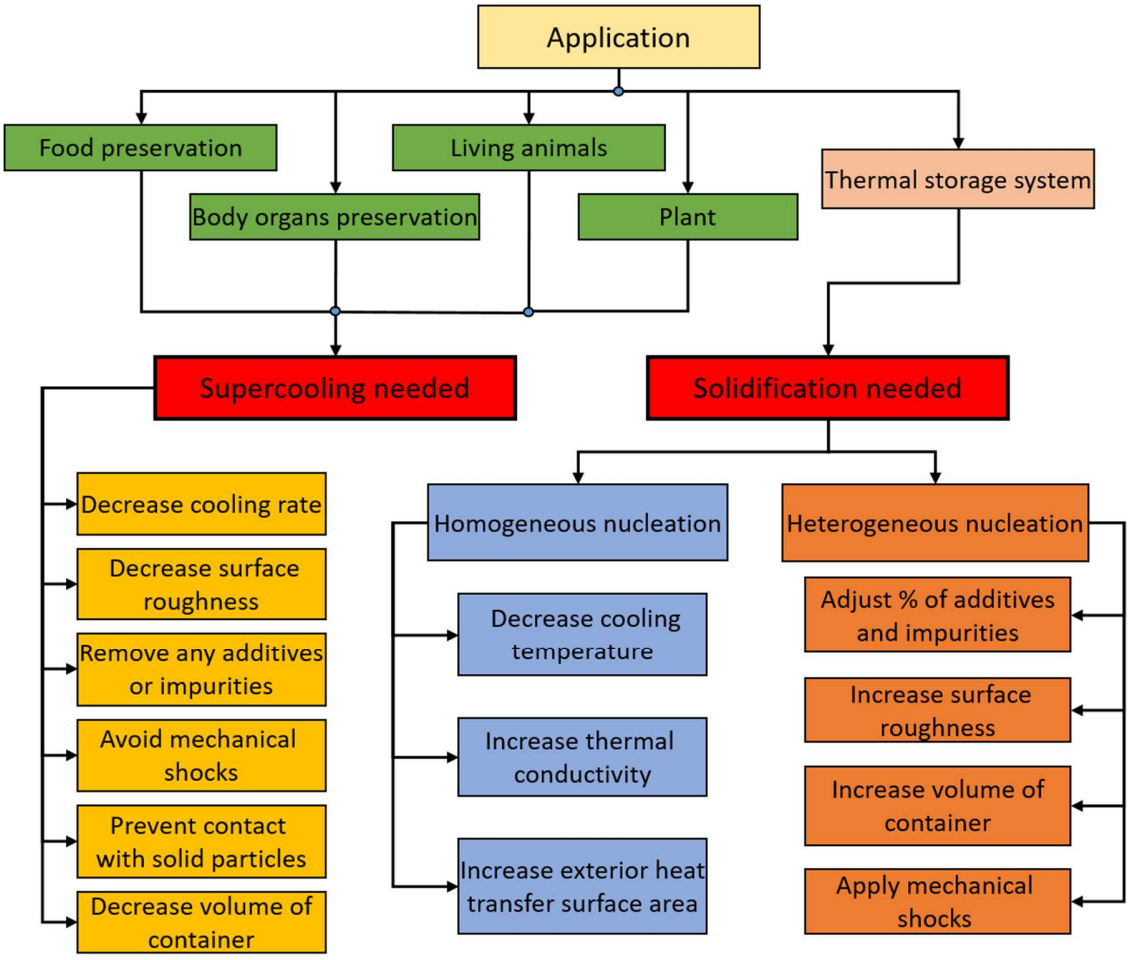

Figure 42 Flow chart showing different solutions to trigger or prevent solidification depending on the application

Acknowledgment

The authors express their sincere thanks to "Le Département de l'Allier" for their financial support for this work.

References

[1] X. Jin, S. Zhang, M. A. Medina, and X. Zhang, "Experimental study of the cooling process of partially-melted sodium acetate trihydrate," *Energy Build.*, vol. 76, pp. 654–660, 2014.

[2] H. Garg, S. Mullick, and V. K. Bhargava, *Solar thermal energy storage*. Springer Science & Business Media, 2012.

[3] T. Kang, Y. You, and S. Jun, "Supercooling preservation technology in food and biological samples: A review focused on electric and magnetic field applications," *Food Sci. Biotechnol.*, vol. 29, no. 3, pp. 303–321, 2020.

[4] D.-K. Liu, C.-C. Xu, C.-X. Guo, and X.-X. Zhang, "Sub-zero temperature preservation of fruits and vegetables: A review," *J. Food Eng.*, vol. 275, p. 109881, 2020.

[5] G. Stonehouse and J. Evans, "The use of supercooling for fresh foods: A review," *J. Food Eng.*, vol. 148, pp. 74–79, 2015.

[6] A. Safari, R. Saidur, F. Sulaiman, Y. Xu, and J. Dong, “A review on supercooling of Phase Change Materials in thermal energy storage systems,” *Renew. Sustain. Energy Rev.*, vol. 70, pp. 905–919, 2017.
[7] N. A. C. Sidik, T. H. Kean, H. K. Chow, A. Rajaandra, S. Rahman, and J. Kaur, “Performance enhancement of cold thermal energy storage system using nanofluid phase change materials: a review,” *Int. Commun. Heat Mass Transf.*, vol. 94, pp. 85–95, 2018.
[8] B. E. Jebasingh and A. V. Arasu, “A detailed review on heat transfer rate, supercooling, thermal stability and reliability of nanoparticle dispersed organic phase change material for low-temperature applications,” *Mater. Today Energy*, vol. 16, p. 100408, 2020.
[9] N. Kumar, J. Hirschey, T. J. LaClair, K. R. Gluesenkamp, and S. Graham, “Review of stability and thermal conductivity enhancements for salt hydrates,” *J. Energy Storage*, vol. 24, p. 100794, 2019.
[10] K. G. Rao, P. Rasoor, G. Anjaneya, J. Nataraj, and M. Srinivas, “A review on methods of preventing super cooling in phase change materials (PCMs),” in *AIP Conference Proceedings*, 2021, vol. 2317, p. 020003.
[11] N. Beaupere, U. Soupremanien, and L. Zalewski, “Nucleation triggering methods in supercooled phase change materials (PCM), a review,” *Thermochim. Acta*, 2018.
[12] Y. Zhao, X. Zhang, X. Xu, and S. Zhang, “Research progress in nucleation and supercooling induced by phase change materials,” *J. Energy Storage*, vol. 27, p. 101156, 2020.
[13] M. H. Zahir, S. A. Mohamed, R. Saidur, and F. A. Al-Sulaiman, “Supercooling of phase-change materials and the techniques used to mitigate the phenomenon,” *Appl. Energy*, vol. 240, pp. 793–817, 2019.
[14] L. Liu, X. Zhang, X. Xu, Y. Zhao, and S. Zhang, “The research progress on phase change hysteresis affecting the thermal characteristics of PCMs: A review,” *J. Mol. Liq.*, p. 113760, 2020.
[15] L. Klimeš *et al.*, “Computer modelling and experimental investigation of phase change hysteresis of PCMs: The state-of-the-art review,” *Appl. Energy*, vol. 263, p. 114572, 2020.
[16] C. A. Goldman and P. L. Hauta, *Tested Studies for Laboratory Teaching. Proceedings of the Workshop/Conference of the Association for Biology Laboratory Education (ABLE)(7th, Las Vegas, Nevada, June 3-7, 1985; 8th, Ithaca, New York, June 16-20, 1986). Volume 7/8.* ERIC, 1993.
[17] G. C. Packard, M. J. Packard, and L. L. McDaniel, “Seasonal change in the capacity for supercooling by neonatal painted turtles,” *J. Exp. Biol.*, vol. 204, no. 9, pp. 1667–1672, 2001.
[18] P. Scholander and J. Maggert, “Supercooling and ice propagation in blood from Arctic fishes,” *Cryobiology*, vol. 8, no. 4, pp. 371–374, 1971.
[19] T. T. Kozlowski and S. G. Pallardy, *Growth control in woody plants*. Elsevier, 1997.
[20] J. Hacker, U. Ladinig, J. Wagner, and G. Neuner, “Inflorescences of alpine cushion plants freeze autonomously and may survive subzero temperatures by supercooling,” *Plant Sci.*, vol. 180, no. 1, pp. 149–156, 2011.
[21] A. Sicular and F. D. Moore, “The postmortem survival of tissues: the effect of time and temperature on the survival of liver as measured by glucose oxidation rate,” *J. Surg. Res.*, vol. 1, no. 1, pp. 16–22, 1961.
[22] K. Monzen *et al.*, “The use of a supercooling refrigerator improves the preservation of organ grafts,” *Biochem. Biophys. Res. Commun.*, vol. 337, no. 2, pp. 534–539, 2005.
[23] B. Rubinsky, A. Arav, J. Hong, and C. Lee, “Freezing of mammalian livers with glycerol and antifreeze proteins,” *Biochem. Biophys. Res. Commun.*, vol. 200, no. 2, pp. 732–741, 1994.
[24] G. Stonehouse and J. Evans, “The use of supercooling for fresh foods: A review,” *J. Food Eng.*, vol. 148, pp. 74–79, 2015.

[25] M. Wisniewski, D. M. Glenn, L. Gusta, and M. P. Fuller, “Using infrared thermography to study freezing in plants,” *HortScience*, vol. 43, no. 6, pp. 1648–1651, 2008.
[26] H. C. J. Godfray *et al.*, “Food security: the challenge of feeding 9 billion people,” *science*, vol. 327, no. 5967, pp. 812–818, 2010.
[27] L. Jeremiah and L. Gibson, “The influence of storage temperature and storage time on color stability, retail properties and case-life of retail-ready beef,” *Food Res. Int.*, vol. 34, no. 9, pp. 815–826, 2001.
[28] S. Sampels, “The effects of storage and preservation technologies on the quality of fish products: A review,” *J. Food Process. Preserv.*, vol. 39, no. 6, pp. 1206–1215, 2015.
[29] Y. Fukuma, A. Yamane, T. Itoh, Y. Tsukamasa, and M. Ando, “Application of supercooling to long-term storage of fish meat,” *Fish. Sci.*, vol. 78, no. 2, pp. 451–461, 2012.
[30] Y. You, J.-Y. Her, T. Shafel, T. Kang, and S. Jun, “Supercooling preservation on quality of beef steak,” *J. Food Eng.*, vol. 274, p. 109840, 2020.
[31] M. Ando, S. Mizuochi, Y. Tsukamasa, and K.-I. Kawasaki, “Suppression of fish meat softening by strict control of storage temperature,” *Fish. Sci.*, vol. 73, no. 3, pp. 705–712, 2007.
[32] A. Duun and T. Rustad, “Quality of superchilled vacuum packed Atlantic salmon (Salmo salar) fillets stored at- 1.4 and- 3.6 C,” *Food Chem.*, vol. 106, no. 1, pp. 122–131, 2008.
[33] C. James, V. Seignemartin, and S. J. James, “The freezing and supercooling of garlic (Allium sativum L.),” *Int. J. Refrig.*, vol. 32, no. 2, pp. 253–260, 2009.
[34] C. James, P. Hanser, and S. J. James, “Super-cooling phenomena in fruits, vegetables and seafoods,” in *11th International Congress on Engineering and Food (ICEF 2011), Athens, Greece*, 2011, pp. 22–26.
[35] A. Arshad, H. M. Ali, M. Ali, and S. Manzoor, “Thermal performance of phase change material (PCM) based pin-finned heat sinks for electronics devices: Effect of pin thickness and PCM volume fraction,” *Appl. Therm. Eng.*, vol. 112, pp. 143–155, 2017, doi: https://doi.org/10.1016/j.applthermaleng.2016.10.090.
[36] A. H. A. Al-Waeli *et al.*, “Evaluation of the nanofluid and nano-PCM based photovoltaic thermal (PVT) system: An experimental study,” *Energy Convers. Manag.*, vol. 151, pp. 693–708, 2017, doi: https://doi.org/10.1016/j.enconman.2017.09.032.
[37] A. Yehya, “Contribution to the experimental and numerical characterization of phase-change materials: consideration of convection, supercooling, and soluble impurities,” PhD Thesis, Artois, 2015.
[38] H. Schranzhofer, P. Puschnig, A. Heinz, and W. Streicher, “Validation of a trnsys simulation model for pcm energy storages and pcm wall construction elements” in *Ecostock conference*, 2006, pp. 2–7.
[39] J. M. Guzman and S. Braga, “Supercooling water in cylindrical capsules,” *Int. J. Thermophys.*, vol. 26, no. 6, p. 1781, 2005.
[40] B. Sandnes and J. Rekstad, “Supercooling salt hydrates Stored enthalpy as a function of temperature,” *Sol. Energy*, vol. 80, no. 5, pp. 616–625, 2006.
[41] H. Hu, X. Jin, and X. Zhang, “Effect of supercooling on the solidification process of the phase change material,” *Energy Procedia*, vol. 105, pp. 4321–4327, 2017.
[42] E. Günther, H. Mehling, and S. Hiebler, “Modeling of subcooling and solidification of phase change materials,” *Model. Simul. Mater. Sci. Eng.*, vol. 15, no. 8, pp. 879–892, Nov. 2007, doi: 10.1088/0965-0393/15/8/005.
[43] R. Waser, S. Maranda, A. Stamatiou, M. Zaglio, and J. Worlitschek, “Modeling of solidification including supercooling effects in a fin-tube heat exchanger based latent heat storage,” *Sol. Energy*, 2018.

[44] T. Adachi, D. Daudah, and G. Tanaka, “Effects of supercooling degree and specimen size on supercooling duration of erythritol,” *Isij Int.*, vol. 54, no. 12, pp. 2790–2795, 2014.
[45] M. C. Flemings and Y. Shiohara, “Solidification of undercooled metals,” *Mater. Sci. Eng.*, vol. 65, no. 1, pp. 157–170, 1984.
[46] J.-P. Dumas, “Etude de la rupture de métastabilité et du polymorphisme de corps organiques,” PhD Thesis, 1976.
[47] K. Nakano, Y. Masuda, and H. Daiguji, “Crystallization and melting behavior of erythritol in and around two-dimensional hexagonal mesoporous silica,” *J. Phys. Chem. C*, vol. 119, no. 9, pp. 4769–4777, 2015.
[48] S.-L. Chen and C.-L. Chen, “Effect of nucleation agents on the freezing probability of supercooled water inside capsules,” *HvacR Res.*, vol. 5, no. 4, pp. 339–351, 1999.
[49] K. Nakano, Y. Masuda, and H. Daiguji, “Crystallization and melting behavior of erythritol in and around two-dimensional hexagonal mesoporous silica,” *J. Phys. Chem. C*, vol. 119, no. 9, pp. 4769–4777, 2015.
[50] R. A. Taylor, N. Tsafnat, and A. Washer, “Experimental characterisation of sub-cooling in hydrated salt phase change materials,” *Appl. Therm. Eng.*, vol. 93, pp. 935–938, 2016.
[51] S.-L. Chen and T.-S. Lee, “A study of supercooling phenomenon and freezing probability of water inside horizontal cylinders,” *Int. J. Heat Mass Transf.*, vol. 41, no. 4–5, pp. 769–783, 1998.
[52] M. Dannemand and S. Furbo, “Supercooling stability of sodium acetate trihydrate composites in multiple heat storage unitsS,” in *12th IIR Conference on Phase-Change Materials and Slurries for Refrigeration and Air Conditioning*, 2018, pp. 227–231.
[53] M. Alizadeh and D. Ganji, “Multi-objective optimization of an externally finned two-phase closed thermosyphon using response surface methodology,” *Appl. Therm. Eng.*, vol. 171, p. 115008, 2020.
[54] K. Kant, P. H. Biwole, I. Shamseddine, G. Tlaiji, F. Pennec, and F. Fardoun, “Recent advances in thermophysical properties enhancement of phase change materials for thermal energy storage,” *Sol. Energy Mater. Sol. Cells*, vol. 231, p. 111309, 2021.
[55] M. Asgari, M. Javidan, M. Nozari, A. Asgari, and D. Ganji, “Simulation of solidification process of phase change materials in a heat exchanger using branch-shaped fins,” *Case Stud. Therm. Eng.*, vol. 25, p. 100835, 2021.
[56] B. Zhao *et al.*, “Phase transitions and nucleation mechanisms in metals studied by nanocalorimetry: A review,” *Thermochim. Acta*, vol. 603, pp. 2–23, 2015.
[57] F. Yin, X. Sun, H. Guan, and Z. Hu, “Effect of thermal history on the liquid structure of a cast nickel-base superalloy M963,” *J. Alloys Compd.*, vol. 364, no. 1–2, pp. 225–228, 2004.
[58] P. Rudolph, H. Koh, N. Schäfer, and T. Fukuda, “The crystal perfection depends on the superheating of the mother phase too—Experimental facts and speculations on the "melt structure" of semiconductor compounds,” *J. Cryst. Growth*, vol. 166, no. 1–4, pp. 578–582, 1996.
[59] Q. Mei and J. Li, “Dependence of Liquid Supercooling on Liquid Overheating Levels of Al Small Particles,” *Materials*, vol. 9, no. 1, p. 7, 2016.
[60] J. A. Noël, L. Kreplak, N. N. Getangama, J. R. de Bruyn, and M. A. White, “Supercooling and Nucleation of Fatty Acids: Influence of Thermal History on the Behavior of the Liquid Phase,” *J. Phys. Chem. B*, vol. 122, no. 51, pp. 12386–12395, 2018.
[61] D. Clause, J. Dumas, P. Meijer, and F. Broto, “Phase transformations in emulsions,” *J Disp Sci Tech*, vol. 8, no. 1, 1987.
[62] D. Clausse, *Research Techniques Utilizing Emulsions, Encyclopedia of Emulsion Technology, vol. 2*. Marcel Dekker, New York, 1985.

[63] T. Wada, K. Matsunaga, and Y. Matsuo, “Studies on salt hydrates for latent heat storage. V. Preheating effect on crystallization of sodium acetate trihydrate from aqueous solution with a small amount of sodium pyrophosphate decahydrate,” *Bull. Chem. Soc. Jpn.*, vol. 57, no. 2, pp. 557–560, 1984.
[64] T. Wada, F. Kimura, and Y. Matsuo, “Studies on Salt Hydrates for Latent Heat Storage. IV. Crystallization in the Binary System CH3CO2Na–H2O,” *Bull. Chem. Soc. Jpn.*, vol. 56, no. 12, pp. 3827–3829, 1983.
[65] T. Wada and Y. Matsuo, “Studies on salt hydrates for latent heat storge. VI. Preheating effect on crystallization of sodium acetate trihydrate from aqueous solution with a small amount of disodium hydrogenphosphate,” *Bull. Chem. Soc. Jpn.*, vol. 57, no. 2, pp. 561–563, 1984.
[66] M. Fashandi and S. N. Leung, “Sodium acetate trihydrate-chitin nanowhisker nanocomposites with enhanced phase change performance for thermal energy storage,” *Sol. Energy Mater. Sol. Cells*, vol. 178, pp. 259–265, 2018.
[67] J. B. Johansen, M. Dannemand, W. Kong, J. Fan, J. Dragsted, and S. Furbo, “Thermal conductivity enhancement of sodium acetate trihydrate by adding graphite powder and the effect on stability of supercooling,” *Energy Procedia*, vol. 70, pp. 249–256, 2015.
[68] T. Schülli, R. Daudin, G. Renaud, A. Vaysset, O. Geaymond, and A. Pasturel, “Substrate-enhanced supercooling in AuSi eutectic droplets,” *Nature*, vol. 464, no. 7292, p. 1174, 2010.
[69] M. Faucheux, G. Muller, M. Havet, and A. LeBail, “Influence of surface roughness on the supercooling degree: Case of selected water/ethanol solutions frozen on aluminium surfaces,” *Int. J. Refrig.*, vol. 29, no. 7, pp. 1218–1224, 2006.
[70] K. Sakurai, N. Yoshinaga, R. Yagi, N. Tomimatsu, and K. Sano, “Effect of embedding sodium acetate trihydrate on the Ag anode in an electrical nucleation cell of a supercooled latent heat storage material,” *Sol. Energy*, vol. 173, pp. 1306–1314, 2018.
[71] S. Akio, U. Yoshio, O. Seiji, M. Kazuyuki, and T. Atsushi, “Fundamental research on the supercooling phenomenon on heat transfer surfaces-investigation of an effect of characteristics of surface and cooling rate on a freezing temperature of supercooled water,” *Int. J. Heat Mass Transf.*, vol. 33, no. 8, pp. 1697–1709, 1990.
[72] P. J. Shamberger and M. J. O’Malley, “Heterogeneous nucleation of thermal storage material LiNO3·3H2O from stable lattice-matched nucleation catalysts,” *Acta Mater.*, vol. 84, pp. 265–274, 2015, doi: https://doi.org/10.1016/j.actamat.2014.10.051.
[73] M. Telkes, “Nucleation of supersaturated inorganic salt solutions,” *Ind. Eng. Chem.*, vol. 44, no. 6, pp. 1308–1310, 1952.
[74] D. Turnbull and B. Vonnegut, “Nucleation catalysis.,” *Ind. Eng. Chem.*, vol. 44, no. 6, pp. 1292–1298, 1952.
[75] G. A. Lane, “Phase change materials for energy storage nucleation to prevent supercooling,” *Sol. Energy Mater. Sol. Cells*, vol. 27, no. 2, pp. 135–160, 1992.
[76] P. Hu, D.-J. Lu, X.-Y. Fan, X. Zhou, and Z.-S. Chen, “Phase change performance of sodium acetate trihydrate with AlN nanoparticles and CMC,” *Sol. Energy Mater. Sol. Cells*, vol. 95, no. 9, pp. 2645–2649, 2011, doi: https://doi.org/10.1016/j.solmat.2011.05.025.
[77] X. Li *et al.*, “Preparation and thermal energy storage studies of CH3COONa·3H2O–KCl composites salt system with enhanced phase change performance,” *Appl. Therm. Eng.*, vol. 102, pp. 708–715, 2016, doi: https://doi.org/10.1016/j.applthermaleng.2016.04.029.
[78] R. Pilar, L. Svoboda, P. Honcova, and L. Oravova, “Study of magnesium chloride hexahydrate as heat storage material,” *Thermochim. Acta*, vol. 546, pp. 81–86, 2012, doi: https://doi.org/10.1016/j.tca.2012.07.021.

[79] S. Ushak, A. Gutierrez, C. Barreneche, A. I. Fernandez, M. Grágeda, and L. F. Cabeza, "Reduction of the subcooling of bischofite with the use of nucleatings agents," *Sol. Energy Mater. Sol. Cells*, vol. 157, pp. 1011–1018, 2016, doi: https://doi.org/10.1016/j.solmat.2016.08.015.
[80] I. M. Sutjahja, S. R. A. U, N. Kurniati, I. D. Pallitine, and D. Kurnia, "The role of chemical additives to the phase change process of CaCl2.6H2O to optimize its performance as latent heat energy storage system," *J. Phys. Conf. Ser.*, vol. 739, p. 012064, Aug. 2016, doi: 10.1088/1742-6596/739/1/012064.
[81] Y. Liu, X. Li, P. Hu, and G. Hu, "Study on the supercooling degree and nucleation behavior of water-based graphene oxide nanofluids PCM," *Int. J. Refrig.*, vol. 50, pp. 80–86, 2015.
[82] S.-L. Chen, P.-P. Wang, and T.-S. Lee, "An experimental investigation of nucleation probability of supercooled water inside cylindrical capsules," *Exp. Therm. Fluid Sci.*, vol. 18, no. 4, pp. 299–306, 1998.
[83] B. Yang, J. H. Perepezko, J. W. Schmelzer, Y. Gao, and C. Schick, "Dependence of crystal nucleation on prior liquid overheating by differential fast scanning calorimeter," *J. Chem. Phys.*, vol. 140, no. 10, p. 104513, 2014.
[84] Z. Zhou, W. Wang, and L. Sun, "Undercooling and metastable phase formation in a Bi95Sb5 melt," *Appl. Phys. A*, vol. 71, no. 3, pp. 261–265, 2000.
[85] R. L. Blaine and C. K. Schoff, *Purity determinations by thermal methods*, vol. 838. ASTM International, 1984.
[86] L. Vinet and A. Zhedanov, "A 'missing'family of classical orthogonal polynomials," *J. Phys. Math. Theor.*, vol. 44, no. 8, p. 085201, 2011.
[87] D. Turnbull, "Formation of crystal nuclei in liquid metals," *J. Appl. Phys.*, vol. 21, no. 10, pp. 1022–1028, 1950.
[88] F. Font, S. Mitchell, and T. Myers, "One-dimensional solidification of supercooled melts," *Int. J. Heat Mass Transf.*, vol. 62, pp. 411–421, 2013.
[89] B. Ralph, *MF Ashby, DRH Jones, Engineering Materials 2 (An Introduction to Microstructures, Processing and Design), Elsevier, Amsterdam (2006), ISBN 978-0-7506-6381-6 and 0-7506-6331-2, 451 pages, US $49.95,\pounds 24.99, 36.75*. Elsevier, 2006.
[90] V. Alexiades, *Mathematical modeling of melting and freezing processes*. Routledge, 2017.
[91] C. Le Bot and D. Delaunay, "Rapid solidification of indium: modeling subcooling," *Mater. Charact.*, vol. 59, no. 5, pp. 519–527, 2008.
[92] A. Y. Uzan, Y. Kozak, Y. Korin, I. Harary, H. Mehling, and G. Ziskind, "A novel multi-dimensional model for solidification process with supercooling," *Int. J. Heat Mass Transf.*, vol. 106, pp. 91–102, 2017.
[93] T. Davin, B. Lefez, and A. Guillet, "Supercooling of phase change: A new modeling formulation using apparent specific heat capacity," *Int. J. Therm. Sci.*, vol. 147, p. 106121, 2020.
[94] A. Safari, R. Saidur, F. Sulaiman, Y. Xu, and J. Dong, "A review on supercooling of Phase Change Materials in thermal energy storage systems," *Renew. Sustain. Energy Rev.*, vol. 70, pp. 905–919, 2017.
[95] S. Liu, Y. Li, and Y. Zhang, "Mathematical solutions and numerical models employed for the investigations of PCMs' phase transformations," *Renew. Sustain. Energy Rev.*, vol. 33, pp. 659–674, 2014.
[96] P. Tittelein *et al.*, "Simulation of the thermal and energy behaviour of a composite material containing encapsulated-PCM: Influence of the thermodynamical modelling," *Appl. Energy*, vol. 140, pp. 269–274, 2015.

[97] P. Lamberg, R. Lehtiniemi, and A.-M. Henell, “Numerical and experimental investigation of melting and freezing processes in phase change material storage,” *Int. J. Therm. Sci.*, vol. 43, no. 3, pp. 277–287, 2004.
[98] Y. Zhang, K. Du, M. A. Medina, and J. He, “An experimental method for validating transient heat transfermathematical models used for phase change materials (PCMs) calculations,” *Phase Transit.*, vol. 87, no. 6, pp. 541–558, 2014.
[99] Y. Kozak and G. Ziskind, “Novel enthalpy method for modeling of PCM melting accompanied by sinking of the solid phase,” *Int. J. Heat Mass Transf.*, vol. 112, pp. 568–586, 2017.
[100] S. Hoseinzadeh, R. Ghasemiasl, D. Havaei, and A. Chamkha, “Numerical investigation of rectangular thermal energy storage units with multiple phase change materials,” *J. Mol. Liq.*, vol. 271, pp. 655–660, 2018.
[101] M. J. Huang, “The effect of using two PCMs on the thermal regulation performance of BIPV systems,” *Sol. Energy Mater. Sol. Cells*, vol. 95, no. 3, pp. 957–963, 2011.
[102] A. V. Sá, M. Azenha, H. de Sousa, and A. Samagaio, “Thermal enhancement of plastering mortars with Phase Change Materials: Experimental and numerical approach,” *Energy Build.*, vol. 49, pp. 16–27, 2012.
[103] S. Sadasivam, D. Zhang, F. Almeida, and others, “An iterative enthalpy method to overcome the limitations in ESP-r’s PCM solution algorithm,” *Ashrae Trans.*, vol. 117, p. 100, 2011.
[104] F. Almeida, D. Zhang, A. S. Fung, and W. H. Leong, “Comparison of corrective phase change material algorithm with ESP-r simulation,” 2011.
[105] S. Liu, Y. Li, and Y. Zhang, “Mathematical solutions and numerical models employed for the investigations of PCMs? phase transformations,” *Renew. Sustain. Energy Rev.*, vol. 33, pp. 659–674, 2014.
[106] Y. Zhang, K. Du, M. A. Medina, and J. He, “An experimental method for validating transient heat transfermathematical models used for phase change materials (PCMs) calculations,” *Phase Transit.*, vol. 87, no. 6, pp. 541–558, 2014.
[107] Z. Chen, X. Guo, L. Shao, S. Li, and L. Gao, “Sensitivity analysis of the frozen soil nonlinear latent heat and its precise transformation method,” *Geophys. J. Int.*, 2021.
[108] D. Heim, “Isothermal storage of solar energy in building construction,” *Renew. Energy*, vol. 35, no. 4, pp. 788–796, 2010.
[109] A. Faghri and Y. Zhang, *Transport phenomena in multiphase systems*. Elsevier, 2006.
[110] Y. Fang and M. Medina, “Proposed modifications for models of heat transfer problems involving partially melted phase change processes,” in *Heat-Air-Moisture Transport, 2nd Volume: Measurements and Implications in Buildings*, ASTM International, 2010.
[111] J. Virgone, J. Noël, and R. Reisdorf, “Numerical study of the influence of the thickness and melting point on the effectiveness of phase change materials: application to the renovation of a low inertia school,” 2009.
[112] F. Kuznik, D. David, K. Johannes, and J.-J. Roux, “A review on phase change materials integrated in building walls,” *Renew. Sustain. Energy Rev.*, vol. 15, no. 1, pp. 379–391, 2011.
[113] L. F. Cabeza, A. Castell, C. de Barreneche, A. De Gracia, and A. Fernández, “Materials used as PCM in thermal energy storage in buildings: A review,” *Renew. Sustain. Energy Rev.*, vol. 15, no. 3, pp. 1675–1695, 2011.
[114] D. Zhou, C.-Y. Zhao, and Y. Tian, “Review on thermal energy storage with phase change materials (PCMs) in building applications,” *Appl. Energy*, vol. 92, pp. 593–605, 2012.
[115] A. Pasupathy and R. Velraj, “Mathematical modeling and experimental study on building ceiling system incorporating phase change material (PCM) for energy conservation,” in

ASME International Mechanical Engineering Congress and Exposition, 2006, vol. 47837, pp. 59–68.

[116] A. Pasupathy, L. Athanasius, R. Velraj, and R. Seeniraj, "Experimental investigation and numerical simulation analysis on the thermal performance of a building roof incorporating phase change material (PCM) for thermal management," *Appl. Therm. Eng.*, vol. 28, no. 5–6, pp. 556–565, 2008.

[117] J. Mazo, M. Delgado, J. M. Marin, and B. Zalba, "Modeling a radiant floor system with Phase Change Material (PCM) integrated into a building simulation tool: Analysis of a case study of a floor heating system coupled to a heat pump," *Energy Build.*, vol. 47, pp. 458–466, 2012.

[118] X. Jin and X. Zhang, "Thermal analysis of a double layer phase change material floor," *Appl. Therm. Eng.*, vol. 31, no. 10, pp. 1576–1581, 2011.

[119] F. Kuznik, J. Virgone, and J. Noel, "Optimization of a phase change material wallboard for building use," *Appl. Therm. Eng.*, vol. 28, no. 11–12, pp. 1291–1298, 2008.

[120] R. Ansuini, R. Larghetti, A. Giretti, and M. Lemma, "Radiant floors integrated with PCM for indoor temperature control," *Energy Build.*, vol. 43, no. 11, pp. 3019–3026, 2011.

[121] P. Damronglerd and Y. Zhang, "Modified temperature-transforming model for convection-controlled melting," *J. Thermophys. Heat Transf.*, vol. 21, no. 1, pp. 203–208, 2007.

[122] Z. Ma and Y. Zhang, "Solid velocity correction schemes for a temperature transforming model for convection phase change," *Int. J. Numer. Methods Heat Fluid Flow*, 2006.

[123] D. U. Sarwe and V. S. Kulkarni, "Thermal behaviour of annular hyperbolic fin with temperature dependent thermal conductivity by differential transformation method and Pade approximant," *Phys. Scr.*, vol. 96, no. 10, p. 105213, 2021.

[124] S. Wang, A. Faghri, and T. L. Bergman, "A comprehensive numerical model for melting with natural convection," *Int. J. Heat Mass Transf.*, vol. 53, no. 9–10, pp. 1986–2000, 2010.

[125] Y. Cao and A. Faghri, "A numerical analysis of phase-change problems including natural convection," 1990.

[126] A. Joulin, Z. Younsi, L. Zalewski, S. Lassue, D. R. Rousse, and J.-P. Cavrot, "Experimental and numerical investigation of a phase change material: Thermal-energy storage and release," *Appl. Energy*, vol. 88, no. 7, pp. 2454–2462, 2011.

[127] A. Joulin, Z. Younsi, L. Zalewski, D. R. Rousse, and S. Lassue, "A numerical study of the melting of phase change material heated from a vertical wall of a rectangular enclosure," *Int. J. Comput. Fluid Dyn.*, vol. 23, no. 7, pp. 553–566, 2009.

[128] Z. A. Hammou and M. Lacroix, "A new PCM storage system for managing simultaneously solar and electric energy," *Energy Build.*, vol. 38, no. 3, pp. 258–265, 2006.

[129] A. Arnault, F. Mathieu-Potvin, and L. Gosselin, "Internal surfaces including phase change materials for passive optimal shift of solar heat gain," *Int. J. Therm. Sci.*, vol. 49, no. 11, pp. 2148–2156, 2010.

[130] M. Costa, D. Buddhi, and A. Oliva, "Numerical simulation of a latent heat thermal energy storage system with enhanced heat conduction," *Energy Convers. Manag.*, vol. 39, no. 3–4, pp. 319–330, 1998.

[131] M. Frémond, R. Gormaz, and J. A. San Martı?n, "A new mathematical model for supercooling," *J. Math. Anal. Appl.*, vol. 261, no. 2, pp. 578–603, 2001.

[132] M. Fremond, "Supercooling: a macroscopic predictive theory," in *Ground freezing 94. Proceedings of the seventh international symposium on ground freezing; Nancy, France; 24-28 October 1994*, 1994, pp. 79–84.

[133] R. Courant, K. Friedrichs, and H. Lewy, “Über die partiellen Differenzengleichungen der mathematischen Physik,” *Math. Ann.*, vol. 100, no. 1, pp. 32–74, 1928.
[134] J. Bony and S. Citherlet, “Numerical model and experimental validation of heat storage with phase change materials,” *Energy Build.*, vol. 39, no. 10, pp. 1065–1072, 2007.
[135] K. Darkwa and P. O'callaghan, “Simulation of phase change drywalls in a passive solar building,” *Appl. Therm. Eng.*, vol. 26, no. 8–9, pp. 853–858, 2006.